Flexible Multicarrier Systems for Ad-hoc Wireless Network

Yafei HOU

A dissertation submitted to
Kochi University of Technology
in partial fulfillment of the requirements
for the degree of

Doctor of Philosophy

(Special Course for International Students)
Department of Engineering
Graduate School of Engineering
Kochi University of Technology
Kochi, Japan

March, 2007

Abstract

Flexible Multicarrier Systems for Ad-hoc Wireless Network

Yafei HOU

The underlying philosophy in all problems that are considered in this dissertation is a synergy between the physical and the MAC layers.

Firstly, we will explain that the flexible transmission including adaptive modulation and variable length of frame can cause different link goodput (to distinguish with 'throughput'), transmission range and energy efficiency. The nodes of ad-hoc network can realize the tradeoff between goodput, range and energy efficiency by the flexible transmissions. We will give the results which shows that there is much to be gained from adaptive modulation and variable frame length in terms of goodput, range and energy consumption for wireless ad-hoc networks. We obtain three rules of design for such a tradeoff for wireless nodes.

Usually, the adaptive modulation and variable length of frame can be achieved using M-QAM modulation with different constellation size M, which can also be treated as the one of technologies of physical layer adaptation. Since the value of M is limited by power of 2, physical layer adaptation using adaptive M-QAM is not easy to choose the appropriate M, and high order M-QAM ($M > 64$) is seldom used for WLAN-based ad-hoc networks. On the other hand, one novel flexible multicarrier system (high compaction multicarrier modulation: HC-MCM) which can attain higher bandwidth efficiency (BWE) than that of the OFDM system has been designed. The HC-MCM can flexibly control the transmission rate and the communication quality. More im-

portantly, only utilizing BPSK or QPSK modulation, it can adaptively achieve the transmission rate of high M-QAM OFDM by transmitting variable length of partial time-domain OFDM signal. Based on the HC-MCM, we propose a novel flexible multicarrier modulation combined with the parallel combinatory OFDM (PC-OFDM), that is, parallel combinatory / high compaction multicarrier modulation (PC/HC-MCM) in this dissertation. The PC/HC-MCM can achieve any transmission rate of M-QAM that corresponds to not only integer M but also real number M. The PC/HC-MCM can also realize the adaptive length of frame which can be utilized to physical layer adaptation with the adaptive length of packets. Two types of PC/HC-MCM systems, which are named as modulated PC/HC-MCM system and PC/HC-MCM system, are designed by this modulation. The modulated PC/HC-MCM system can achieve better BER performance than that of HC-MCM system with the equal BWE by employing appropriate parallel combinatory codes. The PC/HC-MCM system can obtain excellent peak-to-average power ratio (PAPR) characteristics by selecting the optimal constellations for its subcarriers. On the other hand, since the PC/HC-MCM can divide one PC-OFDM symbol duration into multiple time-slots, the advantages of frequency hopping (FH) can be applied in the PC/HC-MCM systems. Therefore, we combine the PC/HC-MCM and frequency hopping multiple access (FHMA) to propose a new multiple access (MA) system. This MA system can synchronously transmit multiple users' data within one symbol duration of the PC-OFDM.

From the flexible multicarrier system, the modulated message data of OFDM signal can be demodulated using the partial time-domain OFDM signal. Therefore, the partial time-domain OFDM signal can be adopted to reconstruct the whole OFDM signal with estimated channel information. So in this dissertation, we will propose a effective method of collision recovery for OFDM-based ad-hoc networks based on the flexible multicarrier system. Since most collisions occur when one user starts to build

a connection or sends a response with a short packet, such as RTS (request-to-send), CTS (clear-to-send) or ACK (acknowledgement), to one node while a principal user is transmitting a long packet including data to an identical destination. Therefore, the collided part is not as long as the principal long packet. Utilizing this advantageous property, a practical method of collision recovery, which is somewhat similar to the scheme of successive interference cancellation, can be realized. We simulate the recovery performance using different modulation for two users with identical SNR and weak near-far effect, and show that the method gives promising results and can be developed to solve the problem of hidden or exposed terminals of ad-hoc networks.

According to the property of flexible multicarrier system, OFDM system can transmit partial time-domain OFDM signals to send the data. Therefore, OFDM system can select the signal among some specific durations, which can reduce the PAPR, to transmit the equal bits of data. So this dissertation also proposes a novel PAPR reduction technique called partial signal transmission (PST) for ad-hoc networks. The PST is a promising technique that dramatically reduces the PAPR with an acceptable BER degradation. Therefore, the PST will decrease the device cost for constructing the ad-hoc networks.

key words Multicarrier System, OFDM, Ad-hoc Networks, Collision Recovery, PAPR Reduction, Physical Layer Adaptation.

Contents

List of Figures

List of Tables

Chapter 1

Introduction

1.1 Introduction

The proliferation of mobile computing and communication devices is driving a revolutionary change in information society. We are moving from the Personal Computer age to the Ubiquitous Computing age in which a user utilizes several electronic platforms through which he can access all the required information whenever and wherever needed [1]. The nature of ubiquitous devices makes wireless networks the easiest solution for their interconnection and, as a consequence, the wireless arena has been experiencing exponential growth in the past decade. Recently, new alternative ways, which have been named as ad-hoc networks and technologies, to deliver the services have been emerging. These are focused around having the devices connect to each other in the transmission range through automatic configuration, setting up an ad-hoc network that is both flexible and powerful. In this way, not only can nodes communicate with each other, but also can receive Internet services through Internet gateway node. As the wireless network continues to evolve, the capabilities of ad-hoc are expected to become more important, the technology solutions used to support more critical and significant future research and development efforts can be expected in industry and academy.

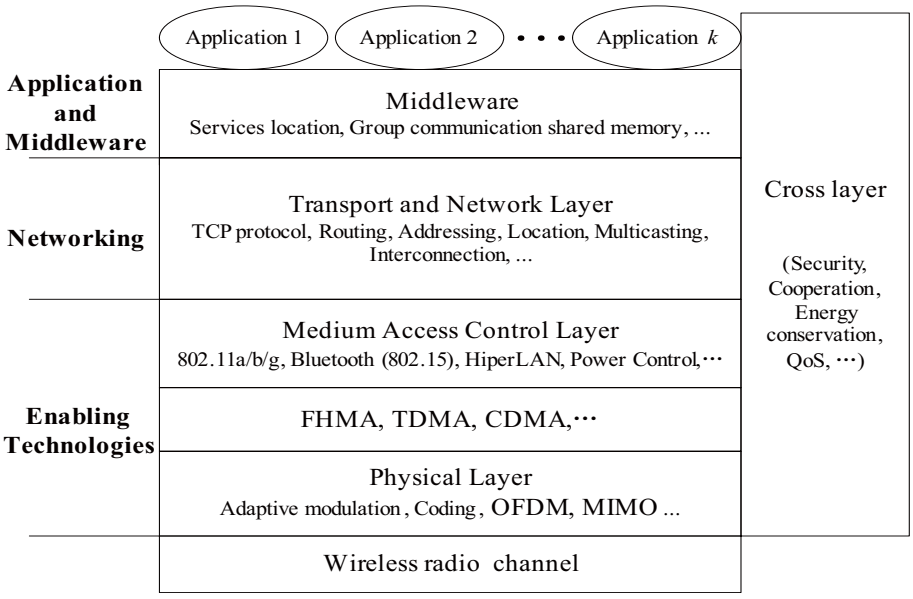

Fig. 1.1 A simple ad-hoc architecture.

1.2 Ad-hoc Network Research

A large body of research has been accumulated to address these specific issues and constraints. In this section, we simple describe the ongoing research activities and the challenges in ad-hoc networks. We will use the simplified architecture shown in Fig. 1.1.

As shown in Fig. 1.1, the research activities will be grouped, according to a layered approach into three main areas:

(1) Applications and middleware;

(2) Network layer reserach;

(3) Enabling technologies.

In addition, as shown in Fig. 1.1, several issues (energy management, security and cooperation, quality of service, network simulation) span all areas, and often such layer is named as the cross layer.

1.2.1 Applications and Middleware of Ad-hoc Networks

The applications and middleware layer operates between the networking layers and the distributed applications (i.e., it mainly implements layers 5 to 7 of the OSI model), with the aim to build on top of raw network services, higher level mechanisms that simplify the development and deployment of applications. Ad-hoc systems developed currently adopt the approach of not having a middleware, but rather rely on each application to handle all the services it needs. This constitutes a major complexity/inefficiency in the development of MANET applications.

Research on middleware for mobile ad-hoc networks is still in its infancy. Ad-hoc networks and self-organization have not yet received the attention they deserve. Existing middleware mainly focus on mobile/nomadic environments, where a fixed infrastructure contains the relevant information. For an overview on middleware for mobile and pervasive systems, see [2]-[4].

1.2.2 Ongoing Research on Network Layer of Ad-hoc Networks

To cope with the self-organizing, dynamic, volatile environment in an ad-hoc netwrok, most of the main functionalities of the network protocols need to be redesigned. The aim of the networking protocols is to use the one-hop transmission services provided by the enabling technologies to construct end-to-end (reliable) delivery services, from a sender to one (or more) receiver(s).

To achieve an end-to-end communication, the sender needs to locate the receiver inside the network. The purpose of a location service is to dynamically map the logical address of the (receiver) device to its current location in the network. Current solutions generally adopted to manage mobile terminals in infrastructure networks are generally inadequate, and new approaches have to be found. Once, a user is located, routing and

forwarding algorithms must be provided to route the information through the ad-hoc network. Finally, the low reliability of communications (due to wireless communications, users' mobility, etc.), and the possibility of network congestion require a redesign of transport layer mechanisms. For an overview on network protocols for ad-hoc netwroks and pervasive systems, see [5]-[8].

1.2.3 Ongoing Research on Enabling Technologies for Ad-hoc Networks

Ad-hoc networks, depending on their coverage area, can be classified into several classes: Body (BAN), Personal (PAN), Local (LAN), Metropolitan (MAN) and Wide (WAN) area networks. Wide- and Metropolitan-area ad-hoc networks are multi-hop wireless networks that present many challenges that are still to be solved and their availability is not on immediate horizon. On the other hand, ad-hoc networks with smaller coverage can be expected to appear soon. Specifically, ad-hoc single-hop BAN, PAN and LAN wireless technologies are already common on the market [9]. For these reasons, BAN, PAN and LAN technologies constitute the Enabling technologies for ad-hoc networking. A detailed discussion of Body, Personal, and Local ad-hoc wireless networks can be found in [10].

Since most ad-hoc networks are constituted by the technologies of wirelss LAN, on the other hand, this dissertation mainly concerns on Enabling technologies for the ad-hoc network, we will describe in detail on the technologies of wireless LAN in the following section.

1.3 Ad-hoc Network Based on Wireless LAN

Wireless LANs (WLANs) have a communication range typical of a single building, or a cluster of buildings, i.e., 30 to 500 [m]. A WLAN should satisfy the same requirements typical of any LAN, including high capacity, full connectivity among attached stations, and broadcast capability. However, to meet these objectives, WLANs need to be designed to face some issues specific to the wireless environment, like security on the air, power consumption, mobility, and bandwidth limitation of the air interface. Two different approaches can be followed in the implementation of a WLAN: an infrastructure-based approach, or an ad-hoc networking one [11].

An infrastructure-based architecture imposes the existence of a centralized controller for each cell, often referred to as AP (access point). The AP is normally connected to the wired network, thus providing the Internet access to mobile devices. In contrast, an ad-hoc network is a peer-to-peer network formed by a set of stations within the range of each other, which dynamically configure themselves to set up a temporary network. In the ad-hoc configuration, no fixed controller is required, but a controller may be dynamically elected among the stations participating in the communication.

The success of a network technology is connected to the development of networking products at a competitive price. A major factor in achieving this goal is the availability of appropriate networking standards. Currently, two main standards are emerging for ad-hoc wireless networks: the IEEE 802.11 standard for WLANs [12], and the Bluetooth specifications 3 [13]-[16] for short-range wireless communications [14]-[16]. Due to its extreme simplicity, the IEEE 802.11 standard is a good platform to implement a single-hop WLAN ad-hoc network. Furthermore, multihop networks covering areas of several square kilometers can potentially be built by exploiting the IEEE 802.11 technology. On a smaller scale, technologies such as Bluetooth can be used to build ad-hoc wireless

Body, and Personal Area Networks, i.e., networks that connect devices on the person, or placed around him inside a circle with radius of 10 [m]. So Bluetooth technology is limited in constructing the ad-hoc networks due to the small coverage.

1.3.1 IEEE 802.11 WLAN

In 1997, the IEEE adopted the first wireless local area network standard, named IEEE 802.11, with data rates up to 2 Mbps [17]. Since then, several task groups (designated by the letters from 'a', 'b', 'c', etc.) have been created to extend the IEEE 802.11 standard. Task groups' 802.11b and 802.11a have completed their work by providing two relevant extensions to the original standard [12], which are often referred to with the friendly name of wireless Fidelity (Wi-Fi). The 802.11b task group produced a standard for WLAN operations in 2.4 GHz band, with data rates up to 11Mbps and backward compatibility. The 802.11a task group created a standard for WLAN operation in the 5 GHz band, with data rates up to 54 Mbps. Among the other task groups, it is worth mentioning the task group 802.11e (attempting to enhance the MAC with QoS features to support voice and video over 802.11 networks), and the task group 802.11g (that is working to develop a higher speed extension to the 802.11b).

The IEEE 802.11 standard defines two operational modes for WLANs: infrastructure-based and infrastructure-less or ad-hoc. Network interface cards can be set to work in either of these modes but not in both simultaneously. Infrastructure mode resembles cellular infrastructure-based networks. It is the mode commonly used to construct the so-called Wi-Fi hotspots, i.e., to provide wireless access to the Internet. In the ad-hoc mode, any station that is within the transmission range of any other, after a synchronization phase, can start communicating. No AP is required, but if one of the stations operating in the ad-hoc mode has a connection also to a wired network, stations forming the ad-hoc network gain wireless access to the Internet.

1.3.2 HiperLAN/2 WLAN

In addition to the IEEE standards, the European Telecommunication Standard Institute (ETSI) has promoted the HiperLAN (high performance radio local area network) family of standard for WLANs [18]. Among these, the most interesting standard for WLAN is HiperLAN/2. The HiperLAN/2 technology addresses high-speed wireless network with data rates ranging from 6 to 54 Mbit/s. Infrastructure-based, and ad-hoc networking on figurations are both supported in HiperLAN/2. More details on this technology can be found in [19]. [20] surveys the off-the-shelf technologies for constructing ad-hoc networks; while [21] presents an in depth analysis of 802.11-based ad-hoc networks, including performance evaluation and some of the open issues.

1.4 Wireless Channel for Ad-hoc Network

The ad-hoc networks flexibility and convenience do come at a price. ad-hoc wireless networks inherit the traditional problems of wireless communications and wireless networking [22]:

(1) the wireless medium has neither absolute, nor readily observable boundaries outside of which stations are known to be unable to receive network frames;

(2) the channel is unprotected from outside signals;

(3) the wireless medium is significantly less reliable than wired media;

(4) the channel has time-varying and asymmetric propagation properties;

(5) hidden-terminal and exposed-terminal phenomena may occur.

To these problems and complexities, the multihop nature, and the lack of fixed infrastructure add a number of characteristics, complexities, and design constraints that are specific to ad-hoc networking. Essentially, above limitations always derive from the wireless channel.

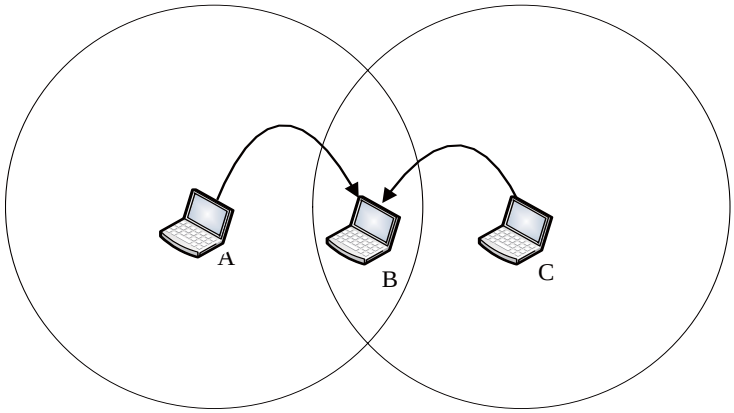

Fig. 1.2 Hidden-terminal problem

1.4.1 The Hidden-terminal or Exposed-terminal Problems

In wireless ad-hoc networks that rely on a carrier-sensing random access protocol, such as the IEEE 802.11, the wireless medium characteristics generate complex phenomena such as the hidden-terminal and the exposed-terminal problems.

The hidden-terminal problem occurs when two (or more) nodes, say A and C, cannot detect each other's transmissions (due to being outside of each other transmission range) but their transmission ranges are not disjoint [23]. As shown in Fig. 1.2, a collision may occur, for example, when the node A and node C start transmitting towards the same receiver, node B in the figure. The exposed-terminal problem results from situations where a permissible transmission from a mobile node to another station has to be delayed due to the irrelevant transmission activity between two other mobile nodes within sender's transmission range. Fig. 1.3 depicts a typical scenario where the "exposed terminal" problem may occur. Let us assume that node A and node C can hear transmissions from B, but node A cannot hear transmissions from C. Let us also assume that node B is transmitting to node A, and node C has a frame to be transmitted to D. According to the CSMA scheme, C senses the medium and finds it busy because of B's transmission, and therefore refrains from transmitting to D, although this transmission

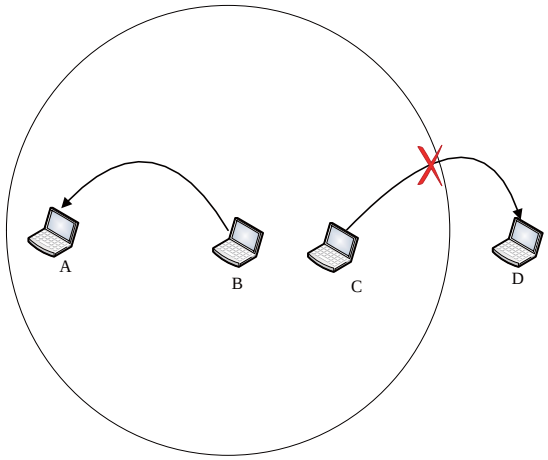

Fig. 1.3 Exposed-terminal problem

would not cause a collision at A. The "exposed terminal" problem may thus result in loss of throughput.

Paper [24] has studied the performance of the IEEE 802.11 MAC protocol in the presence of hidden terminals. The simulations show that the performance of the IEEE 802.11 protocol dramatically deteriorates in the presence of hidden terminals. While the throughput is acceptable when less than 10 percent of station pairs are hidden, the average per frame delay increases by as much as an order of magnitude. Given other system parameters, the system throughput, average packet delay and blocking probability is dependent only on the percentage of station pairs hidden from each other. The average delay, throughput and blocking probability seen by a particular station is not uniform and varies greatly depending on the number of stations hidden from it. To cope with the hidden-terminal and the exposed-terminal problems, many access protocols which are utilized at MAC layer have been proposed, for an overview on network protocols for ad-hoc netwroks, see [5]-[8], [25].

1.4.2 Wireless Channel Model

The inherent volatility of the wireless medium constitutes the major difficulty in the design of ad-hoc networks. The quality of a wireless link between a transmitter and a receiver depends on radio propagation parameters (path loss, shadow fading, multi-path fading) and cochannel interference. Path loss stems from wave propagation attenuation in free space. Shadow fading is caused by large obstacles such as buildings and the incurred loss is modeled as a log-normally distributed random variable. Multi-path fading arises due to additive and subtractive effect of delays and amplitudes from multiple paths.

The time-varying nature of these factors due to transmitter or receiver mobility and movement of the surrounding objects causes the quality of a narrow band wireless link to fluctuate with time. On the other hand, a broadband wireless link is characterized both by time-varying behavior due to the aforementioned factors and by frequency selectivity caused by multi-path propagation and delay spread. The frequency-selectivity can lead to inter-symbol interference (ISI) and thus significantly degrade link quality.

The time-varying wireless channel can be completely characterized by its baseband impulse response $h(t, \tau)$ which is given by

$$h(t,\tau) = \sqrt{G\sigma(t)} \sum_{i=1}^{L_P} A_i e^{j\theta_i} \delta(t - \tau_i), \tag{1.1}$$

where G is the path loss, $\sigma(t)$ denotes time-varying shadow fading, L_P is the number of paths in the multi-path and each path has the relative path delay $\tau_i (\tau_1 \leq \tau_2 \leq \ldots \leq \tau_{L_P} < T_g)$. $A_i = A_i(t)$ and $\theta_i = \theta_i(t)$ are the slowly Rayleigh-fading amplitude attenuation and phase rotation of each path.

The transmitted signal is

$$s(t) = x(t) e^{j 2\pi f_c t}, \tag{1.2}$$

where f_c is the carrier frequency and $x(t)$ is the complex base-band signal. This is

expressed as,

$$x(t) = \sum_{n=-\infty}^{n=+\infty} x(n)g(t-nt), \tag{1.3}$$

where $x(n)$ is the symbol sequence, T is the symbol duration and $g(.)$ is the pulse shaping waveform. The signal at the receiver input is

$$y_r(t) = \int_{-\infty}^{+\infty} x(t-\tau)h(t,\tau)d\tau + n(t), \tag{1.4}$$

where $n(t)$ is the receiver noise process.

To combat the signal distortion over the multipath channel, Many physical layer adaptation technologies, such as modulation and coding, have been proposed and applied in many communication systems [26]. Among them, Orthogonal Frequency Division Multiplexing (OFDM) is one of the proposed modulation and multiple access technique for wireless broadband access [27]. OFDM is included in the IEEE 802.11a and ETSI HiperLAN/2 standards for WLANs, as well as in the digital audio/video broadcasting (DAB/DVB) standards in Europe. It has also been proposed by IEEE 802.15 and IEEE 802.16 working groups for WPANs and fixed BWA respectively. OFDM is based on the principle of multicarrier transmission, also known as Discrete Multi-Tone (DMT), which was applied earlier in high bit-rate DSLs [28]. We will describe in detail on the technologies of physical layer adaptation and, particularly, OFDM system in the following sections.

1.5 OFDM System over Wireless Channel

In OFDM system, the wide-band spectrum is divided into orthogonal narrow-band subcarriers as in frequency division multiplexing. The bit stream is split into subsets, each of which constitutes a subsymbol. Each subsymbol modulates a different subcarrier and several subsymbols of a user are transmitted in parallel over these low-rate subcarriers. Modulation and demodulation of subcarriers during transmission and reception

are implemented with inverse discrete Fourier transform (IDFT) and DFT, respectively. The orthogonality of signals in different subcarriers is preserved by appropriate selection of the frequency spacing between the subcarriers. Due to this orthogonality, the signals are separated at the receiver.

1.5.1 OFDM Transmission and Reception

The schematic diagram of a single-user OFDM transmitter and receiver with N_C subcarriers is depicted in Fig. 1.4. The bit stream is divided into bit groups and each bit group $x(n)(n = 0, \ldots, N_C - 1)$ constitutes one OFDM symbol. Assuming that OFDM symbols do not interfere with each other, it suffices to concentrate on one OFDM symbol. The OFDM symbol is further divided into N_C bit subgroups. The bits in the nth subgroup are fed into the nth modulator and modulate the nth $(n = 0, \ldots, N_C - 1)$ subcarrier, The complex subsymbol $x(n)$ at the output of the nth modulator is selected from a QAM or QPSK constellation and the modulation level of $x(n)$ depends on the number of allocated bits in the nth subcarrier. The number of allocated bits per subcarrier depends on subcarrier quality. Better quality subcarriers can carry more bits and maintain acceptable BER at the receiver. All subsymbols are then fed into an IDFT module and are transformed into time samples $y(n)(n = 0, \ldots, N_C - 1)$, where $y(n)$ is

$$y(n) = \frac{1}{\sqrt{N_C}} \sum_{k=0}^{N_C-1} x(k) e^{j2\pi kn/N_C}, \tag{1.5}$$

where $1/\sqrt{N_C}$ is a scale factor. A cyclic prefix of N_g time samples with total duration larger than the maximum delay spread is appended to the N_C time samples, as a means of eliminating ISI. The sequence $y(n)$ is then passed to a D/A converter, whose output

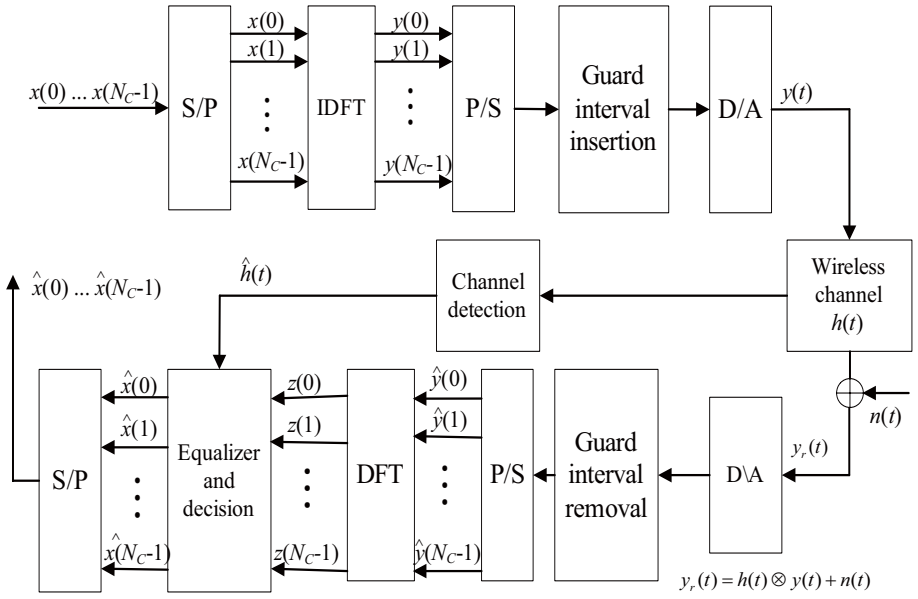

Fig. 1.4 A simple architecture of OFDM system

is the continuous signal,

$$y(t) = \frac{1}{\sqrt{N_C}} \sum_{k=0}^{N_C-1} x(k) e^{j2\pi kt/N_C} \quad t \in [0, T_0], \tag{1.6}$$

where T_0 is the symbol duration. The pulse-shaping filter $g(t)$ is taken to be normalized to unit. Note that the signal in the frequency domain consists of N_C $sinc(\pi f T_0)$ functions, each shifted in frequency (Δf_0) by $1/T_0$, where each such function corresponds to the Fourier transform of the unit pulse. Due to the property of the $sinc(\pi f T_0)$ function that is zero at integer multiples of $1/T_0$, the subsymbols at different subcarriers can be distinguished at the receiver.

The base-band signal $y(t)$ is up-converted and transmitted through the channel. At the receiver, the signal is translated to base-band and its cyclic prefix is removed. We assume that the channel is invariant for the duration of one OFDM symbol. The signal after down-conversion is

$$y_r(t) = \sum_{i=1}^{L_P} \beta_i e^{-j2\pi f_c \tau_i} y(t - \tau_i) + n(t), \tag{1.7}$$

where $n(t)$ is the base-band noise process and $\beta_i = A_i e^{j\theta_i}$. Then, the signal is digitized

by being sampled at time points kT_0/N_C, for $k = 0, \ldots, N_C - 1$. The kth sample is given as

$$\hat{y}_r(k) = \frac{1}{\sqrt{N_C}} \sum_{i=1}^{L_P} \sum_{n=0}^{N_C-1} x(n)\beta_i(n)e^{-j2\pi nk/N_C} + n(k), \tag{1.8}$$

where

$$\beta_i(n) = \beta_i e^{-j2\pi(f_c+n/T_0)\tau_i} \tag{1.9}$$

captures the different impact of the ith path delay on different subcarriers and $n(k)$ are noise samples. The time samples $\hat{y}_r(k)(k = 0, \ldots, N_C - 1)$ enter the DFT module and the subsymbol at subcarrier $k(k = 0, \ldots, N_C - 1)$ is given as

$$z(k) = \frac{1}{\sqrt{N_C}} \sum_{k=0}^{N_C-1} \hat{y}_r(k)e^{-j2\pi kn/N_C}, \tag{1.10}$$

After some algebraic manipulations and by using the orthogonality property we have

$$z(k) = x(k)\sum_{i=1}^{L_P} \beta_i(k) + z(k) = g_k x(k) + n(k), \tag{1.11}$$

where $n(k)$ is the noise level at subcarrier k. The received subsymbols are scaled versions of the transmitted ones and the complex parameter g_k captures the effects of the multi-path channel at subcarrier k.

In order to retrieve the transmitted symbol, the receiver needs channel state information (CSI) in terms of frequency-domain channel transfer function values at subcarrier frequencies. Channel estimation can be performed with pilot symbols that are interspersed with transmitted data symbols. A pilot symbol e consists of known subsymbols $e_k(k = 0, \ldots, N_C - 1)$. The received pilot subsymbol at subcarrier n after DFT is $y_k = e_k g_k + n_k$. Then, the minimum-mean-squared-error (MMSE) estimate of the complex gain g_k is obtained as

$$\hat{g}_k = \frac{y_k}{e_k} = g_k + \frac{z_k}{e_k}, \quad k = 0, \ldots, N_C - 1. \tag{1.12}$$

The estimates $\hat{g}_k$ are used for frequency-domain equalization (FEQ), namely compensation for the phase and amplitude of received subsymbols prior to detection. Given

that the transmitter communicates the utilized modulation level of each subcarrier at the receiver, the ML (maximum likelihood) detector decides about the transmitted subsymbol based on $z(k)/\hat{g}_k(k = 0, \ldots, N_C - 1)$. Here we assume that perfect CSI is available at the transmitter and the receiver. For slowly time-varying channels, the transmitter can obtain reliable CSI with feedback from the receiver. Assuming that all transmitted subsymbols are normalized to unit power, the signal-to-noise ratio (SNR) at the receiver at the kth subcarrier is $SNR_k = G_k/\sigma^2$ where σ^2 is the noise variance and $G_k = |g_k|^2$ is the link gain of subcarrier k. When the transmitter uses power level P_k for subcarrier k, a term $\sqrt{P_k}$ multiplies subcarrier k in (1.5). Then, $SNR_k = G_k P_k/\sigma^2$.

1.5.2 Advantages of OFDM System

The subcarrier spacing of $1/T_0$ in OFDM results in much higher spectral efficiency than that of simple frequency division multiplex. OFDM transmission increases the effective symbol duration and reduces the effective symbol transmission rate, since information is essentially transmitted over narrow-band subcarriers. Thus, it provides high immunity to ISI and delay spread. In addition, since the frequency selective broadband channel is divided into a set of frequency non-selective subcarriers, the equalization procedure at the receiver simplifis to a scalar multiplication for each subcarrier. Furthermore, OFDM provides additional exibility in adapting transmission to varying link conditions, by allowing adaptation for each subsymbol in a subcarrier [29].

1.6 Controllable Parameters for Physical Layer Adaptation

Physical layer adaptation techniques are employed on a link basis in order to achieve high data rate (in bits/s) while maintaining an acceptable BER at the receiver irrespec-

tive of link quality. Often the controllable parameters in this work are coding rate, modulation level and symbol rate.

1.6.1 Coding Rate

Data from higher layers arrive at the input of the block encoder in the form of a bit stream. The block encoder encodes each k-bit data block into a n-bit code word, by appending $(n-k)$ redundant bits, which are used by the receiver decoder for error detection and/or correction. The block code is then referred to as a (n,k) code and the code rate is k/n. A particular class of block codes which are considered in this work is Reed-Solomon (RS) forward error correction (FEC) codes. An (n,k) RS FEC code can correct up to $(n-k)/2$ errors.

Depending on the quality of the wireless link, adaptive error protection can be applied to transmitted data by varying the code rate [30], [31]. The encoder has a set of c available code rates, $\{\frac{k_i}{c}\}_{i=1}^{c}$, which can be generated for example with the aid of a punctured convolutional code [32]. In good channel conditions, few redundant bits are appended to the data block in order to provide the desired level of protection, since transmission errors are not very likely to occur. Hence, a highrate code can be used. On the other hand, when channel conditions deteriorate, lower-rate codes with more redundant bits are required, since errors occur more often.

1.6.2 Modulation Level

The encoded bit stream from the output of the encoder enters the modulator, which maps digital bits into analog waveforms. Each block of $b = log_2 M$ bits from the coded bit stream constitutes a symbol and each symbol is mapped to one of M waveforms. This waveform modulates the carrier and is transmitted over the channel. We fix our

attention to quadrature amplitude modulation (QAM) schemes, for which the amplitude or phase of the carrier changes, but the frequency does not. Each waveform is associated with a signal point in the two-dimensional plane and the ensemble of signal points is the modulation constellation. We are not concerned with the mapping of the b bits to signal points, which is assumed to be accomplished with Gray encoding.

The number of transmitted bits per symbol can be adjusted with adaptive modulation techniques [33]. The modulator has a set $\mathcal{M}$ of L_0 available modulation levels in terms of number of bits per symbol, $\{b_i\}_{i=1}^{L_0}$. Thus, 2-QAM, 4-QAM, 8-QAM and 16-QAM have modulation levels of 1,2,3 and 4 bits/symbol, respectively. In the presence of time-varying link quality, the objective of modulation adaptation is to increase transmission rate and maintain an acceptable BER at the user receiver. High modulation levels provide high transmission rates, but they are more susceptible to interference and noise, since signal points are densely packed in the constellation and hence the probability of error at the receiver is high. Such modulation levels should be used only in good quality channels. On the other hand, low modulation levels provide lower transmission rates but can sustain more interference and noise.

The BER at the output of the detector when a M-QAM modulation level is used (where $M = 2^{b_i}$ for some $b_i \in \mathcal{M}$) is expressed as a function of SINR by the approximation $BER_i \approx 0.2e^{-1.5\frac{SINR}{M-1}}$ [34] . For a maximum allowable BER of ε, the SINR at the output of the detector should satisfy

$$SINR \geq \frac{-ln(5\varepsilon)}{1.5}(M-1). \tag{1.13}$$

Hence, we can map each modulation level $b_i \in \mathcal{M}$ to a minimum SINR value (SINR threshold) γ_i (in dB) through a one-to-one increasing function f, such that $\gamma_i = f(b_i)$ equals the right-hand side of (1.13). Clearly, higher modulation levels should be used only in cases of high SINR in order to guarantee an acceptable BER, while lower modulation levels can achieve the same BER at lower SINRs but with lower transmission

rate.

1.6.3 Symbol Rate

In addition to modulation level, the transmitter can adjust the symbol rate by varying the duration of transmitted symbols as a means of combating ISI [35]. In a link with time-varying multi-path characteristics, the objective of symbol rate control is to increase transmission rate subject to the requirement that delay spread should not exceed a certain fraction of the symbol duration. A high symbol rate with associated small symbol duration yields high transmission rate, but it is more vulnerable to ISI and delay spread. Hence, it should be used when delay spread is small enough and does not constitute a significant fraction of the symbol duration. On the other hand, a low symbol rate with large symbol duration is less vulnerable to delay spread and can be employed even in cases of larger delay spread.

1.7 Motivation of This Research

In the absence of cochannel interference, the use of high order M-QAM ($M > 64$) is restricted by time-varying background noise in the channel. At the same time, wireless channel is subject to severe propagation impairment which results in a serious degradation in the link carrier-to-noise ratio (CNR) and even the efficient techniques of compensation are used, the high order M-QAM cannot achieve the optimal performance. For example, Morinaga et. al. have claimed that 4-QAM (QPSK) is the optimum multilevel modulation for high capacity cellular systems and the option of the higher modulation levels will just reduce the system spectral efficiency [36]. In addition, with the increase of the constellation of QAM, that is, parameter M, the complexity of demodulation and implementation of the demodulator increase rapidly. When the

density of the constellation points increases, the sensitivity to interference also does, the noise which comes from the channel or phase deteriorates the performance of system. To alleviate such influence, more complicated methods and exorbitant devices must be adopted [37], even so, the high order M-QAM is restricted to be adopted in some special applications, for example, 256-QAM and 1024-QAM are often used in wired system such as cable systems or hybrid fiber-coax (HFC) system [38]. On the other hand, Eq. (1.13) often chooses $M = 2^k$ and k is integer. If paramter M could be adopted any positive real number, there would be more useful for the physical layer adaptation.

One novel flexible multicarrier (high compaction multicarrier modulation: HC-MCM) system has been designed. HC-MCM can attain higher spectral efficiency than that of the original OFDM by using the partial time-domain OFDM signal to transmit the equal data of the OFDM signal. HC-MCM system has a high affinity with exiting OFDM system, and can flexibly control the transmission rate and quality of communication. More important, only utilizing BPSK or QPSK modulation, the HC-MCM can achieve the transmission rate of high order M-QAM OFDM, even the M could be any positive real number. It can also flexibly adjust the length of frame according to the radio channel condition. So it is useful to further improve the performance of such a flexible multicarrier system.

Hidden-terminal or exposed-terminal problem is one of the main disadvantages for the ad-hoc networks, which also limits the capacity of the ad-hoc networks. Such a problem is also the bottleneck for the majority of MAC protocal designs of ad-hoc networks. Thus, there have been many attempts to recover collided packets, such as by making use of the capture effect and multiuser detection (MUD). With the capture effect, only the packet that has the highest signal-to-interference-plus-noise ratio (SINR) can be recovered from the collisions and other corrupted packets are discarded. The receiver can utilize the technique of multipacket reception (MPR) by which multiple

packets can be retrieved from the collision. However, such a technique requires all packets to adopt different power levels to ensure that the different SINRs are above the designed thresholds. In situation of WLAN, which also can be treated as a weak near-far situation, nodes transmit packets in an uncoordinated fashion, so it is difficult to realize the above requirement. MUD is a technique by which we can recover all packets at the expense of complexity of the receiver. Since MUD requires user information (signatures), it is often utilized in code division multiple access (CDMA) systems. But CDMA systems often adopt high chip rate to obtain the high transmission rate, therefore, it is difficult to achieve the synchronization between the nodes to utilize the MUD. We will give a novel method utilizing above flexible multicarrier system to solve this problem in this dissertation. Compared with other methods, the most important point is that our proposed method can recover both packets from the collision, which can be utilized in ad-hoc networks based on OFDM. On the other hand, in the near-far situation, our method can achieve better recovery performance in the weak near-far condition which is more realistic in the ad-hoc networks. Therefore, the proposed method can dramatically improve the performance of ad-hoc networks that are based on wireless LAN using OFDM techniques.

One of the main implementation disadvantages of the OFDM systems at the transmitter is the high peak-to-average power ratio (PAPR) of the transmitted signals. When the signals of all subcarriers are added constructively, the peak power can be the number of subcarriers times the average power. The power consumption of a power amplifier depends largely on the peak power than the average power, thus, large peaks leads to lower power efficiency. This necessitates a higher power amplifier in the transmitter even in a lower power mobile communication system, which obviously increases power consumption and the cost of the devices. Since flexible multicarrier system can choose the partial time-domain OFDM signals to send the data, it can select the signal during

some specific durations, which can achieve the promising PAPR, to transmit the equal bits of data. So in this dissertation, based on the flexible multicarrier system, we also propose a novel PAPR reduction technique named as partial signal transmission (PST) for multicarrier systems. PST can dramatically decrease the PAPR of the OFDM signal and achieve the promising BER performance.

1.8 Outline and Organizations of The Dissertation

The underlying philosophy in all problems that are considered in this dissertation is a synergy between the physical and the MAC layer. The contributions of this dissertation, which will be presented in detail in following chapters, are outlined in this section.

It has been shown, in some outstanding papers, that adaptive sizing of the MAC layer frame in the presence of varying channel noise indeed has a large impact on the nodes seen 'goodput' (to distinguish with 'throughput'). In addition, the adaptive frame length control can be exploited to improve the energy efficiency for a desired level of goodput. But those paper assume the modulation is fixed and only changes MTU (maximum transmission unit) according to the wireless channel conditions to tradeoff goodput, range, and energy efficiency of wireless system. However, with the development of modulation techniques such as SDR (software-defined radio), we will explain that adaptive modulation can cause different link goodput, range and energy efficiency. In such a case, the nodes of ad-hoc network can realize the tradeoff between goodput, range and energy efficiency with adaptive modulation. So in Chapter 2, We will give the results which show that there is much to be gained from variable frame length, adaptive modulation in terms of goodput, range and energy consumption for wireless networks. We obtain three rules of design for this tradeoff for wireless networks.

Since physical layer adaptation using adaptive M-QAM is not robust to obtain the appropriate M and high order M-QAM is restricted to be adopted in wired or optical networks, high order M-QAM ($M > 64$) also cannot be used for WLAN-based ad-hoc networks. But HC-MCM system can attain higher BWE than that of the OFDM system. such a flexible multicarrier system can flexibly control the transmission rate and the communication quality. More importantly, only utilizing BPSK or QPSK modulation, it can adaptively achieve the transmission rate of high M-QAM OFDM. So in Chapter 3, based on the parallel combinatory OFDM (PC-OFDM) and HC-MCM, we propose a novel adaptive modulation, that is, parallel combinatory / high compaction multicarrier modulation (PC/HC-MCM). The PC/HC-MCM can achieve any transmission rate of M-QAM, even M is not integer. PC/HC-MCM also can realize the adaptive length of frame which can be utilized to physical layer adaptation with the adaptive length of packets. Two types of PC/HC-MCM systems, which are named as modulated PC/HC-MCM system and PC/HC-MCM system, are designed by this modulation. The modulated PC/HC-MCM system can achieve better BER performance than that of HC-MCM system with the equal BWE by employing appropriate parallel combinatory codes. The PC/HC-MCM system can obtain excellent peak-to-average power ratio (PAPR) characteristics by selecting the optimal constellations for its subcarriers. On the other hand, since PC/HC-MCM can divide one PC-OFDM symbol duration into multiple time-slots, the advantages of frequency hopping (FH) can be applied in PC/HC-MCM systems. Therefore, we also combine the PC/HC-MCM and frequency hopping multiple access (FHMA) to propose a new multiple access (MA) system. This MA system can synchronously transmit multiple users' data within one symbol duration of PC-OFDM.

In Chapter 4, based on the property of the flexible multicarrier system, we will focus our attentions on the collision-recovery issues for ad-hoc network using OFDM-

based WLAN. Since most collisions occur when one user starts to build a connection or sends a response with a short packet, such as RTS (request-to-send), CTS (clear-to-send) or ACK (acknowledgement), to one node while a principal user is transmitting a long packet including data to an identical destination. Therefore, the collided part is not as long as the principal long packet. For example, the long packet of IEEE 802.11a (64 subcarriers) can convey 8184 [bits] (payloads) without preamble and control bits, but the length of ACK, RTS or CTS is no longer than 300 [bits] which can be carried by only six BPSK-modulated OFDM signals or three QPSK-modulated OFDM signals. Undoubtedly, for the long packet, if such collided parts can be recovered, the system performance, such as throughput and delay, will be dramatically improved. On the other hand, it will also benefit the protocol design of ad-hoc networks because short packets often contain much important information, such as positions and power levels. We will propose a method of collision recovery for ad-hoc networks. We will present the property that, for the OFDM packets, the modulated message data can be demodulated using the partial time-domain OFDM signal. Therefore, the partial signal can be adopted to reconstruct the whole OFDM signal with estimated channel information. Utilizing this advantageous property, an effective method of collision recovery can be realized. The proposed method can be developed to solve the problems of hidden terminals and exposed terminals in ad-hoc networks.

Based on adaptive properties of the flexible multicarrier system, OFDM system can choose the partial time-domain OFDM signals to send the data, therefore, OFDM system can select the signal during some specific durations, which can achieve the promising PAPR, to transmit the equal bits of data. So in Chapter 5, we will propose a novel PAPR reduction technique named as partial signal transmission (PST) for ad-hoc network using OFDM-based WLAN. PST can dramatically decrease the PAPR of the OFDM signal and achieve the promising BER performance. Therefore, those technologies will

decrease the devices cost of ad-hoc network.

We will conclude this dissertation and give some discussions on the future research in Chapter 6.

Chapter 2

Adaptive Modulation and Frame Length Using M-QAM Modulation

2.1 Introduction

Wireless ad-hoc networks are characterized by rapidly time-variant channel conditions and battery energy limitations at the wireless terminals. Therefore, control technologies of static link that make sense in comparatively well behaved wired links cannot necessarily apply to wireless radio channel. New techniques are required to provide the robust and energy efficient operation even in the presence of orders of magnitude variations in bit-error rate (BER) and other radio channel conditions. The successful transmission of one node to other nodes depends on two independent processes:

(1) the time-variant radio channel must ensure error-free transmission of packets between nodes;

(2) the packets must avoid collision with other nodes when the system chooses multiple access protocols as the distributed way.

Recent research has advocated many adaptive control techniques for process (1), which include the error control [39], channel state dependent protocols [40], [41] and variable spreading gain [42]. Especially P. Lettieri and M.B. Srivastava explored one

adaptive technique using dynamic sizing of the MAC layer frame [43]. It shows that adaptive sizing of the MAC layer frame in the presence of varying channel noise indeed has a large impact on the nodes seen 'goodput' (to distinguish with 'throughput'). In addition, the adaptive frame length control can be exploited to improve the energy efficiency for a desired level of goodput. But they assume the modulation is fixed and only changes the length of MTU (maximum transmission unit) according to the wireless channel conditions to tradeoff goodput, range, and energy efficiency of wireless system. However, with the development of modulation techniques such as SDR (software-defined radio), we will explain that the flexible modulation can cause different link goodput, range and energy efficiency. In such a case, the ad-hoc nodes can also realize the tradeoff between goodput, range and energy efficiency by adaptive modulation. On the other hand, many papers expatiate on the relation of transmission ranges or powers with the throughputs of ad-hoc network such as [44]-[47], but M. Krunz et.al. have pointed out that variable rate support is an optimization, which can increase spectral efficiency, by transmission power control or adapting the adaptive length of packets and coding schemes, and such issues have not been fully considered till now [48].

So in this Chapter, we present the results which shows that there is much to be gained from variable frame length, flexible modulation in terms of goodput, range and energy consumption for the ad-hoc nodes. We obtain three rules of design for the tradeoff of goodput range and energy consumption for wireless networks [51], [52]. Then we propose the disadvantages of adaptive modulation and frame length using M-QAM modulation and show the importantance for the flexible multicarrier system.

2.2 Adaptive Modulation and Length of Frame for Link Goodput, Range and Power Consumption

Radio channel is time-variant one and the channel variations are inherently uncontrollable. Therefore, many techniques of modulation and coding are developed in order to successfully transmit a packet through wireless channel. Fig. 2.1 gives the BER performance of system when it uses M-QAM with rectangular constellations, a Gaussian channel, and matched filter reception. Each parameter M can obtain the identical BER by choosing different SNR(signal-to-noise ratio) Eb/No [46]. It can be seen from Fig. 2.1, if the system needs the BER $\leq 10^{-4}$, the corresponding SNR is about 19.40 [dB] for 256-QAM, 14.7 [dB] for 64-QAM, 10.5 [dB] for 16-QAM and 6.8 [dB] for QPSK, respectively. However different parameter M will cause different link throughput (or goodput), range and energy efficiency which we will elaborate the results in following subsections. The way we utilize is similar to that of P. Lettieri and M.B. Srivastava [43], but in [43], they only adopt QPSK modulation . We develop it to M-QAM modulation with different parameter M.

We analyse a link with following parameters:

(1) The radio uses M-ary QAM modulations (here we use M-QAM with M=4, 16, 64, 256 and incoherent symbol detection);

(2) The channel symbol rate is $1M$ symbols/second;

(3) MAC uses a CRC field: "bad" frames are reliably detected and dropped.

For analysis, we assume a free-space path loss model, with unity gain antennas, no system loss. Note that the results are quite general despite these assumptions. The analysis is elaborated along three dimensions, presented in the next three subsections. In all cases, we consider some metrics of the wireless system with respect to variations in frame length and different modulations. In the first case, we present the throughput

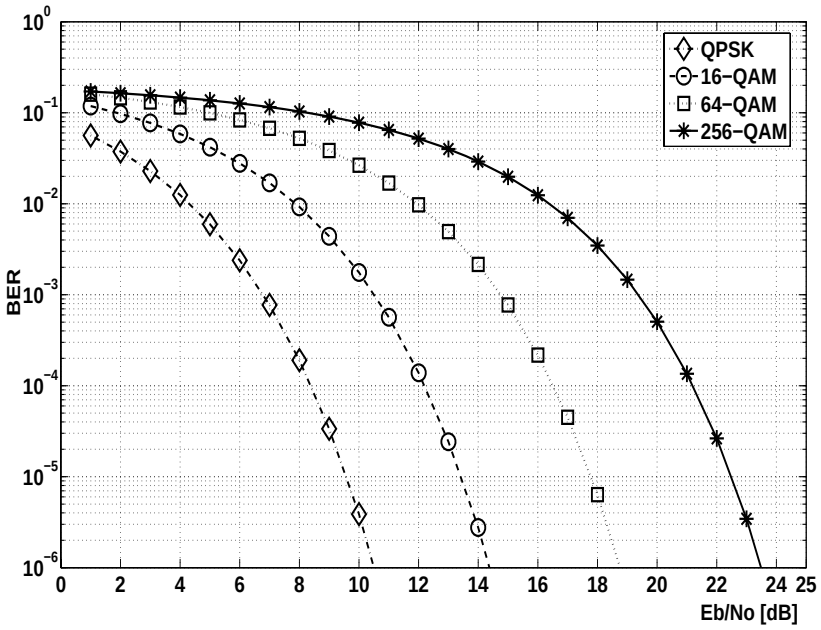

Fig. 2.1 BER characteristics for several kinds of QAM constellations.

(goodput) of system, in the second case, we will extrapolate effective transmission range with different modulations and frame length. Finally, we show the transmissimg power consumption, as important metric in the design of portable, battery operated devices with those variables.

2.2.1 Frame Length Versus Node Throughput

Firstly, we consider the system's throughput and hereafter referred to as goodput, as a function of frame length over varying BER. The goodput refers to the bandwidth the user actually receives after all overheads are calculated, including such as the MAC and PHY overheads. Beyond these costs, however, the goodput will be reduced by the occurrence of frames lost to bit error, even one bit error inside a frame will result in the loss of that frame, as the CRC will not pass. Each lost frame directly results in wasted bandwidth, as in the time spent sending that frame achieved no forward progress. This loss might also result in the additional signaling overhead of an ARQ protocol.

In order to examine the behavior of the system, let us first specify various quantities of interest [43]. We assume

(1) L_D = length of node data;

(2) L_O = length of PHY overhead = 52.5 bytes;

(3) L_H = length of MAC and IP header overhead = 40 bytes;

(4) MTU = L_D+20bytes;

(5) R_C = raw bit rate of radio channel = 2 Mbps (QPSK), 4Mbps (16-QAM), 8Mbps (64-QAM), 10Mbps (256-QAM);

(6) BER = probability of channel bit error, a function of transmitter power and path loss;

(7) G= goodput (i.e. real user level good throughput).

With these quantities in hand, we can specify the normalized goodput as:

$$\frac{G}{R_C}=\frac{L_D(1-BER)^{(L_D+L_H)}}{L_D+L_O+L_H}=\frac{(1-BER)^{(L_D+L_H)}}{1+(L_H+L_O)/L_D}. \tag{2.1}$$

The equation (2.1) gives a value for the goodput normalized against raw data in terms of frame length and BER. With the overheads taken constant, we vary the size $L(=L_D+L_O+L_H)$ of the user data. The theoretical value of Eq.(2.1) for a variety of BER is shown in Fig. 2.2. The main observation to make from this figure is that as the channel conditions deteriorate, it would be helpful to use a smaller MTU instead of the naive selection of the maximum allowed MTU of constant length. A properly chosen MTU can even improve the goodput on an apparently dead link giving zero goodput. For instance, if the radio channel BER is equal to 5×10^{-4} and the length of frames is longer than 950 bytes, the goodput of system will be zero. But the goodput will be improved to maximum with 0.3 if the length of frame is shortened to the 150 bytes. On the other hand, Figure 2.1 shows that the identical Eb/No for $M-$QAM modulation with different parameter M can cause different BER, different BER will result in different

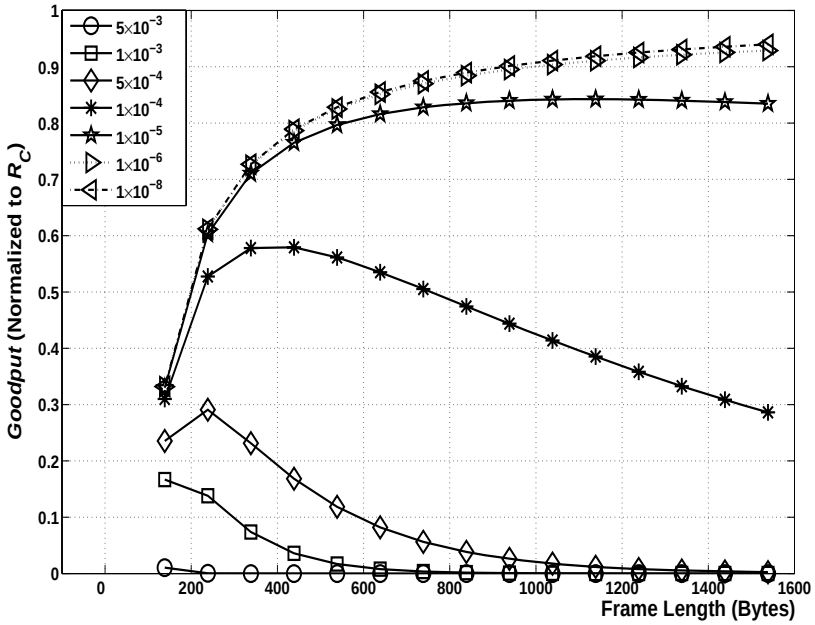

Fig. 2.2 Frame length versus the Goodput for different BER.

goodput which can be seen from Fig. 2.2. For the identical Eb/No, the BER of QPSK is the smallest of all four modulations and 256-QAM can obtain maximal BER than QPSK, 16-QAM and 64-QAM. However, 256-QAM can obtain higher R_C than that of QPSK.

With the above analyses, we can get Rule 1:

Rule 1: when the power consumption is not the major problem for one node, it is more beneficial for the node to adopt modulations with higher number of constellations of QAM, longer length of frame to transmit the packets for obtaining high goodput and R_C. But when the energy is limited, the node can maintain high goodput by decreasing number of constellations of QAM so that the system can maintain the constant BER. For example, using 64-QAM, 16-QAM and then QPSK with longer length of frame (but shorter length of frame when BER is large($> 10^{-4}$)) to replace 256-QAM.

2.2.2 Frame Length versus Transmission Range

Another metric to consider when the frame length is varied in the presence of different modulation is the transmission range. Range of transmitter-receiver (Tr-Re) distance also means the connectivity of the wireless network. We analyze it in two ways. First, we analyze goodput vs. the normalized distance for different length of frames using different modulations as shown in Fig. 2.3. To achieve this, we note that for M-QAM, the bit error rate is [46].

$$BER \approx \frac{2(1-L^{-1})}{log_2 L} Q[\sqrt{(\frac{6log_2 L}{L^2-1})\frac{E_b}{N_o}}], \tag{2.2}$$

where $Q(x) = \frac{1}{\sqrt{2\pi}} \int_x^\infty exp(-\frac{u^2}{2})du$ and L represents the number of amplitude levels in one dimension (L=2 for QPSK, L=4 for 16-QAM, L=6 for 64-QAM and L=10 for 256-QAM).

If we further assume a free space path loss model with path loss exponent equal to 2, this simplifies to:

$$BER \approx \frac{2(1-L^{-1})}{log_2 L} Q[\sqrt{(\frac{6log_2 L}{L^2-1})}\frac{1}{d}], \tag{2.3}$$

where $d = \frac{d_r}{\sqrt{(E_b/N_o)}d_0}$ is the transmitter-receiver separation in some normalized units of distance. E_b/N_o is the value measured at a receiving point which is distinct from transmitting point with d_0 [m] and d_r [m]is the real distance. With the relation between distance and BER, and substituting (2.2) into the (2.1), we can obtain the goodput as a function of distance at a particular MTU in the presence of different modulations.

Fig. 2.3 shows the impact of three types of frame length on the Tr-Re distance with different goodput and the modulations are QPSK, 16-QAM, 64-QAM and 256-QAM, respectively. At moderate distances the large MTU is the certainly desirable since goodput is higher. Using QPSK as an example, the goodput degrades rapidly with the Tx-Rx distance increasing from 0.4 to 0.6. Over a relatively short distance, goodput goes from maximum to nothing. But if the MTU is variable however, an

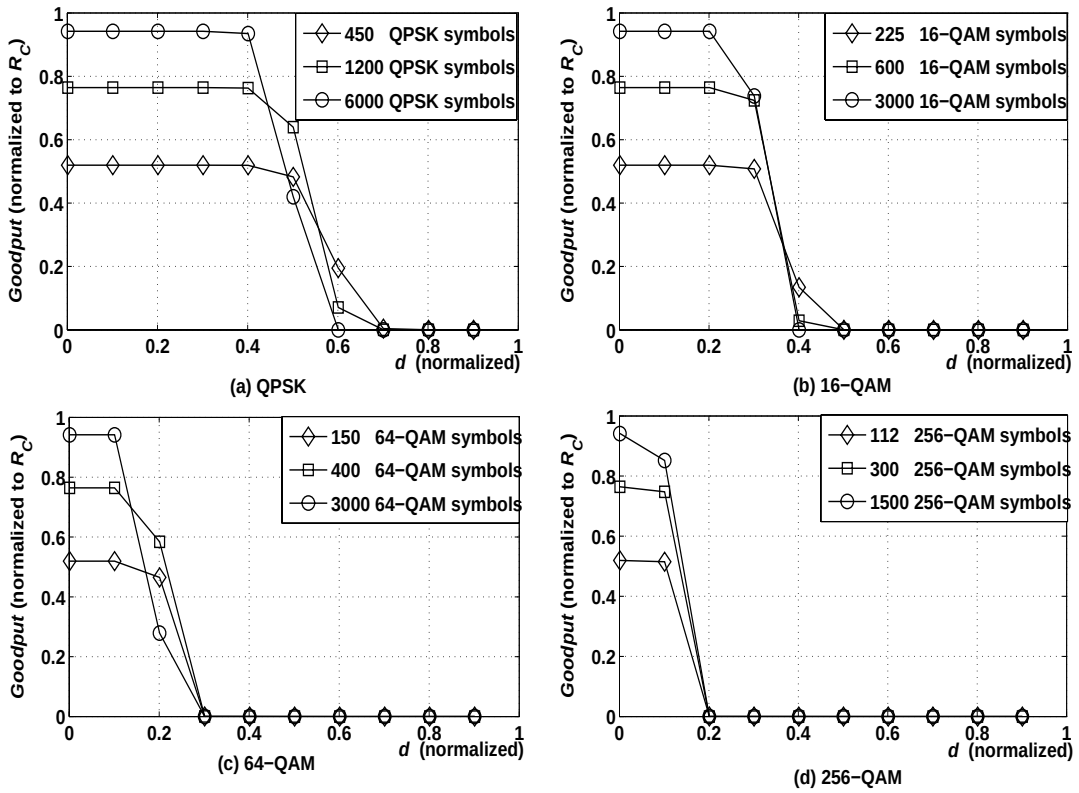

Fig. 2.3 Goodput versus normalized transmission range d with varying frame length for different modulation.

amount of extension of the range is possible over which meaningful data can be sent. But when the system increases the number of rectangular constellations, that is, using 16-QAM, 64-QAM, 256-QAM to increase the R_C, the Tr-Re distance will decrease when the system adopts the same length of frame. On the other hand, in effect, adaptively changing the length of frame can allow one to smooth the degradation in goodput of a wireless link as distance is increased, but the effect decreases by increasing the parameter M of M-QAM.

Alternatively, we plot range vs. MTU for various values of normalized goodput in the presence of different modulation with the identical energy as shown in Fig. 2.4. It is another way of viewing the same equation. At first, we choose a constant goodput that the specific application can accept, then, we set various MTU sizes to obtain the

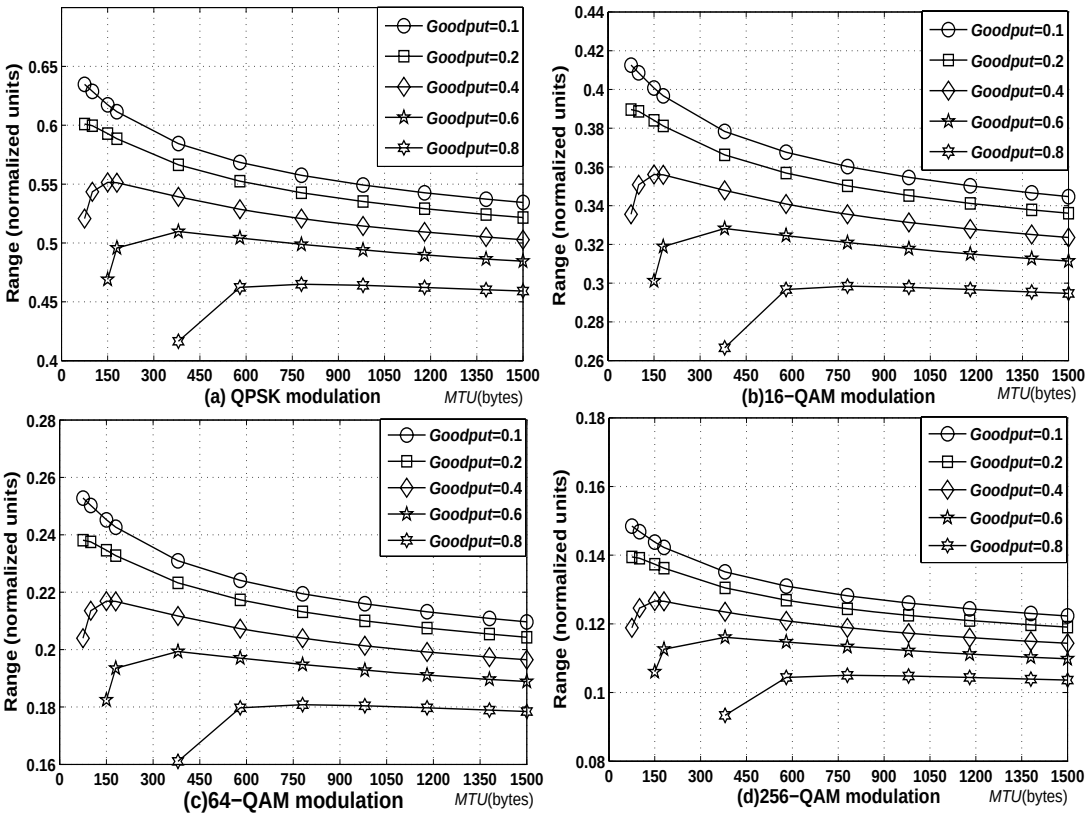

Fig. 2.4 Frame length versus normalized transmission range d with varying Goodput for different modulation.

range using four types of modulations which can be achieved.

What these plots shows is that for low levels of desired goodput, a substantial extension in range is possible by reducing MTU to a certain value. If the goodput could be set to 0.1, all four modulations can improve up to 20% in range using minimum length of frame to instead of maximum one. But the improvement of range decreases when the goodput increases. On the other hand, by increasing the number of constellations of the modulation, The Tr-Re distance will decrease when the system adopts the same goodput and energy.

With the above analyses, we can get Rule 2:

Rule 2: when the power consumption is not the major problem for one node, it is more beneficial for the node to adopt the modulations using higher number of

constellations of QAM, longer length of frame to transmit the packets for obtaining high goodput and R_C. But with the same energy, the higher number of constellations of QAM is, the less the range is. So when the energy is limited, the node can maintain high range by decreasing number of constellations of QAM. For example, using 64-QAM, 16-QAM and then QPSK and shorter length of frame (but longer length of frame when goodput is high(>0.8)) to replace 256-QAM.

2.2.3 Frame Length Versus Power Consumption

Another relationship can be found for battery power and frame sizes in the presence of different modulations over various allowable goodput. It can be obtained by analysing the energy per bit vs. frame length which has been shown in Fig. 2.5.

Fig. 2.5 shows that there is a substantial improvement in energy consumption for a given level of goodput, especially for the high goodput. For all four modulation, the power consumption increases with increasing the number of constellations of QAM. 256-QAM needs much more power than that of QPSK at the identical level of goodput. On the other hand, it is more benefitful for the system to use longer packet when the goodput is more than 0.8, in such a case, shorter packet which is smaller than 400 bytes will consume more power than that of 800 bytes. More power will be saved with increasing the number of constellation of QAM. For QPSK modulation, 1.3 units power will be saved but 26 units for the 256-QAM modulation.

With the above analyses, we can get Rule 3:

Rule 3: when the power consumption is not the major problem for one node, it is more beneficial for the node to adopt modulations with higher number of constellations of QAM, moderate length of frame to transmit the packets for obtaining high goodput and R_C. But the larger the number of constellation of QAM is, the more power consumption is required. So when the energy is limited, the node can save power by

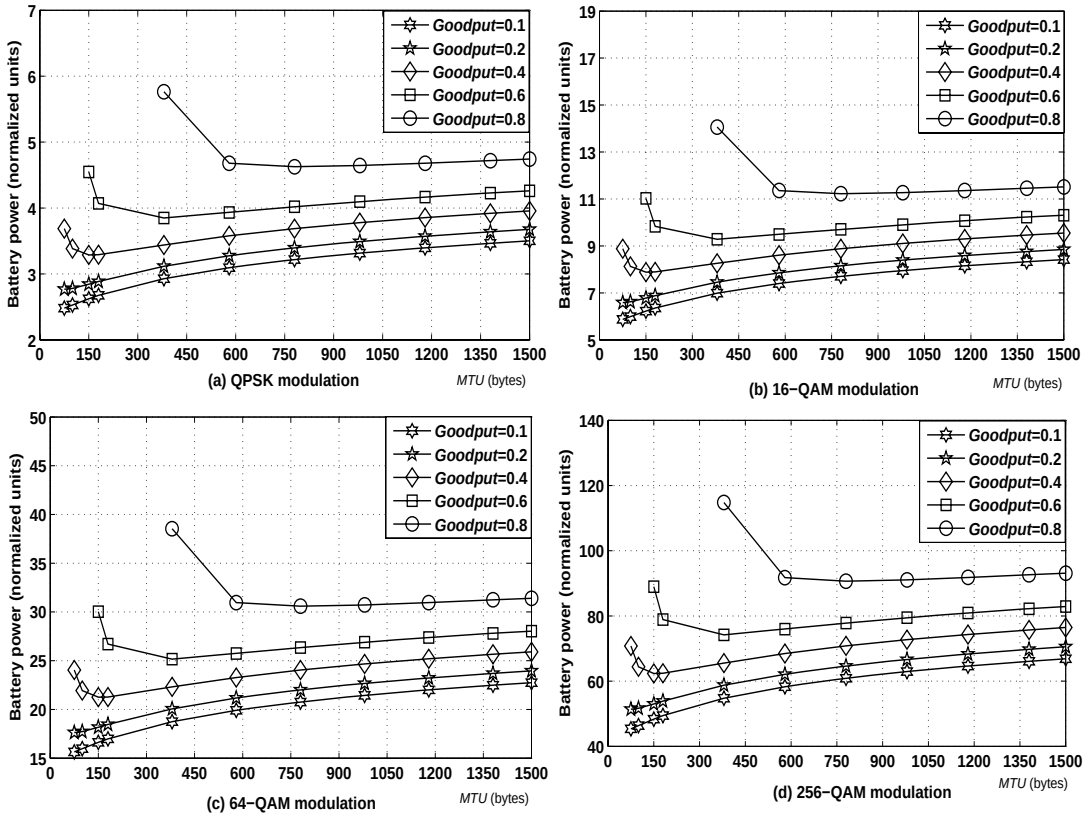

Fig. 2.5 Frame length versus normalized power consumption with varying Goodput for different modulation.

decreasing number of constellations of QAM. For example, using 64-QAM, 16-QAM and then QPSK with moderate length of frame (but shorter length of frame when goodput is small($<$0.2)) to replace 256-QAM.

2.3 Disadvantages of High Order M-QAM

Spectral efficiency (SE), measured in [bits/sec/Hz], is the primary concern in the design of future communication systems. One efficient technique to increase the spectral efficiency is to utilize multilevel modulation, such as M-QAM, which increases the spectral efficiency of link by sending multiple bits per symbol, the spectral efficiency can be dramatically improved with high-order M-QAM [38]. For example, the use

of 256-QAM has become more prevalent in cable system, as both a video and data modulation and it offers almost the highest spectral efficiency available today among digital cable signals [53].

However, with the increase of the constellation of QAM, that is, parameter M, the complexity of demodulation and implementation of the demodulator increase rapidly. When the density of the constellation points increases, the sensitivity to interference also does [54], the noise which comes from the channel or phase deteriorates the performance of system. To alleviate such influence, more complicated methods and exorbitant devices must be adopted [37], even so, the high order M-QAM is restricted to be adopted in some special applications. 256-QAM and 1024-QAM are often used in wired system such as cable systems or hybrid fiber-coax (HFC) system [38].

On the other hand, the radio spectrum available for wireless data services and systems is extremely scarce and the radio channel is viewed as band-limited one [46]. Wireless channel is subject to severe propagation impairment which results in a serious degradation in the link carrier-to-noise ratio (CNR) and even the efficient techniques of compensation are used, the high order QAM cannot achieve the optimal performance. For example, Morinaga et. al. have claimed that 4-QAM (QPSK) is the optimum multilevel modulation for high capacity cellular systems and the option of the higher modulation levels will just reduce the system spectral efficiency [36]. Therefore, the OFDM of high order M-QAM will also be limited to the special applications with the above reason.

In addition, the high order M-QAM often chooses $M = 2^k$ and k is an integer. So physical layer adaptation using adaptive M-QAM is not robust to obtain the appropriate M. According to the analysis of above section, if the system can adopt random value of paramter M, particularly the M could be plus real number, there will be more useful for the physical layer adaptation, that is, the tradeoff for ad-hoc network between the

different reqirments of link goodput, range and energy efficiency can be controled in a more flexible way.

Moreover, for OFDM systems, plural subcarriers are transmitted with orthogonal frequency spacing. Usually, the frequency spacing Δf_0 is chosen as the reciprocal of symbol duration T_0. In this case, no interference of adjacent subcarriers appears even when M-PSK and/or M-QAM are used to modulate the subcarriers. When the subcarriers are modulated by BPSK and are coherently detected, the minimum frequency separation Δf_0 will be reduced to $1/2T_0$ [46]. One novel flexible multicarrier system (high compaction multi-carrier modulation: HC-MCM) has been designed which can attain higher spectral efficiency than that of the original OFDM. HC-MCM system has a high affinity with exiting OFDM system, and can flexibly control the transmission rate and quality of communication. More important, only utilizing BPSK or QPSK modulation, the HC-MCM can achieve the transmission rate of high order M-QAM OFDM, even the M could be plus real number. It can also flexibly adjust the length of frame according to the radio channel condition. In the following Chapers, we will develop this flexible multicarrier system to the ad-hoc networks.

Chapter 3

A Flexible High Compaction Multi-Carrier Modulation Using Parallel Combinatory Coding

3.1 Introduction

3.1.1 Related Work

For the OFDM systems, each subcarrier transmits data using orthogonal frequency spacing Δf_0. Usually, Δf_0 is chosen as the reciprocal of symbol duration T_0. Therefore, the normalized symbol duration (or modulation index) of the OFDM system is equal to one ($\Delta f_0 T_0 = 1$). Due to multipath fading and Doppler effect of wireless channel, standard OFDM systems often utilize a guard interval (GI) T_g to combat intersymbol interference (ISI), then the normalized symbol duration of the standard OFDM systems can be regarded as $\Delta f_0(T_0 + T_g) > 1$. According to Balian-Low theorem [55], [56], the OFDM systems must utilize entire duration ($\Delta f_0 T_0 \geq 1$) to keep orthogonality between subcarriers and to minimize the intercarrier interference (ICI), otherwise, if $\Delta f_0 T_0 < 1$, the ICI cannot be avoided.

On the other hand, in the OFDM, serial data stream is first converted to parallel and then parallel data are transmitted by subcarriers synchronously. Parallel transmission method including the OFDM can divide the high rate signal into sub-flows with lower rate, therefore, can mitigate the influence due to multipath. One of the advantages for the use of the parallel transmission is that the transmission with the parallel combinatory coding is available in addition to the parallel data transmission [58], [59]. The system selects some subcarriers and transmits the special signals according to the combinatory rule, for example, only zero amplitude point. In the receiver, the system recovers the additional bits by the position of the zero and nonzero amplitude subcarriers with the combinatory rule. The paper [60] has proposed such method to reduce the peak-to-average power ratio (PAPR) of OFDM system without reducing the bandwidth efficiency and without increasing the bit error probability. The system was named as parallel combinatory OFDM (PC-OFDM) systems.

The OFDM system achieves a high transmission rate using high order M-QAM constellation. However, according to Chapter 2, with increasing the size M of constellation of M-QAM, the implementation complexity of the demodulator increases. To alleviate such an influence, the complicated methods and exorbitant devices must be adopted. In addition, since wireless channel is subject to severe propagation impairment which results in a serious degradation in the link carrier-to-noise ratio (CNR), even the efficient techniques of compensation are used, high order M-QAM OFDM cannot achieve the optimal performance.HC-MCM system can make the normalized symbol duration smaller than one [61]-[64]. Compared with T_0 or Δf_0 of OFDM system, HC-MCM system can transmit the equal bits of data using T ($< T_0$) or Δf ($< \Delta f_0$). Only utilizing BPSK or QPSK modulation, the HC-MCM can achieve the transmission rate of high order M-QAM OFDM, even the M could be plus real number. It can also flexibly adjust the length of frame according to the radio channel condition.

The BWE of HC-MCM can be increased by employing smaller ΔfT, but ICI, which deteriorates bit-error rate (BER) performance, will also be increased with smaller ΔfT. Therefore, we apply the parallel combinatory coding to the HC-MCM system to reduce the ICI since zero-amplitude subcarriers will reduce the ICI if $\Delta fT < 1$. On the other hand, by an appropriate choice of the parallel combinatory coding, we can achieve the identical BWE of the HC-MCM system using larger ΔfT.

3.1.2 Contributions and Outline of This Chapter

In this Chapter, based on parallel combinatory coding, we further improve the performance of flexible HC-MCM system and propose a novel modulation, that is, parallel combinatory/high compaction multi-carrier modulation (PC/HC-MCM). Two types of PC/HC-MCM systems, which are named as modulated PC/HC-MCM system and (unmodulated) PC/HC-MCM system, can be designed. The modulated PC/HC-MCM system can achieve better BER performance than that of HC-MCM system with the equal BWE by employing appropriate parallel combinatory coding. The PC/HC-MCM system can obtain better PAPR characteristics by selecting the suitable constellations for its subcarriers. Furthermore, since PC/HC-MCM can divide the PC-OFDM symbol duration into multiple time-slots, the advantages of frequency hopping (FH) can be applied in the PC/HC-MCM system. Therefore, we also combine the PC/HC-MCM and frequency hopping multiple access (FHMA) to propose a new multiple access (MA) system. This MA system can synchronously transmit multiple users' data within one symbol duration of PC-OFDM [57].

The remainder of this Chapter is organized as follows. The PC-OFDM and the PC/HC-MCM models are introduced in Sect. 3. 2. The BWE, BER performance and PAPR of both PC/HC-MCM systems are presented in Sect. 3. 3. We show the performance of multiple access for the downlink system when the system adopts the

PC/HC-MCM with frequency hopping in Sect. 3. 4. Conclusions are presented in Sect. 3. 5.

3.2 Parallel Combinatory/High Compaction Multi-Carrier Modulation Systems

3.2.1 Parallel Combinatory OFDM Systems

PC-OFDM [58]-[60] is based on expanding M-PSK signal constellation with one extra, zero-amplitude, point. From this larger signal constellation, containing $(M+1)^{N_C}$ (N_C is the number of subcarriers) different waveforms, a subset of waveforms with lower PAPR may be chosen. If chosen properly, compared with the original OFDM system, the system with new signal constellation can realize least bandwidth requirement and lower BER.

The PC-OFDM system can be viewed as two subsystems, that is, original symbol transmission implemented by nonzero modulated subcarriers and combinatory bits of information transmission decided by the position of nonzero and zero subcarriers. At first, the system sets the number of nonzero subcarriers, N_{PC}, and the number of zero subcarriers, $N_C - N_{PC}$, respectively. Therefore, PC-OFDM system is equivalent to the OFDM system when $N_C = N_{PC}$. Then N_{PC} nonzero subcarriers are modulated by M-ary PSK. Here we map m_{PC} [bits] into a subset of subcarriers and m_{PSK} [bits] into the phase of the selected subcarriers. For this case m_{PSK} [bits] can be represented by

$$m_{PSK} = N_{PC} \log_2 M. \tag{3.1}$$

Selecting N_{PC} subcarriers out of N_C subcarriers can be realized in $\binom{N_C}{N_{PC}}$ different ways, so the combinatory bits per PC-OFDM symbol, m_{PC} [bits], can be represented

by

$$m_{PC} = \left\lfloor \log_2 \binom{N_C}{N_{PC}} \right\rfloor, \tag{3.2}$$

where $\lfloor x \rfloor$ is the largest integer smaller than or equal to x.

Therefore, the number of bits per PC-OFDM symbol m_{tot} is

$$m_{tot} = m_{PSK} + m_{PC} = N_{PC} \log_2 M + \left\lfloor \log_2 \binom{N_C}{N_{PC}} \right\rfloor. \tag{3.3}$$

When $(N_C - N_{PC}) \log_2 M < \left\lfloor \log_2 \binom{N_C}{N_{PC}} \right\rfloor$, PC-OFDM will achieve higher bandwidth efficiency than the OFDM systems with N_C subcarriers of M-QAM constellation.

By the demodulation, the data that consist of m_{PSK} [bits] can be first recovered and then the m_{PC} bits can be obtained by the combinatory rule with the position of the N_C zero and non-zero subcarriers.

3.2.2 Parallel Combinatory/High Compaction Multi-Carrier Modulation (PC/HC-MCM)

Spectra of PC/HC-MCM signal

PC-OFDM system transmits subcarriers of symbol duration T_0[s] arranged with a minimum orthogonal frequency spacing $\Delta f_0 = 1/T_0$ [Hz] for M-PSK and M-QAM as shown in Fig. 3.1(a) (For (8, 4) PC-OFDM, only 4 subcarriers are transmitted in each symbol duration (SD), e.g. the solid lines for the first SD and dotted lines for the next SD). Therefore, the PC-OFDM system can be characterized as a system with a modulation index $\Delta f_0 T_0 = 1$. The modulation index $\Delta f_0 T_0$ can be interpreted as a normalized frequency spacing or normalized symbol duration. Therefore, high compaction multi-carrier modulation (HC-MCM [61], [62]) system can basically be characterized by modulation indices $\Delta f T < 1$. We utilize the HC-MCM and PC-OFDM to design the new modulation system called PC/HC-MCM. Fig. 3.1(b) illustrates the spectrum of a PC/HC-MCM signal for a modulation index $\Delta f T = 0.375$. In this case,

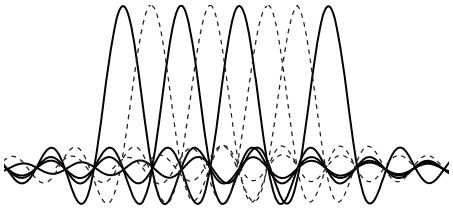

(a) Spectrum of a PC-OFDM signal.

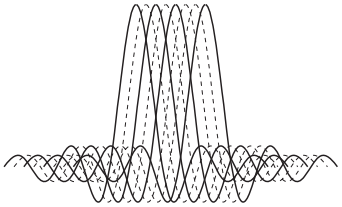

(b) Spectrum of a PC/HC-MCM signal (1).

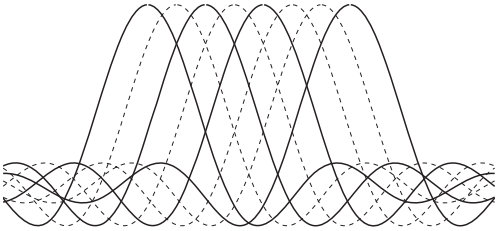

(c) Spectrum of a PC/HC-MCM signal (2).

Fig. 3.1 Spectra of a PC-OFDM and PC/HC-MCM ($\Delta fT = 0.375$).

the transmission rate is identical to that of the PC-OFDM illustrated in Fig. 3.1(a) ($T = T_0, \Delta f = 0.375\Delta f_0$), because the bandwidth of each individual subcarrier is identical to that of the PC-OFDM illustrated in Fig. 3.1(a), whereas the frequency spacing is smaller than that of the PC-OFDM. Thus, the PC/HC-MCM can achieve an identical transmission rate to the PC-OFDM with a narrower bandwidth.

Another form of the spectrum of a PC/HC-MCM signal is illustrated in Fig. 3.1(c). The modulation index for the spectrum of Fig. 3.1(c) is identical to that of Fig. 3.1(b). In this case, the frequency spacing is identical to that the PC-OFDM illustrated in Fig. 3.1(a) ($\Delta f = \Delta f_0, T = 0.375T_0$). However, a fast transmission rate can be

achieved, because the bandwidth of each individual subcarrier is larger than that of the PC-OFDM. Therefore, PC/HC-MCM (or HC-MCM) system can flexibly adjust its bandwidth efficiency or transmission rate and the length of frame using aprropriate parameter ΔfT.

Compared to the PC-OFDM, the PC/HC-MCM can change BWE by adopting different ΔfT. The PC/HC-MCM can be classified into two systems which are named as the modulated PC/HC-MCM system and the (unmodulated) PC/HC-MCM system. The modulated PC/HC-MCM system adopts m_{tot} [bits] in (3. 3) for each PC/HC-MCM waveform to transmit data. The PC/HC-MCM system only employs m_{PC} [bits] in (3. 2) for each PC/HC-MCM waveform to transmit data, that is, the transmitter chooses N_{PC} from N_C subcarriers to transmit $e^{j\theta_i}$ and $\theta_i (i = 1, \ldots, N_{PC})$ can be arbitrary values, but other (N_C-N_{PC}) subcarriers adopt zero-amplitude points to generate different PC/HC-MCM waveforms. Both systems can achieve the higher BWE than that of the M-QAM modulated OFDM system with N_C subcarriers if the systems choose appropriate combination of (N_C, N_{PC}) and ΔfT.

Modulated PC/HC-MCM system model

Figure 3.2 shows the transmitter and receiver for the modulated PC/HC-MCM system. Suppose m_{tot} [bits] (or m_{PC} [bits] for PC/HC-MCM system) can be transmitted in each symbol duration using the specific combination (N_C, N_{PC}) and modulation. It can be expressed with a vector whose elements are $x(k)(k = 0, \ldots, N_C - 1)$ including N_{PC} modulated subcarriers and $(N_C - N_{PC})$ zeros. In the transmitter of modulated PC/HC-MCM, K_0 zeros are tacked on to the subcarrier symbols $x(k)$ as padding at the input of the IDFT and $(N_C + K_0 - M_1)$ samples are removed at the IDFT output. The operation of padding zeros is for mitigating the aliasing in the frequency domain caused

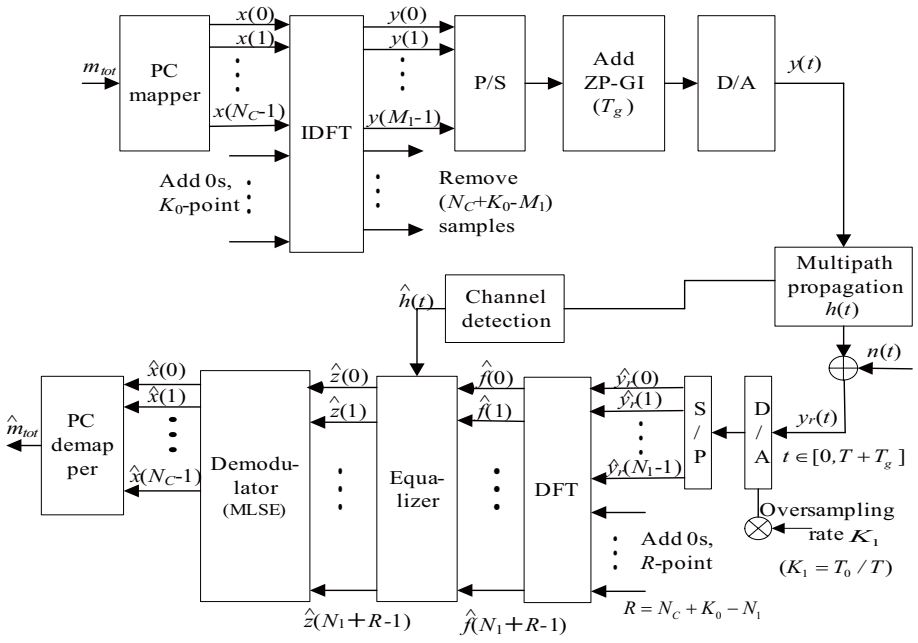

Fig. 3.2 Transmitter and receiver of the modulated PC/HC-MCM system.

by the IDFT and for interpolation for the samples in the time domain. When the entire samples produced by the inverse discrete Fourier transform (IDFT) are transmitted, the transmitter output $y(t)$ forms an ordinary PC-OFDM waveform. In the modulated PC/HC-MCM transmitter, only a portion of IDFT output samples is transmitted. This operation makes its transmitting symbol compact in the time domain, and makes its spectrum high density in the frequency domain, relative to its transmission rate. Suppose M_1 samples out of $N_C + K_0$, i.e., $y(m)(m = 0, \ldots, M_1 - 1)$, are transmitted as shown in Fig. 3.2, in this case, the modulation index ΔfT for modulated PC/HC-MCM signals can be represented as $M_1/(N_C + K_0)$. After IDFT and parallel-to-serial (P/S) conversion process, several zeros are padded as the postfix guard interval (GI) to alleviate the influence of multipath fading. The duration of zero postfix (ZP) is T_g. The reason we choose ZP as GI is that such a method simplifies the demodulation and equalization of the receiver [65]. After digital-to-analog (D/A) conversion, the modulated PC/HC-MCM signal $y(t)$ is transmitted into the channel.

For simplicity, the time-domain modulated PC/HC-MCM signal is expressed in complex base-band notation as

$$y(t) = \sum_{n=0}^{N_C-1} x(n)e^{j2\pi n\Delta f t}, \quad t \in [0, T] \tag{3.4}$$

Suppose that the impulse response $h(t)$ of the fading channel is

$$h(t) = \sum_{i=1}^{L_P} A_i e^{j\theta_i}\delta(t-\tau_i) \quad t \in [0, T+T_g], \tag{3.5}$$

where L_P means the number of paths and each path has the relative path delay $\tau_i (\tau_1 \leq \tau_2 \leq \ldots \leq \tau_{L_P} < T_g)$. $A_i = A_i(t)$ and $\theta_i = \theta_i(t)$ are the slowly Rayleigh-fading amplitude attenuation and phase rotation of each path. We assume A_i and θ_i are constant during each PC/HC-MCM symbol duration.

Therefore the received signal, $y_r(t)$ $(t \in [0, T+T_g])$, can be represented as

$$\begin{aligned} y_r(t) &= h(t) \otimes y(t) + n(t) \\ &= \sum_{i=1}^{L_P} A_i e^{j\theta_i} y(t-\tau_i) + n(t) \quad t \in [0, T+T_g], \end{aligned} \tag{3.6}$$

where $n(t)$ is the additive white Gaussian noise (AWGN).

The receiver generates N_1 discrete-time samples, $\hat{y}_r(m)(m = 0, \ldots, N_1 - 1)$, from the received signal $y_r(t)$ after analog-to-digital (A/D) conversion with oversampling rate K_1. We assume $K_1 = T_0/T$ and the number of time-domain samples of GI is N_g. The N_1 received samples, $\hat{y}_r(m)$, followed by R zeros yield $\hat{f}(n)(n = 0, \ldots, N_1 + R - 1)$ by DFT, as shown in Fig. **??**. Here R $(R = K_1 N - N_1)$ is the number of samples corresponding to the vanished period of the entire PC-OFDM samples. If $T + T_g > T_0$, we assume that $R = 0$ and the samples from $y_r(t)$ during $[T_0, T+T_g]$ will be overlapped with the samples of $y_r(t)$ during $[0, T + T_g - T_0]$, which is identical to the process that ZP-OFDM utilizes the guard interval to eliminate the ISI [65]. In such a case, N_1 will be decreased to $N_1 T_0/(T+T_g)$. It should be pointed out that we can set arbitrary integers for N_1 and R such that the relations $K_1 = T_0/T = (R+N_1)/(N_1-N_g) = (N_C+K_0)/M_1$

and $N_C \leq N_1 - N_g$ hold. For simplicity of analysis, we assume that $R + N_1 = N_C + K_0$ and $M_1 = N_1 - N_g$.

Then the DFT outputs $\hat{f}(n)(n = 0, \ldots, N_1+R-1)$ are equalized with the estimation $\hat{h}(t)$ of the channel impluse response $h(t)$. The goal of equalization is to reduce the multipath interference and we adopt the zero-forcing equalizer as described below.

Suppose each path delay τ_i corresponds to the duration of $N_{\tau_i}(i = 1, \ldots, L_P)$ samples after A/D conversion. At the receiver front, discrete-time samples $\hat{y}_r(m)(m = 0, \ldots, N_1 - 1)$ of the received signal $y_r(t)$ are

$$\begin{aligned}\hat{y}_r(m) = &\sum_{i=1}^{L_P} A_i e^{j\theta_i} \sum_{k=0}^{N_C-1} x(k) e^{j\frac{2\pi k(m-N_{\tau_i})}{N_1+R}} \\ &\times [u(m - N_{\tau_i}) - u(m - N_{\tau_i} - M_1 + 1)] + n(m),\end{aligned} \tag{3.7}$$

where $n(m)$ is the discrete value of $n(t)$ and $u(m)$ is the unit step function. Therefore, after DFT operation, as was shown in Fig. 3.2, the receiver output $\hat{f}(n)(n = 0, \ldots, N_1 + R - 1)$ can be expressed as

$$\begin{aligned}\hat{f}(n) = \frac{1}{N_1+R}\Big(&\sum_{i=1}^{L_P} A_i e^{j\theta_i} \sum_{k=0}^{N_C-1} x(k) e^{-j\frac{2\pi n N_{\tau_i}}{N_1+R}} \\ &\times \sum_{m=0}^{M_1-1} e^{j\frac{2\pi m(k-n)}{N_1+R}} + n'(n)\Big),\end{aligned} \tag{3.8}$$

where $n'(n)$ is the frequency response of $n(m)$. Suppose that $H(f)$ is the frequency response of channel $h(t)$ and its discrete representation is $H(n)(n = 0, \ldots, N_1 + R - 1)$, where $H(n) = H(f)|_{f=nf_0}$. Then the zero-forcing equalizer can be defined as

$$H_{ZF}(n) = H^{-1}(n) = \left(\frac{1}{N_1+R}\sum_{i=1}^{L_P} A_i e^{j\theta_i} e^{-j\frac{2\pi n N_{\tau_i}}{N_1+R}}\right)^{-1}.$$

After being passed through the equalizer, the received signal $\hat{f}(n)$ will be changed to

$\hat{z}(n)$. $\hat{z}(n)(n = 0, \ldots, N_1 + R - 1)$ can be expressed as

$$\begin{aligned}
&\hat{z}(n) = \hat{f}(n) \times H_{ZF}(n) \\
&= \frac{\sum_{i=1}^{L_P} A_i e^{j\theta_i} \sum_{k=0}^{N_C-1} e^{-j\frac{2\pi n N_{\tau_i}}{N_1+R}} x(k) \sum_{m=0}^{M_1-1} e^{j\frac{2\pi m(k-n)}{N_1+R}} + n'(n)}{\sum_{i=1}^{L_P} A_i e^{j\theta_i} e^{-j\frac{2\pi n N_{\tau_i}}{N_1+R}}}.
\end{aligned}$$

Therefore, the perfect zero-forcing equalizer can remove the multipath interference, and $\hat{z}(n)$ can be expressed as

$$\begin{aligned}
\hat{z}(n) &= \sum_{m=0}^{M_1-1} \sum_{k=0}^{N_C-1} x(k) e^{j\frac{2\pi m(k-n)}{N_1+R}} + n''(n) \\
&= \sum_{k=0}^{N_C-1} x(k) \frac{1 - e^{j\frac{2\pi M_1(k-n)}{N_C+K_0}}}{1 - e^{j\frac{2\pi(k-n)}{N_C+K_0}}} + n''(n) \\
&= \sum_{k=0}^{N_C-1} x(k) \frac{1 - e^{j2\pi(k-n)\frac{T}{T_0}}}{1 - e^{j\frac{2\pi(k-n)}{M_1}\frac{T}{T_0}}} + n''(n), \qquad (3.9)
\end{aligned}$$

where $n''(n) = n'(n)/(\sum_{i=1}^{L_P} A_i e^{j\theta_i} e^{-j\frac{2\pi n N_{\tau_i}}{N_1+R}})$.

Finally, the estimates $\hat{x}(k)(k = 0, \ldots, N_C - 1)$ of $x(k)$ that contains m_{tot} [bits] are recovered through the demodulation stage with the samples $\hat{z}(n)(n = 0, \ldots, N_1+R-1)$.

From (3.9), we can find that the ICI will appear if $\Delta f T < 1$. The modulated PC/HC-MCM cannot keep orthogonality between subcarriers. Therefore, the usual demodulation algorithm, that is, each subcarrier is demodulated independently, cannot utilized in the modulated PC/HC-MCM systems. A reasonable approach for attaining a good demodulation performance will be the maximum likelihood sequence estimation (MLSE) at the decision stage in the receiver. The BER performance of the MLSE often depends on the minimum Euclidean distance (MED) between all modulated PC/HC-MCM waveforms. The computation process of the MED can be shown in the following example. Since BPSK-modulated PC/HC-MCM with $(N_C, N_{PC}) = (8, 4)$ can generate 1120 different vectors $\mathbf{X}_i(i = 1, \ldots, 1120)$ whose elements are $x_i(k)(k = 0, \ldots, N_C - 1)$,

each vector will generate the samples $z_i(n)$ ($z_i(n) = \hat{z}_i(n) - n_i''(n); n = 0, \ldots, N_1 + R - 1$) of (3.9) after the equalization of receiver without the noise. Therefore, we can calculate a value of the MED $D_i (i = 1, \ldots, 1120)$ for $\mathbf{X}_i$ using other vectors $\mathbf{X}_j$ ($j = 1, \ldots, 1120; j \neq i$) as follows:

$$D_i = min_j \left(\sqrt{\sum_{n=0}^{N_1+R-1} |z_i(n) - z_j(n)|^2} \right).$$

We evaluate the minimum value $min_i(D_i)$ ($i = 1, \ldots, 1120$) of D_i as the MED of modulated PC/HC-MCM. We also evaluate the average MED (AMED) ($\sum_{i=1}^{1120} D_i/1120$) to represent an average property.

Figure 3.3 shows the MED and average MED (AMED) properties of three modulations as a function of ΔfT, which are BPSK-modulated HC-MCM with $N_C = N_{PC} = 8$ (Modulation A), BPSK-modulated PC/HC-MCM with $(N_C, N_{PC}) = (8, 4)$ (Modulation B) and PC/HC-MCM with $(N_C, N_{PC}) = (8, 4)$ (Modulation C). Signal power per bits is assumed to be unity. For a specific value of ΔfT, the transmission rate of HC-MCM becomes faster than that of the OFDM by a factor of $1/\Delta fT$, provided that the frequency spacing of the HC-MCM Δf is identical to that of the OFDM Δf_0 (e.g., the transmission rates of BPSK-modulated HC-MCM with $\Delta fT = 0.25, 0.125$ are identical to that of 16-QAM and 256-QAM-modulated OFDM). The AMEDs for the HC-MCM becomes larger than that the OFDM when the transmission rates are identical, as can been seen in Fig. 3.3. Therefore, only using BPSK and QPSK modulation, HC-MCM can achieve the transmission rate of high M-QAM OFDM. It should be pointed out that the bandwidth efficiency of OFDM system is higher than that of HC-MCM because both edges of HC-MCM spectra shown in Fig. 3.1(c) are increased with smaller ΔfT. Such a loss of BWE can be alleviated by increasing N_C. Figure 3.3 also shows the influences of ICI over three modulations. The smaller ΔfT will increase ICI and decrease the MEDs and AMEDs.

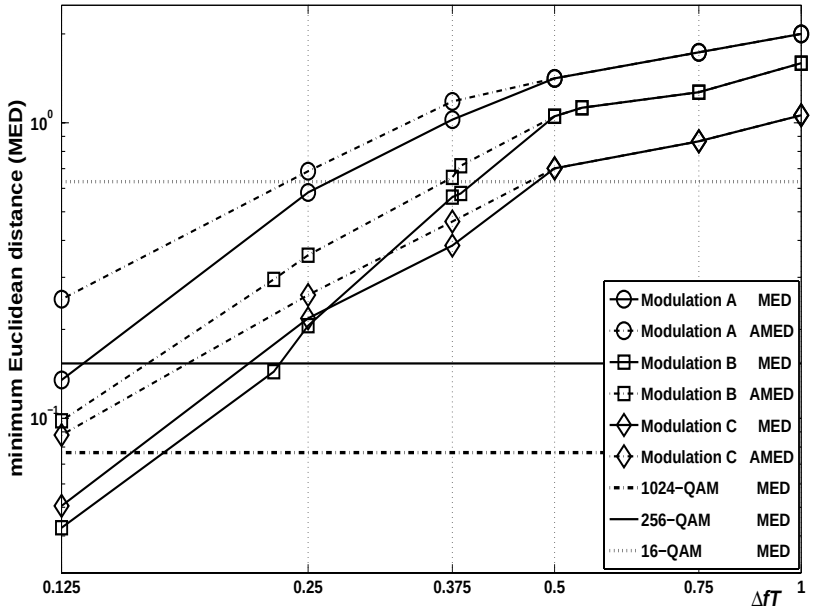

Fig. 3.3 The minimum Euclidean distances (MEDs) and average MEDs (AMEDs) of three modulations with different ΔfT.

Since the amount of computations required for Euclidean distance increases exponentially with N_C, the MLSE can only be utilized for small N_C. For large N_C, a demodulation method using the M-algorithm, which the calculation complexity preserves a linear increase with N_C, has been proposed [64]. In this study, we adopt the MLSE to obtain $\hat{x}(i)(i = 1, \ldots, N_C - 1)$. After that, utilizing the rule of PC mapper, the system can recover the m_{tot} [bits] of data.

On the other hand, the spectrum illustrated in Fig. 3.1(b) can be obtained by time-scaling the duration of the waveform, whose spectrum is illustrated in Fig. 3.1(c), to the equal time duration of the original PC-OFDM waveform. The time-scaling can be accomplished by an appropriate choice of D-A conversion rate, or by adjusting the zero-padding in the transmitter.

3.3 Performance of PC/HC-MCM System

3.3.1 Bandwidth Efficiency of PC/HC-MCM

The BWE of multicarrier systems depends on the number of subcarriers and the type of pulse shaping employed. For ordinary OFDM system with M-QAM, the BWE η_1 will be

$$\eta_1 = \frac{(N_C \log_2 M)/T_0}{2/T_0 + (N_C - 1)\Delta f_0} = \frac{N_C \log_2 M}{N_C + 1}. \tag{3.10}$$

And for HC-MCM system with M-QAM, the BWE η_2 will be

$$\eta_2 = \frac{(N_C \log_2 M)/T}{2/T + (N_C - 1)\Delta f} = \frac{N_C \log_2 M}{2 + (N_C - 1)\Delta f T}. \tag{3.11}$$

We define the BWE η_3 of the modulated PC/HC-MCM system and η_4 of the PC/HC-MCM system as follows:

$$\eta_3 = \frac{m_{tot}/T}{2/T + (N_C - 1)\Delta f} = \frac{N_{PC}\log_2 M + \left\lfloor \log_2 \binom{N_C}{N_{PC}} \right\rfloor}{2 + (N_C - 1)\Delta f T}, \tag{3.12}$$

$$\eta_4 = \frac{m_{PC}/T}{2/T + (N_C - 1)\Delta f} = \frac{\left\lfloor \log_2 \binom{N_C}{N_{PC}} \right\rfloor}{2 + (N_C - 1)\Delta f T}. \tag{3.13}$$

Figure 3.4 plots the BWEs of above four systems. We choose $N_C = 8$ for BPSK-modulated HC-MCM and $N_C = 32$ for QPSK-modulated HC-MCM systems, respectively. We choose for the BPSK- and QPSK-modulated PC/HC-MCMs, (N_C, N_{PC})=(8, 4) and (32, 28), respectively, that maximize the value of m_{tot}. For PC/HC-MCM system, (N_C, N_{PC})=(8, 4) and (32, 16) are chosen to maximize the values of m_{PC}. From (3.11), (3.12) and Fig. 3.4, the modulated PC/HC-MCM system will improve the BWE of the HC-MCM system if $(N_C - N_{PC}) \log_2 M < \left\lfloor \log_2 \binom{N_C}{N_{PC}} \right\rfloor$ holds. Since the ICI will be enlarged by smaller values of $\Delta f T$, we can employ larger $\Delta f T$ of the modulated PC/HC-MCM system to achieve identical BWE of HC-MCM system using the

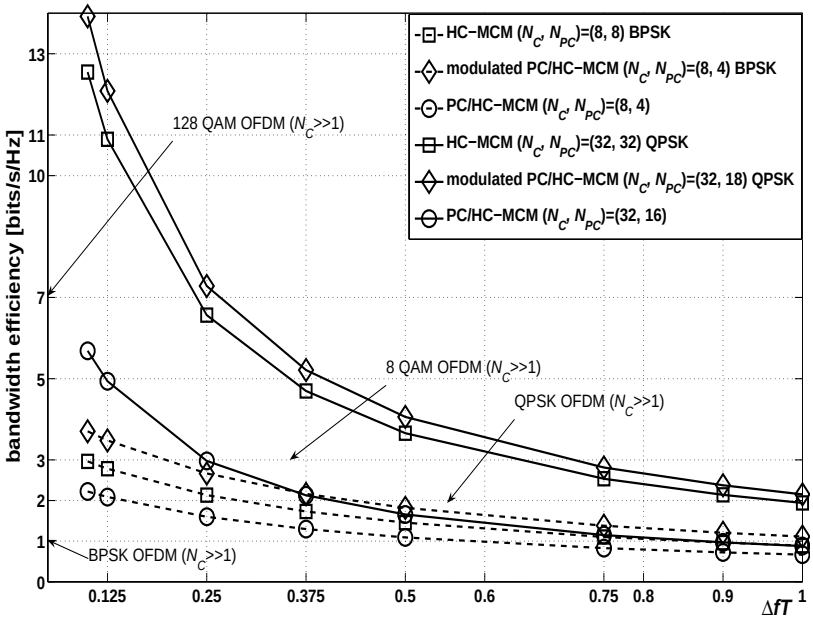

Fig. 3.4 Bandwidth efficiency for four types of different multicarrier systems.

appropriate combination (N_C, N_{PC}). For example, the BWEs of the BPSK-modulated HC-MCM systems ($N_C = 8$) with ΔfT=0.125, 0.25 and 0.375 will be identical to that of the BPSK-modulated PC/HC-MCM systems ((N_C, N_{PC})=(8, 4)) with ΔfT=0.227, 0.384 and 0.54, respectively. And the BWEs of the QPSK-modulated HC-MCM systems ($N_C = 32$) with ΔfT=0.125, 0.25 and 0.375 will be identical to that of the QPSK-modulated PC/HC-MCM systems $(N_C, N_{PC}) = (32, 28)$ with ΔfT=0.145, 0.2844 and 0.4231, respectively. Therefore, compared to the HC-MCM system, the modulated PC/HC-MCM can decrease the ICI by employing the larger ΔfT.

For the PC/HC-MCM system, we can still achieve the identical BWE to the M-QAM OFDM using an appropriate combination of (N_C, N_{PC}) and ΔfT. However, the modulated PC/HC-MCM system will outperform the PC/HC-MCM system because of $m_{PC} < m_{tot}$ for any specific (N_C, N_{PC}). Whereas the PC/HC-MCM system can choose arbitrary value of $e^{j\theta}(i = 1, \ldots, N_{PC})$ for N_{PC} subcarriers. Therefore the PC/HC-MCM system can reduce the PAR.

Table 3.1 Specifications of simulations for modulated PC/HC-MCM system over AWGN channel.

System Item	Parameter
Combination (N_C, N_{PC})	(8, 4)
Subcarrier modulation	BPSK
Synchronization	Complete
Demodulation	MLSE
Channel type	AWGN

3.3.2 Simulated BER Performance of Modulated PC/HC-MCM System over AWGN Channel

Common specifications of simulations are listed in Table 3.1. Figure 3.4 shows BER performance of BPSK-modulated PC/HC-MCM system with $(N_C = 8, N_{PC} = 4)$ over the AWGN channel. The modulation indices ΔfT are 0.227, 0.384 and 0.54, which have the identical BWEs to the BPSK-modulated HC-MCM system with $N_C = 8$ and $\Delta fT = 0.125, 0.25$ and 0.375, respectively. We also plot the theoretical results for the M-QAM-modulated OFDM with N_C=8 and M=16 and 256, since their transmission rates are equal to the modulated PC/HC-MCM system with $\Delta fT = 0.384$ and 0.227, respectively, provided that the frequency spacing of PC/HC-MCM (Δf) is identical to that of the OFDM system (Δf_0). From the results, we can find that the BPSK-modulated PC/HC-MCM system can achieve better BER performance. For $\Delta fT = 0.227, 0.384$ and BER=10^{-4}, the modulated PC/HC-MCM system obtains 7.4 [dB] gain and 1.25 [dB] gain compared to the 256-QAM OFDM and 16-QAM OFDM systems, respectively.

It should be pointed out that the BWEs of 16-QAM and 256-QAM OFDM are

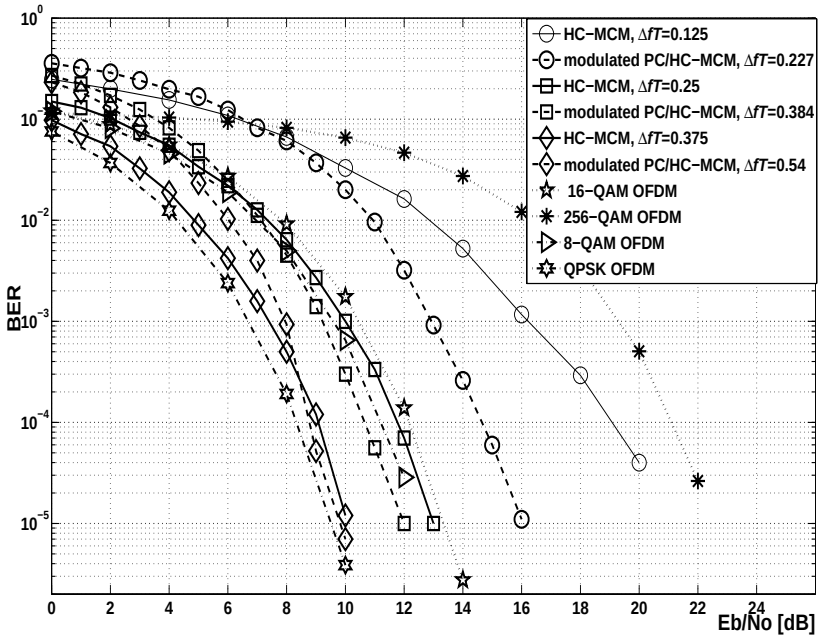

Fig. 3.5 BER performance of BPSK-modulated PC/HC-MCM system $(N_C, N_{PC}) = (8, 4)$ over AWGN channel.

higher than that of the BPSK-modulated HC-MCM system with $(N_C = 8)$ and $\Delta fT = 0.25, 0.125$ because both edges of HC-MCM spectra shown in Fig. 3.1(c) are increased with smaller ΔfT. Such a loss of BWE can be alleviated by increasing N_C. From Fig. 3.4, we can find that the BWEs of QPSK and 8-QAM OFDM are identical to that of the above BPSK-modulated HC-MCM systems. The BER performance of QPSK and 8-QAM OFDM is better than that of the BPSK-modulated HC-MCM systems which can be found in the Fig. 3.4. For $\Delta fT = 0.125$ and BER=10^{-4}, the BPSK-modulated HC-MCM system has 8 [dB] gap between the 8-QAM OFDM system. But the BPSK-modulated PC/HC-MCM system with $\Delta fT = 0.227$ will improve 4.5 [dB] for BER=10^{-4} than that of the BPSK-modulated HC-MCM system.

Table 3.2 Specifications of simulations for modulated PC/HC-MCM system over multipath fading channel.

System Item	Parameter
Subcarrier modulation	BPSK
Combination (N_C, N_{PC})	(8, 4) for PC/HC-OFDM $N_C = 8$ for HC-MCM
Synchronization	Complete
Channel type	JTC' 94 (indoor residential B) (L_P=8)
Equalization	zero-forcing equalization
Supported PC/HC-MCM rate (symbol/second)	570k ($T + T_g = 1.75\mu$s)
Relative delay for each path (ns)	0, 50, 100, 150 200, 250, 300, 350
Relative power attenuation for each path (dB)	0, -2.9, -5.8, -8.7, -11.6, -14.5, -17.4, -20.3
Maximum Doppler frequency shift f_D (Hz)	15
Duration of zero guard signal	T_g=0.25T
ΔfT	0.125, 0.25, 0.375 for HC-MCM 0.227, 0.384, 0.54 for modulated PC/HC-MCM
Noise	Additive White Gaussian Noise

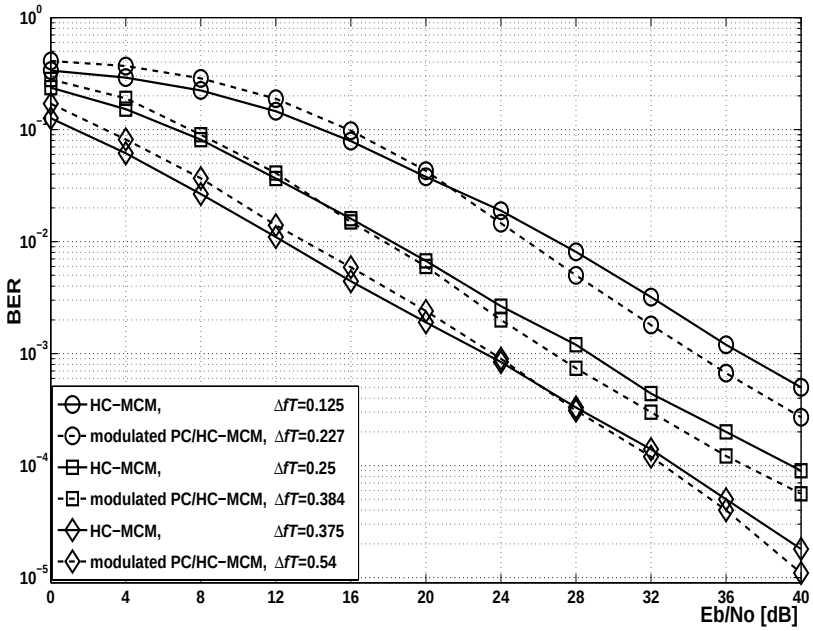

Fig. 3.6 BER performance of BPSK-modulated PC/HC-MCM system with $(N_C, N_{PC}) = (8, 4)$ over a multipath channel.

3.3.3 Simulated BER Performance of Modulated PC/HC-MCM System over Multipath Fading Channel

Specifications of simulations are listed in Table 3.2. Figure 3.6 shows BER performance of BPSK-modulated PC/HC-MCM system with $(N_C, N_{PC}) = (8, 4)$ over a multipath fading channel in comparison with the HC-MCM. We assume the transmission rates of both systems are identical for all values of ΔfT; thus the frequency spacing (Δf) is reduced by decreasing ΔfT. The modulation indices ΔfT are 0.227, 0.384 and 0.54, which have the identical BWEs to the BPSK-modulated HC-MCM system ($N_C = 8$) with ΔfT=0.125, 0.25 and 0.375, respectively. We choose the fading channel model of JTC' 94 (indoor residential B) [66] to compare the BER performance of both systems. It is assumed that the receiver knows the channel information $h(t)$ and carries out the perfect zero-forcing equalization. From the results, we can find that the BPSK-modulated PC/HC-MCM system can achieve better BER performance. For

Table 3.3 Specifications of simulations for PC/HC-MCM system over AWGN channel.

System Item	Parameter
Combination (N_C, N_{PC})	(8, 4), (16, 3), (16, 13), (16, 5)
Subcarrier modulation	N_{PC} subcarriers use $e^{i\theta_i}$ (θ_i is random for ith subcarrier), $(N_C - N_{PC})$ subcarriers adopt zero-amplitude points
Synchronization	Complete
Demodulation	MLSE
Channel type	AWGN

example, using $\Delta fT = 0.227$, the modulated PC/HC-MCM system can achieve 3 [dB] gain for BER=10^{-3} than that of the HC-MCM system with the equal BWE.

3.3.4 Simulated BER Performance of PC/HC-MCM System over AWGN Channel

Specifications are listed in Table 3.3. Figure 3.7 shows the characteristics of the bandwidth efficiency (BWE) versus Eb/No required for BER=10^{-4}. We adopt the combinations of (N_C, N_{PC}) = (16, 5), (16, 3), (16, 13) and (8, 4). N_{PC} subcarriers are modulated by $e^{j\theta_i}(i = 1, \ldots, N_{PC})$ where θ_i is the phase angle of the i-th subcarrier. In order to evaluate the impact of the ICI, θ_i $(i = 1, \ldots, N_{PC})$ are chosen to be random values ($\theta \in [0, 2\pi]$). When ΔfT=1, the PC/HC-MCM system reduces to the PC-OFDM system without m_{PSK}. For a specific Eb/No, different combination and ΔfT can cause different bandwidth efficiency. For example, when Eb/No $\simeq$ 12.5 dB, the PC/HC-MCM with ΔfT=0.375 and (N_C, N_{PC}) = (16, 5) achieves BWE $\simeq$1.6 bits/s/Hz, whereas

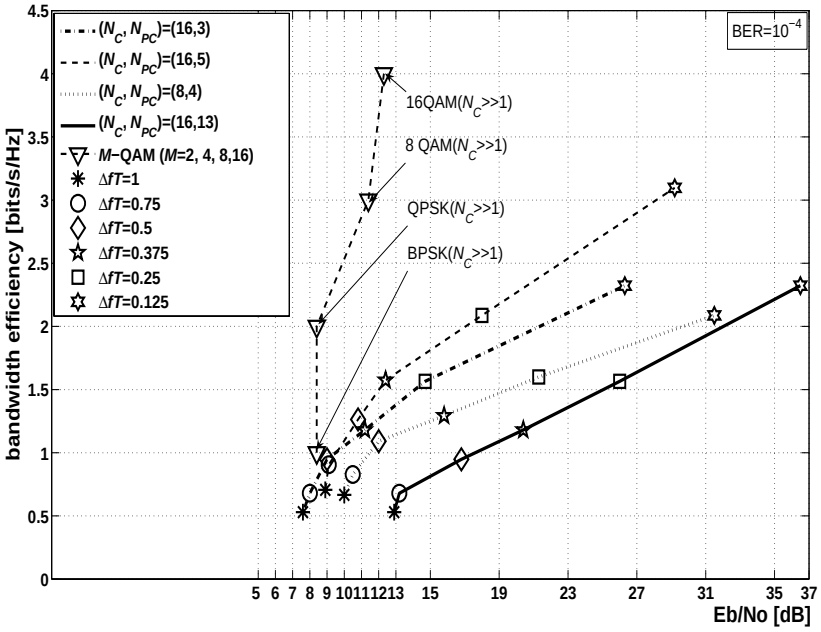

Fig. 3.7 BER versus Eb/No [dB] required at BER=10^{-4} for PC/HC-MCM system over AWGN channel.

the (nomodulated) PC-OFDM with ΔfT=1.0 and (N_C, N_{PC})=(8, 4) achieves BWE $\simeq$ 0.7bits/s/Hz. This means that twice the bandwidth efficiency is obtained by the PC/HC-MCM system. On the other hand, the PC/HC-MCM system with combinations of (N_C, N_{PC}) = (16, 3) and (16, 13) can achieve the equal bandwidth efficiency because the values of m_{PC} for both systems are the same. However, we can find that (N_C, N_{PC}) = (16, 13) will consume more power than that of (N_C, N_{PC}) = (16, 3).

Figure 3.8 shows the simulated BER performance of the PC/HC-MCM system with (N_C, N_{PC}) = (16, 5) and θ_i $(i = 1, \ldots, N_{PC})$ are chosen to be random values $(\theta \in [0, 2\pi])$. From the results we can find that for the same BER, more power is consumed with the smaller ΔfT but the BWE can be improved. It is remarkable that the PC/HC-MCM with ΔfT=0.5, 0.75 and 1 achieves almost the same BER performance. Note that ΔfT=0.375 also indicates comparable BER performance.

Figure 3.8 also shows the tradeoff between the BWE and the demodulation com-

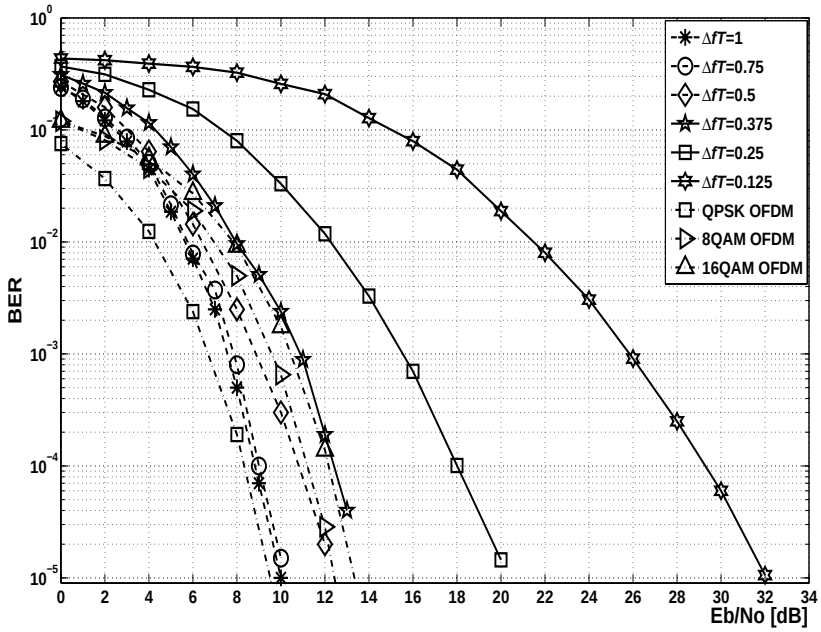

Fig. 3.8 BER performance of PC/HC-MCM system with combination with $(N_C, N_{PC}) = (16, 5)$ over AWGN channel.

plexity of the PC/HC-MCM system. Large number N_C of PC/HC-MCM system results in high complexity, especially for the MLSE of demodulation. By utilizing the method we proposed to the decision stage [61], it can preserve a linear increase with N_C for the calculation complexity. On the other hand, Figs. 3.7 and 3.8 also show the BER performance of OFDM system using QPSK, 8 QAM, 16 QAM modulation. PC/HC-MCM system cannot achieve better performance than that of the OFDM systems, but PC/HC-MCM system can realize better characteristics of PAPR which will be presented in following subsection.

3.3.5 PAPR of Two PC/HC-MCM Systems

One of the major drawbacks of OFDM system is that the time-domain OFDM signals exhibit large value of PAPR. Therefore, complicated methods and exorbitant devices must be utilized to OFDM system to decrease the value of PAPR. The PAPR

will be enlarged if N_C or M-QAM modulation order M increases [67].

Let us denote the data block of length N_C as a vector $\mathbf{X} = [x(0), \ldots, x(N_C - 1)]$. The symbol duration of the PC/HC-MCM is T. Each subcarrier modulates one of the set of frequencies $f_n (n = 0, \ldots, N_C - 1)$ and $f_n = n\Delta f$. The complex envelope of the transmitted PC/HC-MCM signal is given by

$$y(t) = \frac{1}{\sqrt{N_C}} \sum_{n=0}^{N_C-1} x(n) e^{j2\pi n \Delta f t} \quad t \in [0, T]. \tag{3.14}$$

The PAPR of the signal of PC/HC-MCM can be defined as

$$PAPR = \frac{\max_{0<t<T} |y(t)|^2}{P_{AV}}, \tag{3.15}$$

where P_{AV} is the ensemble average of the power of time-domain PC/HC-MCM signals $y(t)$. We randomly generate millions of time-domain PC/HC-MCM signals by computer to obtain the approximate value $\hat{P}_{AV}$ of P_{AV}. The simulated $\hat{P}_{AV}$ for modulated PC/HC-MCM signals $(N_C, N_{PC}) = (64, 48)$ are almost identical for all values of $\Delta f T$. To capture the peaks of the PC/HC-MCM signal, we adopt 4 times oversampling time-domain samples which can totally approximate the continus time-domain signal [68]. We use the complementary cumulative density function (CCDF) of the PAPR (Prob[PAPR>PAPR$_0$]) to represent the PAPR characteristics. In the following simulations, we can confirm that the PAPR of modulated PC/HC-MCM system will be reduced by decreasing $\Delta f T$.

For PC-OFDM signals with large N_C, the peak values of the signals appear uniformly in the PC-OFDM symbol duration $[0, T_0]$. The modulated PC/HC-MCM only utilizes the partial time-domain signal during $[0, T]$ of the entire PC-OFDM time-domain signal ($[0, T_0]$) to transmit the equal bits of data, as can be seen in Fig. 3.2. Therefore, if the peak values of the PC-OFDM signal appears in the duration $(T, T_0]$, the peak values of the modulated PC/HC-MCM signal will be smaller than that of PC-OFDM signal. On the other hand, the simulated $\hat{P}_{AV}$ for the modulated PC/HC-MCM signals

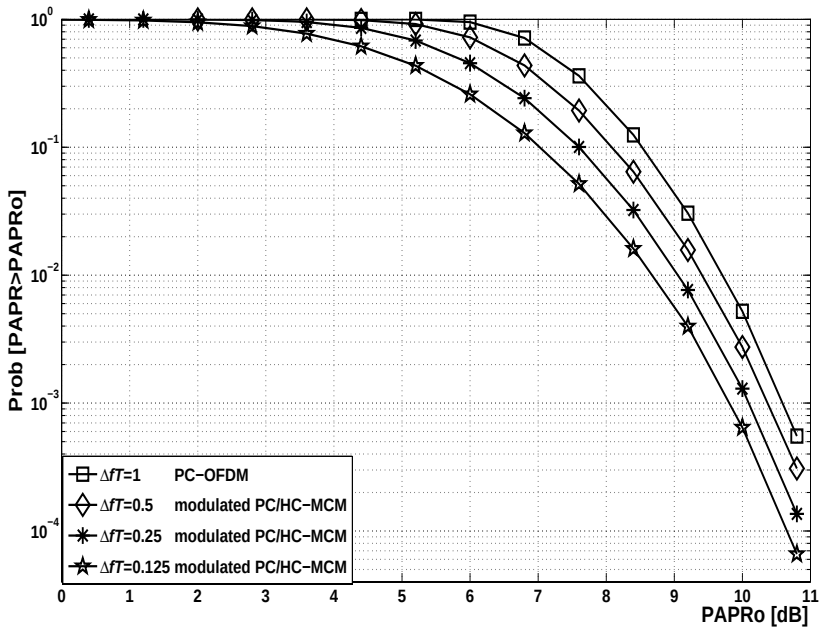

Fig. 3.9 CCDFs of PAPR of the modulated PC/HC-MCM with (N_C,N_{PC})=(64, 48), the modulation is QPSK.

$(N_C, N_{PC}) = (64, 48)$ are almost identical for all values of ΔfT. So it can be intuitively inferred that the PAPR (Prob[PAPR>PAPR$_0$]) will be reduced by decreasing ΔfT compared to the ordinary PC-OFDM waveforms.

Figure 3.9 gives the CCDFs of the PAPR of the modulated PC/HC-MCM signals. The PC-OFDM is the special case of the modulated PC/HC-MCM when $\Delta fT = 1$. QPSK is used to modulate the subcarriers. We use $N_C = 64$ to simulate the PAPR because large subcarriers can further distinctly exhibit the CCDF property of PAPR during the adjustment of ΔfT. From the results, we can confirm that the PAPR of the modulated PC/HC-MCM system can be reduced with ΔfT.

For the PC/HC-MCM system, we can utilize the values of $e^{j\theta_i}(i = 1, \ldots, N_{PC})$ to obtain small PAPR. In this paper, we assume that a certain set of θ_i is used for all the PC/HC-MCM signals, and that each element of the set takes a value $\theta_i \in \{\pi/2, \pi, 3\pi/2, 2\pi\}$. The best set that minimizes the PAPR was searched through the

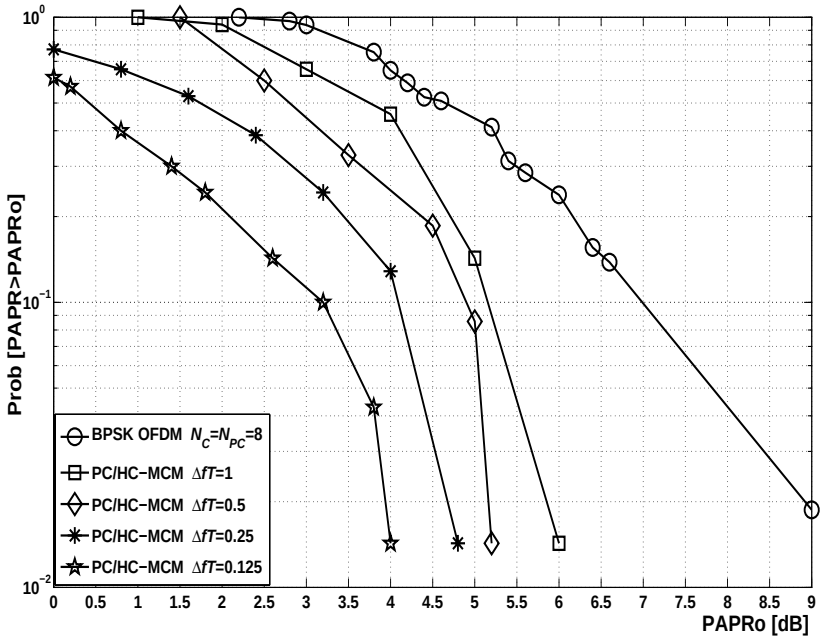

Fig. 3.10 CCDFs of PAPR of the PC/HC-MCM with (N_C, N_{PC})=(8, 4) by the selection process.

simulations from all $4^{N_{PC}}$ kinds. The results plotted in Fig. 3.10 indicate that the PAPR is dramatically improved by such a simple way.

3.4 PC/HC-MCM with Frequency Hopping for Multiple Access

Multiple access (MA) in telecommunications systems refers to techniques that enable multiple users to share limited network resources efficiently. So many papers focus the attention on the MA based on OFDM [69], [70]. In this section, we develop a new frequency hopping code division MA (FH-CDMA) technique based on PC/HC-MCM.

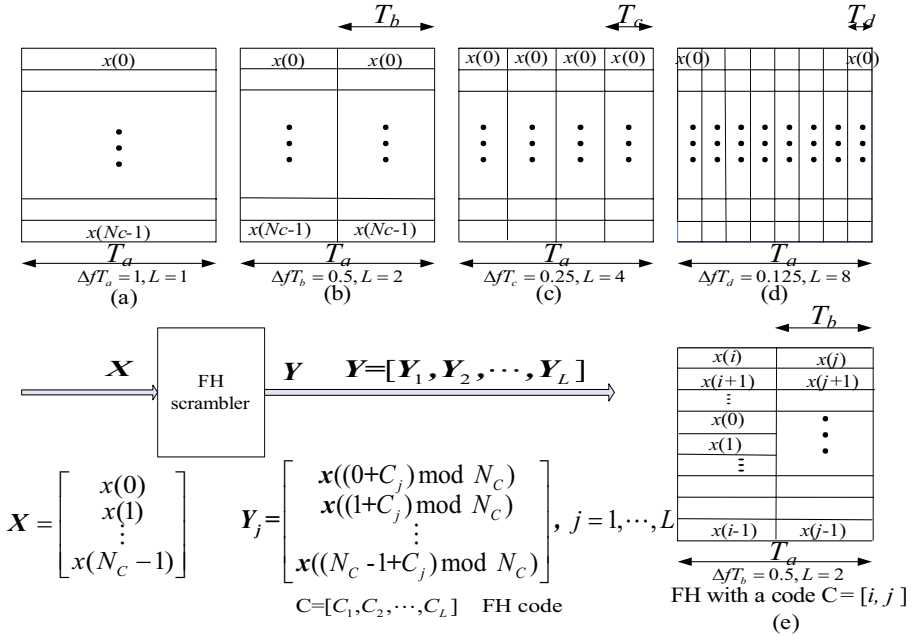

Fig. 3.11 Frequency hopping for the PC/HC-MCM system.

3.4.1 PC/HC-MCM with Frequency Hopping

The PC/HC-MCM system can improve the transmitting rate if the system keeps frequency spacing (Δf) constant for arbitrary values of modulation index ΔfT. In this case, a fast transmission rate can be achieved with a smaller value of ΔfT. In other words, during the same symbol duration of the PC-OFDM, the PC/HC-MCM can transmit the symbol repeatedly.

Let T_a be the symbol duration of PC-OFDM with ΔfT_a =1 and let $T_b = T_a/2, T_c = T_a/4$, and $T_d = T_a/8$ be the symbol durations of the PC/HC-MCM with ΔfT_b=0.5, ΔfT_c=0.25 and ΔfT_d=0.125, respectively. Since T_b, T_c,and T_d are shorter than T_a, frequency-time map for each modulation index can be illustrated as shown in Figs. 3.11(a)-(d). As can been seen in Figs. 3.11(a)-(d), during T_a, the PC/HC-MCM systems can transmit two symbols for ΔfT_b, four symbols for ΔfT_c and eight symbols for ΔfT_d. Therefore, we can adopt frequency hopping (FH) technique, i.e., L=2 for ΔfT_b, L=4 for ΔfT_c and L=8 for ΔfT_d with different length of time-slots (L) to obtain the gain

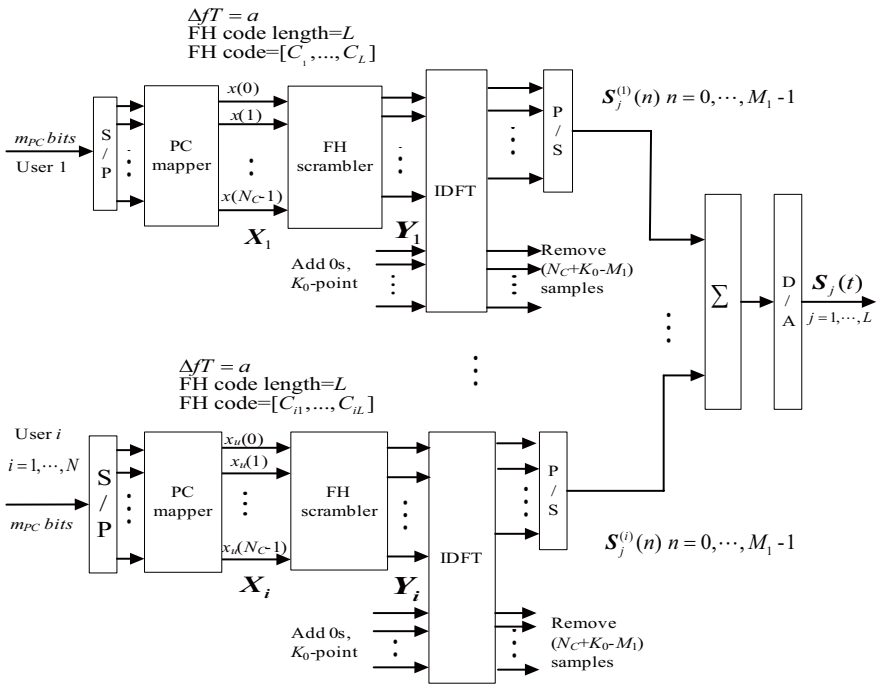

(a) Base station (BS) transmitter.

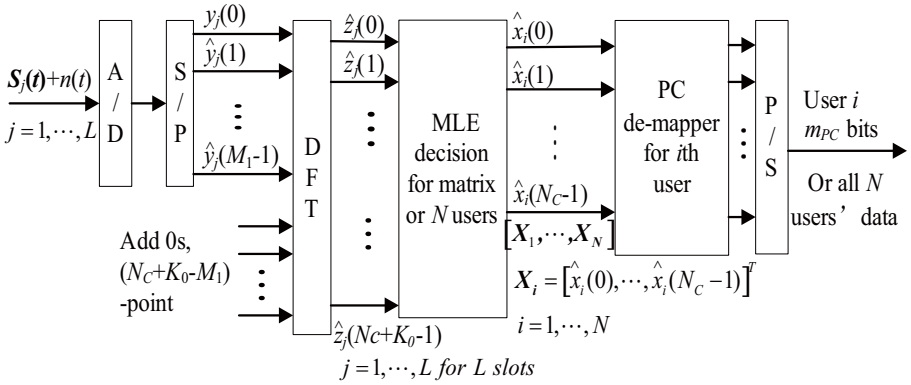

(b) Receiver.

Fig. 3.12 Downlink of MA with PC/HC-MCM techniques.

of FH.

System introduction

Suppose that the FH code $C = [C_1, \ldots, C_L]$, where $C_j (j = 1, \ldots, L)$ is a jth chip value that takes an integer limited over $[0, N_C - 1]$. By the FH code, the input $x(k)(k = 0, \ldots, N_C - 1)$ to the IDFT in the transmitter (Fig. 3.2) is scrambled as $x((k + C_j) mod N_C)$ for the jth time-slot. The process of scrambling is also illustrated in Fig. 3.11. In this paper, we assume FH code whose elements (chips) are randomly generated with uniform distribution.

3.4.2 Multiple Access for PC/HC-MCM with Frequency Hopping

In the receiver (Fig. 3.2), the decision stage utilizes the $(N_C + K_0) \times L$ input matrix to demodulate m_{PC} [bits] with the MLSE in this paper.

The benefits of FH for the PC/HC-MCM can be applied in multiple access especially for downlink of system which is presented in the following subsection.

Figures 3.12(a) and (b) show a base station (BS) transmitter and a receiver for downlink of MA with PC/HC-MCM techniques. We assume that each user adopts the same ΔfT, L and combination of (N_C, N_{PC}). The base station transmits all data of N users synchronously. Input m_{PC} [bits] of each user can be denoted by the matrix $\boldsymbol{Y}_i(N_C \times L)$ after the function model of FH scrambler in Fig. 3.12(a), and $\boldsymbol{Y}_i$ is processed by the IDFT column by column. After the process of P/S, M_1 samples $\boldsymbol{S}_j^{(i)}(n)(n = 1, \ldots, M_1 - 1)$ of the ith $(i = 1, \ldots, N)$ user's signal for the jth $(j = 1, \ldots, L)$ time-slot can be obtained. $\boldsymbol{S}_j^{(i)}(n)$ of all users are added to be one transmitting signal $S_j(t)$ after the D/A, and all users' m_{PC} [bits] are transmitted in time duration of L slots. Each receiver receives the transmitting signal $S_j(t)$ polluted by noise. After the A/D and S/P, the samples of $\hat{\mathbf{Z}}_j$ are obtained by the DFT of Fig. 3.12(b). By performing

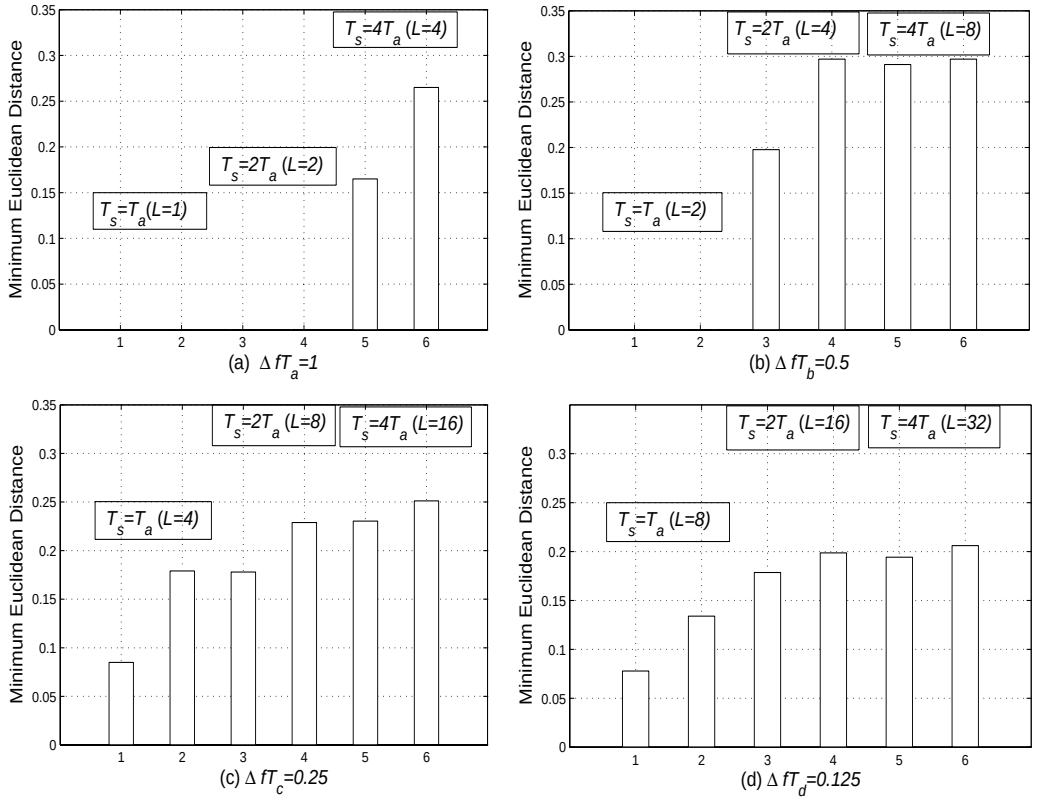

Fig. 3.13 Simulated minimum Euclidean distance (MED) for different L (FH code length) with different ΔfT for four users.

the DFT L times slot by slot, we can produce a received matrix $\hat{\mathbf{Z}} = [\hat{\mathbf{Z}}_1, \ldots, \hat{\mathbf{Z}}_L]$. The receiver can recover all data of the users from the received matrix $\hat{\mathbf{Z}}$ based on the MLSE. The outputs of the MLSE decision stage are the estimates of the frequencies $\hat{\mathbf{X}}_i = [\hat{x}_i(0), \ldots, \hat{x}_i(N_C - 1)]^T$ utilized for transmitting the N_{PC} PC tones for the ith user.

System performance

We adopt $(N_C, N_{PC}) = (4,\ 1)$, $e^{i\theta_i} = 1 (i = 1, \ldots, N_{PC})$ for all users and N=4 (4 users) to explain this method. Since $(N_C, N_{PC}) = (4,\ 1)$, $m_{PC} = \lfloor \log_2 \binom{4}{1} \rfloor$=2 [bits] for each user.

Figure 3.13 shows the minimum Euclidean distance (MED), that is, for all $m(m = 256$ in this simulation) combinations of input data of 4 users, there will be m received matrices with size of $(N_C + K_0) \times L$ ($\hat{\mathbf{Z}}$) after the DFT of the receiver. The power of each transmitted matrix $\sum_{i=1}^{i=N} S_j^{(i)}(n)(n = 1, \ldots, M_1 - 1; j = 1, \ldots, L)$ in Fig. 3.13(b) is assumed to be unity. Here we make the system generate 100 different FH codes for 4 users randomly to simulate the MED with different ΔfT and L. All users choose the FH codes randomly but codes of each user are different. For each ΔfT and L, we use the average MED to represent the average of all 100 MEDs of the system with different FH codes. So average MED is the scale of difference between all m matrices with random FH codes. At the same time, we also give the optimal MED among 100 MEDs to compare with the average MED for each ΔfT and L (1, 3, 5: average MED between 100 FH codes; 2, 4, 6: optimal MED among 100 FH codes).

We define a new notation T_s to represent the duration for transmitting the m_{PC} data bits. Three types of selection of L are shown in Fig. 3.13, where $T_s = T_a$ means the m_{PC} data block are transmitted in one PC-OFDM symbol duration (T_a). In this case $\Delta fT_a = 1, L = 1$; $\Delta fT_b = 0.5, L = 2$; $\Delta fT_c = 0.25, L = 4$; $\Delta fT_d = 0.125, L = 8$ can achieve the same transmission rate which is analyzed in the above section. Again, $T_s = 2T_a$ means the m_{PC} data block are transmitted in two PC-OFDM symbol durations, so $\Delta fT_a = 1, L = 2$; $\Delta fT_b = 0.5, L = 4$; $\Delta fT_c = 0.25, L = 8$; $\Delta fT_d = 0.125, L = 16$ generate the same transmission rate, and $\Delta fT_a = 1, L = 4$; $\Delta fT_b = 0.5, L = 8$; $\Delta fT_c = 0.25, L = 16$; $\Delta fT_d = 0.125, L = 32$ for $T_s = 4T_a$. Utilizing this way, L can be increased with T_s.

For the case of $T_s = T_a$, the average MED and optimal MED are equal to zeros when L=1 ($\Delta fT_a = 1$) and L=2 ($\Delta fT_b = 0.5$) and it is no way to recover the data. But with increasing L, such as L=4 ($\Delta fT_c = 0.25$) and 8 ($\Delta fT_d = 0.125$), the average MED becomes larger. On the other hand, average MED increases with T_s. For $T_s =$

$2T_a, L = 2(\Delta f T_a = 1)$ still makes the average MED and optimal MED zero, but for $L = 4(\Delta f T_b = 0.5)$, $L = 8(\Delta f T_c = 0.25)$ and $L = 16(\Delta f T_b = 0.125)$, the average MED can be highly improved, especially for $L = 4(\Delta f T_b = 0.5)$. The similar phenomena can be found with $T_s = 4T_a$, $L = 8(\Delta f T_b = 0.5)$ has the maximal average MED for all different and L.

The distribution of MED varies with $\Delta f T$ and L. For the case of $T_s = 4T_a$ and $L = 4(\Delta f T_a = 1)$, we make the system generate 100 different FH codes combination for 4 users randomly to simulate the MED, and the MEDs of 17 combinations are zeros. But for other $\Delta f T$, especially for $\Delta f T_{c,d} = 0.25, 0.125$, the above phenomena never happens. So it is very important for the system to adopt the appropriate FH codes and $\Delta f T$.

Figure 3.14(a)-(c) show the simulated results of the BER performance with 4 users over the AWGN channel($(N_C, N_{PC}) = (4, 3)$, $e^{j\theta_i} = 1, i = 1, \ldots, N_{PC}$ and T_s =1, 2, 4 PC-OFDM symbol duration (T_a) for different L with optimal FH codes). Note that here we make each user choose the FH codes with the optimal MED from all simulated FH codes. From Fig. 3.14(a), we can find that with $T_s = T_a, L = 1$ and 2, the BER performance vibrate between 0.05 and 0.1, so no any data can be recovered from the received matrices with white noise. But when the system adopts L=4 ($\Delta f T_c = 0.25$) and L=8 ($\Delta f T_d = 0.125$), the data of users can be recovered. It also means that the system can support 4 users to transmit synchronously in one symbol duration of PC-OFDM when system adopts PC/HC-MCM. For $T_s = 2T_a$, L=4 ($\Delta f T_b = 0.5$) can achieve the best BER performance, and for the $T_s = 4T_a$, L=8 ($\Delta f T_a = 0.5$) can also get the optimal performance.

Figure 3.14(a)-(c) also show that the system can change its transmission rate to improve the BER performance over the AWGN channel. For $T_s = T_a$, if the system chooses L=4 ($\Delta f T_c = 0.25$) to hold 4 users at BER=10^{-4}, the required Eb/No$\simeq$ 20

[dB]. But for $T_s = 2T_a$, if the system chooses L=8 ($\Delta f T_c = 0.25$) to hold 4 users, the required Eb/No reduces to 16 [dB], but the transmission rate for $T_s = 2T_a$ is half of that for system with $T_s = T_a$.

Figure 3.15 shows the simulated results of the BER performance of the PC/HC-MCM MA system with 4 users over the multipath channel ($(N_C, N_{PC}) = (4,\ 1)$, $e^{j\theta_i} = 1, \theta = 1, \ldots, N_{PC}$ with optimal FH codes). The channel model is JTC'94 (indoor residential B) which has been listed in Table 3. 2. We assume the duration of T_a is 2.8 μs and duration of GI (T_g) is 350 ns($= T_a/8$). We also assume that the symbol duration of the PC/HC-MCM symbols are identical for all values of $\Delta f_a T_a, \Delta f_b T_b, \Delta f_c T_c$ and $\Delta f_d T_d$, which can be realized by time-scaling the duration of the PC/HC-MCM waveforms. Because of $T_a = T_b = T_c = T_d = 2.8\mu$s. the frequency spacings Δf_b, Δf_c and Δf_d can be represented as $\Delta f_b = 0.5\Delta f_a$, $\Delta f_c = 0.25\Delta f_a$ and $\Delta f_d = 0.125\Delta f_a$, respectively. Therefore the required bandwidths for smaller $\Delta f_i T_i (i = b, c, d)$ are reduced. It is assumed that the receiver carries out the perfect zero-forcing equalization.

Figure 3.15 shows the BER performance of system with time-slots $L = 4$ and $L = 8$. Since the symbol duration of the PC/HC-MCM symbols are identical, PC/HC-MCM MA system with $L = 4$ will achieve double transmission rate than that of $L = 8$. For $L = 4$, the system with $\Delta f_b T_b = 0.5$ obtains 8 dB than that of system with $\Delta f_b T_b = 0.25$ for BER $=10^{-4}$. But the system with $\Delta f_b T_b = 0.25$ occupies smaller bandwidth that that of system with $\Delta f_b T_b = 0.5$. The similar BER performance can also be obtained for the systems with $L = 8$. Since the system with L=4, $\Delta f_b T_b = 0.5$ has large value of MED as can be seen in Fig. 3.13, it can achieve both the optimal transmission rate and better BER performance than that of other $\Delta f_i T_i (i = a, b, c, d)$ and L.

3.5 Conclusions of This Chapter

In this Chapter, we further improve the performance of flexible HC-MCM system and propose a new modulation named parallel combinatory/high compaction multi-carrier modulation (PC/HC-MCM) using the techniques of parallel combinatory orthogonal frequency division multiplexing (PC-OFDM) and high compaction multi-carrier modulation (HC-MCM). Two types of PC/HC-MCM systems, which are named as modulated PC/HC-MCM system and (unmodulated) PC/HC-MCM system, can be designed. The modulated PC/HC-MCM system achieves better bit-error rate (BER) performance than that of HC-MCM system with equal bandwidth efficiency (BWE). The PC/HC-MCM system can obtain the better peak-to-average power ratio (PAPR) characteristics by selecting appropriate constellation for each subcarrier. On the other hand, since PC/HC-MCM can divide the PC-OFDM symbol duration into multiple time-slots, the advantages of frequency hopping (FH) can be applied in the PC/HC-MCM system. Therefore, we also combine the PC/HC-MCM and frequency hopping multiple access (FHMA) to propose a novel multiple access (MA) system. It can simultaneously transmit multiple users' data within one symbol duration of PC-OFDM.

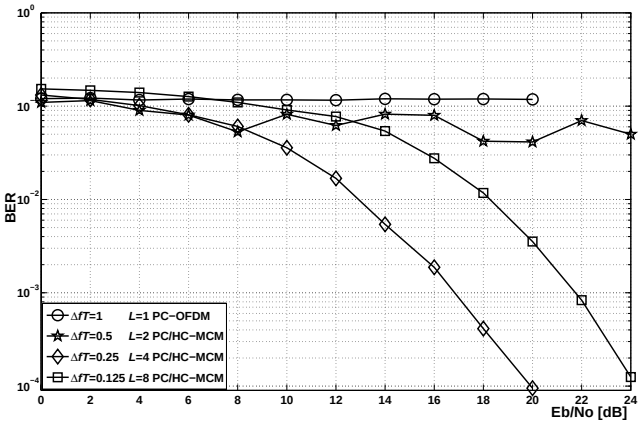

(a) $T_s = T_a$,

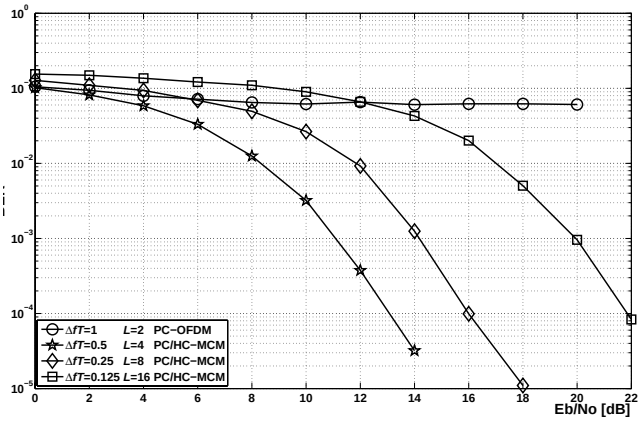

(b) $T_s = 2T_a$,

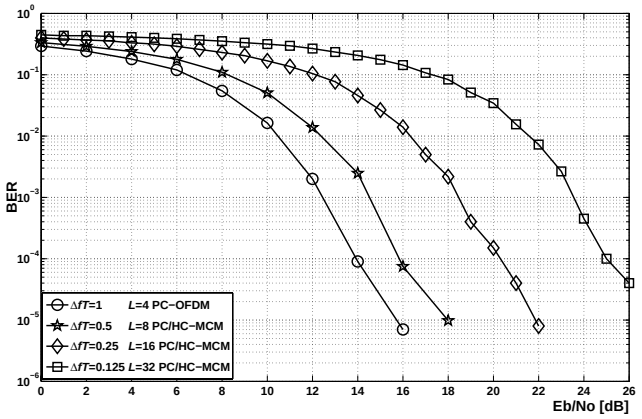

(c) $T_s = 4T_a$

Fig. 3.14 BER performance of FH-CDMA utilizing the PC/HC-MCM with four users over AWGN channel.

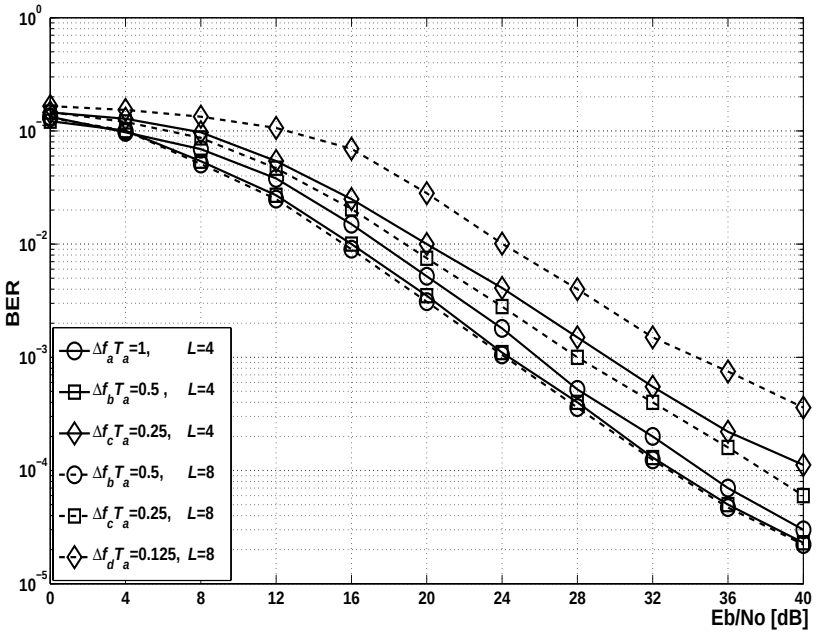

Fig. 3.15 BER performance of FH-CDMA utilizing the PC/HC-MCM with four users over multipath channel.

Chapter 4

Collision Recovery for Ad-hoc Network Using Flexible Multicarrier System

4.1 Introduction

4.1.1 Related Work

Packet collisions occur when two or more packets from different transmitters are simultaneously transmitted and interfere with each other over the common medium. It is often assumed that, except for the spread spectrum system, collided packets are discarded and must be retransmitted. Such a retransmission decreases the system throughput and increases the transmission delay. The performance of wireless communications and ad-hoc networks in distributed random multiple access is influenced by this restriction [71]. Such phenomena also have been named as the hidden-terminal or exposed-terminal problems, which dramatically decrease the performance of ad-hoc networks. Thus, there have been many attempts to recover collided packets, such as by making use of the capture effect and multiuser detection (MUD).

With the capture effect [73], only the packet that has the highest signal-to-interference-plus-noise ratio (SINR) can be recovered from the collisions and other

corrupted packets are discarded. The receiver can utilize the technique of multipacket reception (MPR) by which multiple packets can be retrieved from the collision [74]. However, such a technique requires all packets to adopt different power levels to ensure that the different SINRs are above the designed thresholds. In distributed random multiple access, nodes transmit packets in an uncoordinated fashion, so it is difficult to realize the above requirement [75]. MUD is a technique by which we can recover all packets at the expense of complexity of the receiver [76]. Since MUD requires user information (signatures), it is often utilized in code division multiple access (CDMA) systems. Furthermore, the error correction coding (ECC) [77] and diversity reception [78] enhance the capture effect and result in high probability that the collided packets are recovered.

On the other hand, most collisions occur when one user starts to build a connection or sends a response with a short packet, such as RTS (request-to-send), CTS (clear-to-send) or ACK (acknowledgement), to one node while a principal user is transmitting a long packet including data to an identical destination. Therefore, the collided part is not as long as the principal long packet. For example, the long packet of IEEE 802.11a (64 subcarriers) can convey 8184 [bits] (payloads) without preamble and control bits, but the length of ACK, RTS or CTS is no longer than 300 [bits] which can be carried by only six BPSK-modulated OFDM signals or three QPSK-modulated OFDM signals [79]. Undoubtedly, for the long packet, if such collided parts can be recovered, the system performance, such as throughput and delay, will be dramatically improved [74]. On the other hand, it will also benefit the protocol design of wireless networks because short packets often contain much important information, such as positions and power levels [80]-[82].

4.1.2 Contributions and Outline of This Chapter

In this Chapter, we will propose a effective method of collision recovery for OFDM-based ad-hoc networks. Since that, which has been presented in above Chapters, from the flexible multicarrier system, the modulated message data of OFDM signal can be demodulated using the partial (ΔfT) time-domain OFDM signal. Therefore, the partial signal can be adopted to reconstruct the whole OFDM signal with estimated channel information. Utilizing this advantageous property, an effective method of collision recovery, which is somewhat similar to the scheme of successive interference cancellation (SIC) [83], can be realized. We simulated the recovery performance using different modulations for two users with identical SNR and weak near-far effect, and showed that the method gives promising results and can be developed to solve the problem of hidden terminals [72].

Compared with other methods, the most important point is that our proposed method can recover both long and short packets from the collision, which can be utilized in ad hoc networks based on OFDM. For example, the short packets such as RTS often contain much important information of wireless nodes, such as their positions and desired transmission duration. If the nodes which have sent the RTS have not obtained the responses, they will retransmit the short packets (RTS) after a random delay and such the process will result in another collision. By utilized our proposed method, the receiver can separate the short packets without any synchronization when they are collided with the long packet. So in the next step, the receiver can send the responses according to the scheduling strategies to all nodes which have sent the RTS packets. On the other hand, in the near-far situation, our method can achieve better recovery performance in the weak near-far condition which is more realistic in the wireless LAN. Therefore, the proposed method can be utilized to solve the hidden terminal or exposed

terminal problems and improve the performance of ad-hoc networks that are based on wireless LAN using OFDM techniques.

This Chapter is organized as follows. A basic model of the OFDM system with partial signals and its performance using BPSK and QPSK modulations over a multipath fading channel are described in Sect. 4.2. Then the method of collision recovery is presented in Sect. 4.3. We discuss some factors that influence the performance of recovery in Sect. 4.4. The performance of the proposed method is simulated in Sect. 4.5. We further discuss the performance of the OFDM system with partial signals using 8-QAM and 16-QAM modulations in Sect. 4.6 and the paper ends with conclusions presented in Sect. 4.7.

4.2 OFDM System with Partial Signal

4.2.1 Model of OFDM System with Partial Signal

For simplicity, the time-domain OFDM signal is expressed in complex base-band notation as

$$y(t) = \sum_{n=0}^{N_C-1} x(n) e^{j2\pi n \Delta f_0 t}, \qquad t \in [0, T_0] \tag{4.1}$$

with $\Delta f_0 = 1/T_0$, T_0 being the symbol duration of OFDM, $j = \sqrt{-1}$. $x(n)$ is the information-bearing message symbol that modulates the nth subcarrier ($n = 0, \ldots, N_C - 1$), and N_C is the number of subcarriers. Since the minimum frequency spacing Δf_0 between adjacent subcarriers is $1/T_0$, the normalized symbol duration of the OFDM signal is equal to or larger (with additional guard interval T_g) than one. Usually, the OFDM receiver utilizes the whole duration ($\Delta f_0 T_0$=1) of the OFDM signal, except the guard interval (GI), to recover the message symbols. It has been shown that for some types of high-compaction multicarrier modulation (HC-MCM) [61]-[64], we can recover the message symbols even when only a partial

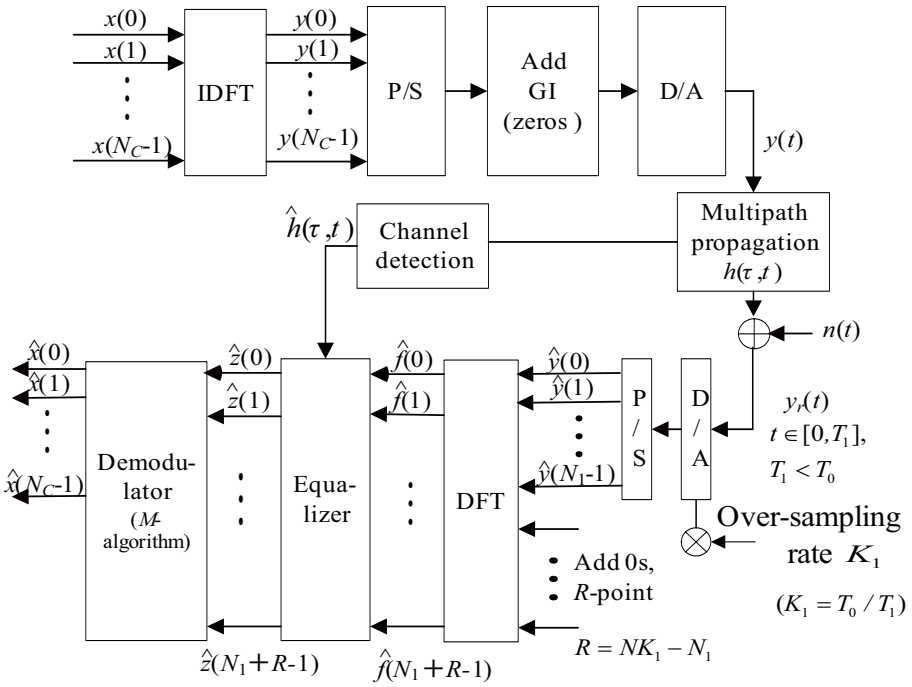

Fig. 4.1 Transmitter and receiver for OFDM system with partial signal.

duration of the OFDM signal can be utilized at the receiver.

Figure 4.1 shows the transmitter and receiver for the OFDM system with a partial signal. $x(n)(n = 0, ..., N_C - 1)$ is a message-bearing subcarrier symbol that takes a complex value to modulate a corresponding subcarrier. After the inverse discrete Fourier transform (IDFT) and parallel-to-serial (P/S) conversion process, several zeros are padded as the postfix GI to alleviate the influence of multipath fading. The duration of zero postfix (ZP) is T_g. The reason we choose ZP as GI is that such a method simplifies the demodulation and equalization of the receiver [65]. After digital-to-analog (D/A) conversion, the whole OFDM signal $y(t)$ $(t \in [0, T_0 + T_g])$ is transmitted into the channel.

Suppose that the impulse response $h(t)$ of the fading channel is

$$h(t) = \sum_{i=1}^{L_P} A_i e^{j\theta_i} \delta(t - \tau_i) \quad t \in [0, T_0 + T_g], \tag{4.2}$$

where L_P means the number of paths and each path has the relative path delay $\tau_i(\tau_1 \leq$

$\tau_2 \leq \ldots \leq \tau_{L_P} < T_g$). $A_i = A_i(t)$ and $\theta_i = \theta_i(t)$ are the slowly Rayleigh-fading amplitude attenuation and phase rotation of each path. We assume A_i and θ_i are constant during each OFDM symbol duration.

Suppose that only a portion of the OFDM signal, $y_r(t)$ ($t \in [0, T_1](T_1 \leq T_0)$), can be utilized in the receiver. $y_r(t)$ can be represented as

$$\begin{aligned} y_r(t) &= h(t) \otimes y(t) + n(t) \\ &= \sum_{i=1}^{L_P} A_i e^{j\theta_i} y(t - \tau_i) + n(t) \quad t \in [0, T_1], \end{aligned} \tag{4.3}$$

where $n(t)$ is the additive white Gaussian noise (AWGN).

The receiver generates N_1 discrete-time samples, $\hat{y}_r(m)(m = 0, \ldots, N_1 - 1)$, from the received signal $y_r(t)$ after analog-to-digital (A/D) conversion with oversampling rate K_1. We assume $K_1 = T_0/T_1$. The N_1 received samples, $\hat{y}_r(m)$, followed by R zeros yield $\hat{f}(n)(n = 0, \ldots, N_1 + R - 1)$ by DFT, as shown in Fig. 4.1 ($R = K_1 N_C - N_1$, where R is the number of samples corresponding to the vanished period of the entire OFDM signal). It should be pointed out that the relation $K_1 = T_0/T_1$ is not necessary and we can set arbitrary integers for K_1 and R such that the relations $N_1/(R+N_1)$=T_1/T_0 and $N_C \leq N_1$ hold. Then the DFT outputs $\hat{f}(n)(n = 0, \ldots, N_1 + R - 1)$ are equalized with the estimation $\hat{h}(t)$ of the channel impluse response $h(t)$. The goal of equalization is to reduce the multipath interference and we adopt the zero-forcing equalizer as described below.

Suppose each path delay τ_i corresponds to the duration of $N_{\tau_i}(i = 1, \ldots, L_P)$ samples after A/D conversion. At the receiver front, discrete-time samples $\hat{y}_r(m)(m = 0, \ldots, N_1 - 1)$ of the received signal $y_r(t)$ are

$$\begin{aligned} \hat{y}_r(m) = &\sum_{i=1}^{L_P} A_i e^{j\theta_i} \sum_{k=0}^{N_C - 1} x(k) e^{j\frac{2\pi k(m - N_{\tau_i})}{N_1 + R}} \\ &\times [u(m - N_{\tau_i}) - u(m - N_1 + 1)] + n(m), \end{aligned} \tag{4.4}$$

where $n(m)$ is the discrete-time sample of $n(t)$ and $u(m)$ is the unit step function. Therefore, after DFT operation, as shown in Fig. 4.1, the receiver output $\hat{f}(n)(n = 0, \ldots, N_1 + R - 1)$ can be expressed as

$$\hat{f}(n) = \frac{1}{N_1 + R}\Big(\sum_{i=1}^{L_P} A_i e^{j\theta_i} \sum_{k=0}^{N_C-1} x(k) e^{-j\frac{2\pi n N_{\tau_i}}{N_1+R}} \times \sum_{m=0}^{N_1-N_{\tau_i}-1} e^{j\frac{2\pi m(k-n)}{N_1+R}} + n'(n)\Big), \tag{4.5}$$

where $n'(n)$ is the DFT output of $n(m)$.

Suppose that $H(f)$ is the frequency response of channel $h(t)$ and its discrete representation is $H(n)(n = 0, \ldots, N_1 + R - 1)$, where $H(n) = H(f)|_{f=n\Delta f_0}$. Then the zero-forcing equalizer can be defined as

$$H_{ZF}(n) = \frac{1}{H(n)} = \left(\frac{1}{N_1 + R} \sum_{i=1}^{L_P} A_i e^{j\theta_i} e^{-j\frac{2\pi n \tau_i}{T_0}} \right)^{-1}. \tag{4.6}$$

After being passed through the equalizer, the received signal $\hat{f}(n)$ will be changed to $\hat{z}(n)$. $\hat{z}(n)(n = 0, \ldots, N_1 + R - 1)$ can be expressed as

$$\begin{aligned} \hat{z}(n) &= \hat{f}(n) \times H_{ZF}(n) \\ &= \frac{\sum_{i=1}^{L_P} A_i e^{j\theta_i} \sum_{k=0}^{N_C-1} x(k) e^{-j\frac{2\pi n \tau_i}{T_0}} \sum_{m=0}^{N_1-N_{\tau_i}-1} e^{j\frac{2\pi m(k-n)}{N_1+R}} + n'(n)}{\sum_{i=1}^{L_P} A_i e^{j\theta_i} e^{-j\frac{2\pi n \tau_i}{T_0}}}. \end{aligned} \tag{4.7}$$

For a multipath fading channel, the transmitted OFDM signals will be superposed by L_P signals. Figure 4.2 illustrates the received signals over a two-path fading channel (the complex amplitude of each path is $A_1 e^{j\theta_1}$ and $A_2 e^{j\theta_2}$ in Fig. 4.2). Suppose that one OFDM time-domain signal $y_{11}(t)(t \in [t_1, t_4])$ is transmitted over this channel and the receiver uses a partial signal $y_r(t)$ $(t \in [t_1, t_3], T_1 = (t_3 - t_1))$ to demodulate message symbols. From Fig. 4.2, $y_r(t)$ $(t \in [t_1, t_3])$ is the sum of the first-path partial

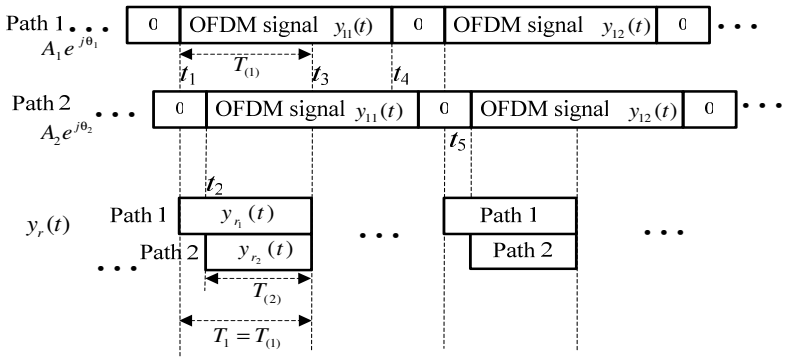

Fig. 4.2 Two-path fading channel.

signal $y_{r_1}(t)(t \in [t_1, t_3])$ and the second-path partial signal $y_{r_2}(t)(t \in [t_2, t_3])$. We use $T_{(i)}$ to represent the partial duration for the ith partial signal in a multipath channel. Therefore, $\Delta f_0 T_{(1)} = (t_3 - t_1)/(t_4 - t_1)$ and $\Delta f_0 T_{(2)} = (t_3 - t_2)/(t_4 - t_1) = \Delta f_0 T_{(1)} - \tau_1/T_0)$, where $\tau_1 = t_2 - t_1$ is the relative delay. Then, $y_r(t)$ $(t \in [t_1, t_3])$ can be represented as

$$y_r(t) = y_{11}(t)A_1 e^{j\theta_1} + y_{11}(t-\tau)A_2 e^{j\theta_2}. \tag{4.8}$$

Therefore, for an L_P-path multipath channel, received signal $y_r(t)$ in Fig. 4.2 will be superposed with L_P partial signals, and $\Delta f_0 T_{(1)} \geq \Delta f_0 T_{(2)} \geq \ldots \geq \Delta f_0 T_{(L_P)}(\Delta f_0 T_1 = \Delta f_0 T_{(1)})$. The differences between $\Delta f_0 T_{(i)}$ and τ_i/T_0 can be decreased by increasing T_0. From (4.7), if the values of $\tau_i/T_0 (= N_{\tau_i}/(N_1 + R))$ for $i = 1, \ldots, L_P$ are approximately identical, the multipath interference can almost completely be removed. Suppose that τ_i/T_0 in (4.7) can be approximated as $\tau_i/T_0 << 1$ and $N_{\tau_1}/(N_1+R) \approx N_{\tau_2}/(N_1+R) \approx \ldots \approx N_{\tau_{L_P}}/(N_1 + R)$. In this case, (4.7) is reduced to

$$\begin{aligned}
\hat{z}(n) &= \sum_{m=0}^{N_1 - N_{\tau_1} - 1} \sum_{k=0}^{N_C - 1} x(k) e^{j\frac{2\pi m(k-n)}{N_1+R}} + n''(n) \\
&= \sum_{k=0}^{N_C-1} x(k) \frac{1 - e^{j\frac{2\pi(N_1 - N_{\tau_1})(k-n)}{N_1+R}}}{1 - e^{j\frac{2\pi(k-n)}{N_1+R}}} + n''(n) \qquad (4.9) \\
&= \sum_{k=0}^{N_C-1} x(k) \frac{1 - e^{j2\pi(k-n)\frac{T_1-\tau_1}{T_0}}}{1 - e^{j\frac{2\pi(k-n)}{N_1}\frac{T_1-\tau_1}{T_0}}} + n''(n), \qquad (4.10)
\end{aligned}$$

where $n''(n) = n'(n)/(\sum_{i=1}^{L_P} A_i e^{j\theta_i} e^{-j\frac{2\pi n \tau_i}{T_0}})$.

Finally, the estimates $\hat{x}(n)(n = 0, \ldots, N_C - 1)$ of the message symbols $x(n)$ are recovered through the demodulation stage with the samples $\hat{z}(n)(n = 0, \ldots, N_1 + R - 1)$. Due to intercarrier interference (ICI), which is evident in (4.10), a reasonable approach for attaining a good demodulation performance will be the maximum likelihood sequence estimation (MLSE). However, the demodulation complexity (C_p) of MLSE increases exponentially with the number of subcarriers N_C and modulation type P(BPSK: $P = 2$; QPSK: $P = 4, \ldots$), that is, $C_p = P^{N_C}$, which is impractical for the demodulation for large N_C. But for large N_C, a demodulation method using the M-algorithm, in which the calculation complexity preserves a linear increase with N_C, has been proposed [64]. In this study, we adopt the M-algorithm to demodulate the message symbols.

4.2.2 M-Algorithm for OFDM System with Partial Signal

We briefly introduce the M-algorithm to demodulate the partial OFDM signal. Readers can find the detailed process and performance in [64].

Step 1: Generate partial message vectors $\mathbf{X}_u^{(1)} = [x(0), \ldots, x(U-1), \ldots, 0](u = 0, \ldots, P^U - 1;\ U \leq N_C;\ P = 2$ for BPSK, $P = 4$ for QPSK) of length N_C. Utilizing $\mathbf{X}_u^{(1)}$, produce P^U kinds of replica vectors $\mathbf{Z}_u^{(1)} = [z(0), \ldots, z(N_1 + R - 1)]$ by the same operation as shown in Fig. 4.1 without noise and fading. Therefore, the elements $z(l)(l = 0, \ldots, N_1 + R - 1)$ of $\mathbf{Z}_u^{(1)}$ can be expressed as

$$z(l) = \sum_{k=0}^{U-1} x(k) \frac{1 - e^{j2\pi(k-l)\frac{T_1}{T_0}}}{1 - e^{j\frac{2\pi(k-l)}{N_1}\frac{T_1}{T_0}}}. \tag{4.11}$$

Euclidian distances $d_u^{(1)}(u = 0, 1, \ldots, P^U - 1)$ between $\mathbf{Z}_u^{(1)}$ and $\hat{\mathbf{Z}}$ are first evaluated using their elements partially as

$$d_u^{(1)} = \left(\sum_{l=0}^{U-1} |z(l) - \hat{z}(l)|^2 + \sum_{l=N_C}^{N_1+R-1} |z(l) - \hat{z}(l)|^2 \right)^{1/2}. \tag{4.12}$$

Then $M(M < P^U)$ kinds of $\mathbf{Z}_u^{(1)}$, which indicate small Euclidean distances, are chosen as $\mathbf{Z}^{(1)(r)}(r = 0, 1, 2, ..., M-1)$ from among P^U kinds of $\mathbf{Z}_u^{(1)}$, and vectors $\mathbf{X}_u^{(1)}$ which produce $\mathbf{Z}^{(1)(r)}$ are stored as $\mathbf{X}^{(1)(r)}$ $(r = 0, \ldots, M-1)$. The elements of vectors $\mathbf{X}^{(1)(r)}$ become candidates for the partial message symbols $\hat{x}(0), \ldots, \hat{x}(U-1)$.

Step 2: Redefine partial message vectors $\mathbf{X}_w^{(2)}(w = 0, \ldots, MP-1)$ of length N_C as $\mathbf{X}_w^{(2)}$=$[\mathbf{X}^{(1)(r)}, x(U), 0, \ldots, 0]$. Therefore, MP kinds of replica vectors $\mathbf{Z}_w^{(2)} = [z(0)...z(N_1+R-1)]$ are produced. Euclidian distances $d_w^{(2)}(w = 0, \ldots, MP-1)$ between $\mathbf{Z}_w^{(2)}$ and $\hat{\mathbf{Z}}$ are evaluated by

$$d_w^{(2)} = \left(\sum_{l=0}^{U} |z(l) - \hat{z}(l)|^2 + \sum_{l=N_C}^{N_1+R-1} |z(l) - \hat{z}(l)|^2 \right)^{1/2}. \tag{4.13}$$

Then, M kinds of $\mathbf{Z}_w^{(2)}$, which indicate small Euclidian distances, are chosen as $\mathbf{Z}_w^{(2)(r)}(r = 0, \ldots, M-1)$ from among MP kinds of $\mathbf{Z}_w^{(2)}$, and vectors $\mathbf{X}_w^{(2)}$ which produce $\mathbf{Z}_w^{(2)(r)}$ are stored as $\mathbf{X}^{(2)(r)}(r = 0, \ldots, M-1)$. The elements of vectors $\mathbf{X}^{(2)(r)}$ become new candidates for the partial message symbols $\hat{x}(0), \ldots, \hat{x}(U)$. Thus, $\hat{x}(U)$ is added to the candidates obtained in Step 1.

Step 3: MP kinds of $\mathbf{Z}_w^{(N_C-U+1)}$ are obtained by repeating Step 2 $N_C - U$ times. Finally, vector $\mathbf{X}^{(N_C-U+1)}$, which produces the minimum Euclidian distance, contains all the message symbols $\hat{x}(0), \ldots, \hat{x}(N_C-1)$.

From three steps, we can find that the M-algorithm can keep demodulation complexity as $C_p = P^U + (N_C - U)MP$ and C_p preserves a linear increase with N_C. The M-algorithm produces the replica vectors $\mathbf{Z}_u^{(i)}$ for each iteration according to (4.11). It should be pointed out that the HC-MCM system in [63] has the same $\Delta f_0 T_{(i)}(i = 1, \ldots, L_P)$ since the transmitter of HC-MCM utilizes the partial signal with ZP-GI to transmit message symbols $x(n)$ in Chapter 3. However in this Chapter, only the receiver adopts the partial signal to demodulate $x(n)$. This causes different values for $\Delta f_0 T_{(i)}(i = 1, \ldots, L_P)$ over the multipath channel. Nevertheless the algorithm

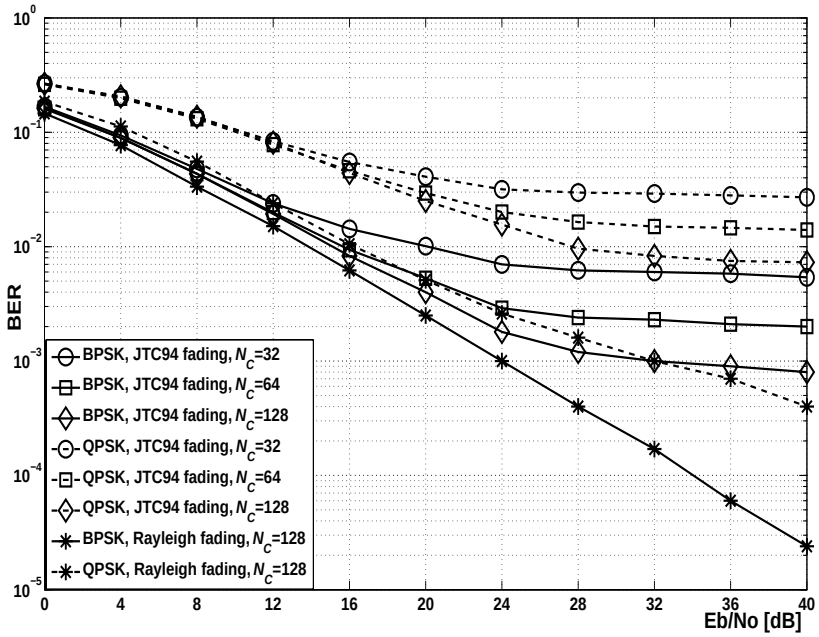

Fig. 4.3 BER of OFDM system with partial signal, $\Delta f_0 T_1$=0.5.

can achieve an acceptable performance if relative values of τ_i/T_0 are small enough to make $\Delta f_0 T_{(i)}$ ($i \in [1, \ldots, L_P]$) almost the same over all the paths of the channel. Note that τ_i/T_0 can be decreased with the increase of T_0 (or equivalently, N_C).

4.2.3 Simulated Performance of OFDM System with Partial Signal over Multipath Fading Channel

We choose the fading channel model of JTC' 94 (indoor residential B) [66] to simulate the performance of our system. The duration of each OFDM signal is T_S ($T_S = T_0 + T_g$). The receiver utilizes the partial signals with durations $\Delta f_0 T_1 = 0.5$ and 0.625 to demodulate all symbols $x(n)$ ($n = 0, 1, ..., N_C - 1$) by the M-algorithm. The common specifications of simulations are listed in Table 4.1.

Figure 4.3 shows the BER performance for $\Delta f_0 T_1 = 0.5$, which means half the OFDM signal for the first path, which results in $\Delta f_0 T_{(i)} < 0.5$ for $i \in [2, \ldots, L_P]$. We assume that the receiver knows the channel information and carries out the zero-forcing

Table 4.1 Specifications of simulations for OFDM system with partial signal over multipath fading channel.

System Item	Parameter
Subcarrier modulation	BPSK, QPSK
Synchronization	Complete
Channel type	JTC' 94 (indoor residential B) (L_P=8)
Equalization	zero-forcing equalization
Supported symbol rate (OFDM symbol/second)	250k ($T_0 + T_g = 4\mu$s), N_C=32; 125k ($T_0 + T_g = 8\mu$s), N_C=64; 62.5k ($T_0 + T_g = 16\mu$s), N_C=128
Relative delay for each path (ns)	0, 50, 100, 150 200, 250, 300, 350
Relative power attenuation for each path (dB)	0, -2.9, -5.8, -8.7, -11.6, -14.5, -17.4, -20.3
Maximum Doppler frequency shift f_D (Hz)	20
Duration of zero guard signal	T_g=0.25T_0
$\Delta f_0 T_1$	0.4, 0.5, 0.625, 1
Noise	additive white Gaussian noise
Values U, M for M-algorithm	BPSK U=4, $M = 16$; QPSK U=2, $M = 16$

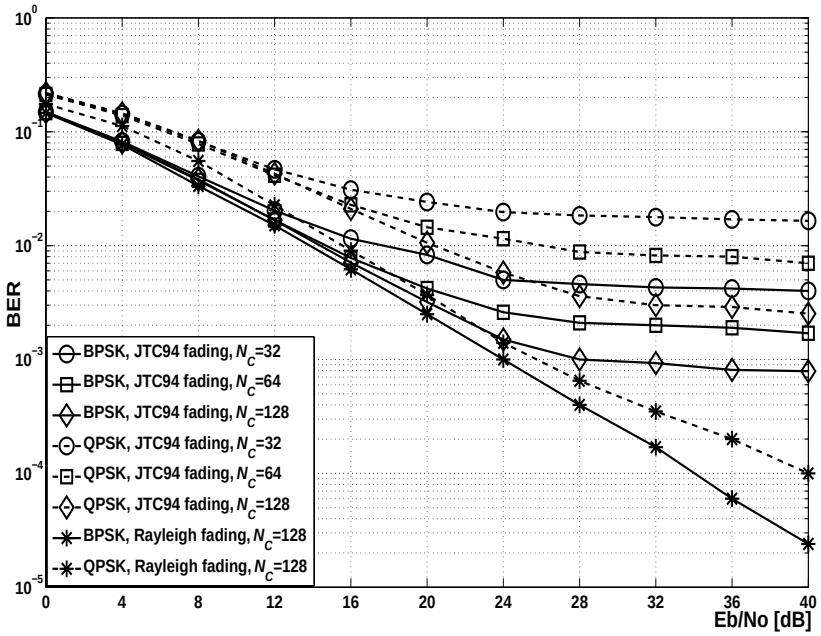

Fig. 4.4 BER of OFDM system with partial signal, $\Delta f_0 T_1$=0.625.

equalization. From Fig. 4.3, we confirm that the partial signal can be used to demodulate all symbols $x(n)$ $(n = 0, 1, ..., N_C - 1)$ with the M-algorithm. Particularly for BPSK, we can achieve a better BER performance. We also can confirm that the performance is improved with increasing N_C. The reason is that τ_i/T_0 and the differences between $\Delta f_0 T_{(1)}$ and $\Delta f_0 T_{(L_P)}$ are decreased. On the other hand, from (4.7), due to the effect of different τ_i/T_0, the equalizer cannot totally remove ISI of the multipath channel. Therefore, an error floor appears for large SNR. Such an influence is severer for QPSK than that for BPSK.

Figure 4.4 shows the BER performance for $\Delta f_0 T_1 = 0.625$. Compared with the results in Fig. 4.3, the performance is improved, particularly for QPSK-modulated OFDM. We also give the simulated performance of the system over a one-path Rayleigh-fading channel (N_C=128), which can be regarded as the performance of the system over the multipath fading channel with N_C increasing to infinity. The results also prove that we can improve the system performance by increasing N_C.

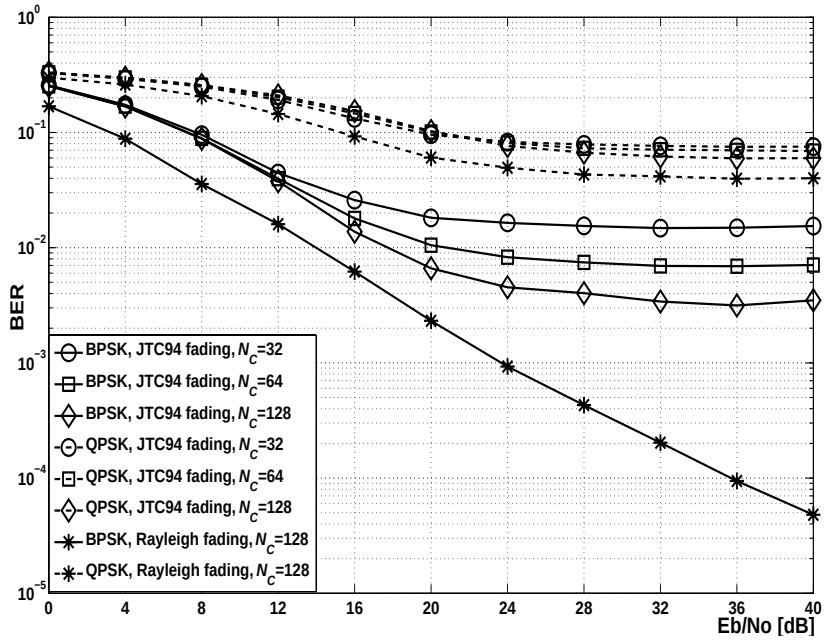

Fig. 4.5 BER of OFDM system with partial signal, $\Delta f_0 T_1$=0.4.

We assume that the system utilizes the partial OFDM signal to demodulate the data and reconstruct the whole OFDM signal. To achieve better recovery performance, the parameter $\Delta f_0 T_1$ should be adopted appropriately when collision happens. For system design that the proposed method achieves better recovery performance, the value of $\Delta f_0 T_1$ must be in [0.5, 0.625] or similar values which will be described in the following sections. To further evaluate the effectiveness and performance limit of the system that utilizes the partial OFDM signal, we simulate the BER performance of OFDM system with partial signal using BPSK and QPSK for $\Delta f_0 T_1$=0.4 in Fig. 4.5 and for $\Delta f_0 T_1$=1 in Fig. 4.6, respectively. The BER performance degrades severely for QPSK modulation with $f_0 T_1 = 0.4$, even over a one-path Rayleigh-fading channel (N_C=128). The reason is that ICI is dramatically increased by smaller value of $\Delta f_0 T_1$ and intensify the error propagation during the each iteration of M-algorithm. It should be mentioned that for $\Delta f_0 T_1 = 1$, the error floor will still appear because $\Delta f_0 T_1 = 1$ means the intact OFDM signal for the first path, but $\Delta f_0 T_{(i)} < 1$ for $i \in [2, \ldots, L_P]$, which causes the different

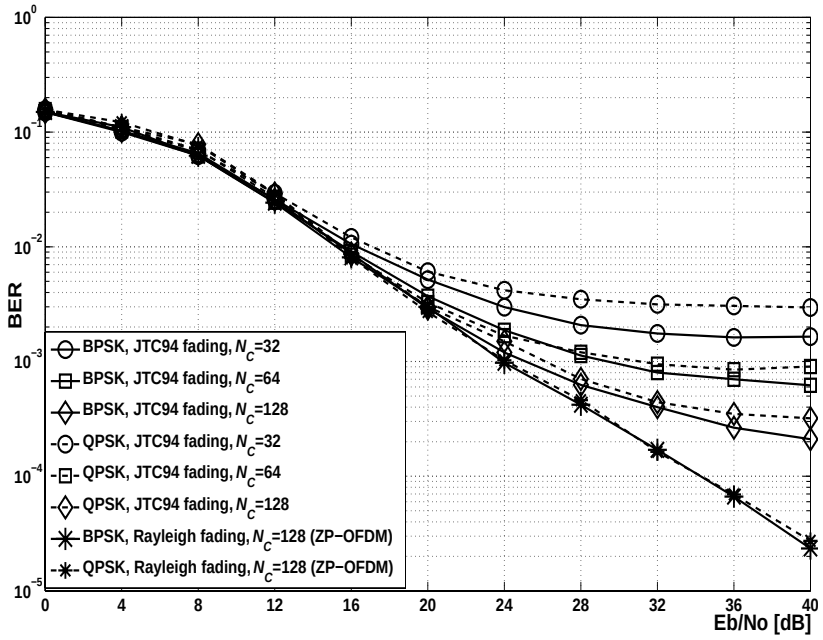

Fig. 4.6 BER of OFDM system with partial signal, $\Delta f_0 T_1$=1.

τ_i/T. Therefore, the equalizer cannot totally remove ISI due to the multipath channel. On the other hand, we also give the simulated BER performance of the system with $\Delta f_0 T_1 = 1$ over a one-path Rayleigh-fading channel (N_C=128). It can be regarded as the performance of the system over the multipath fading channel with N_C increasing to infinity. For $\Delta f_0 T_1 = 1$, the system over a one-path Rayleigh-fading channel can also be treated as the ZP-OFDM [65] system over a one-path Rayleigh-fading. The simulated results also confirm that performance degradation always appears for the different τ_i/T and smaller $\Delta f_0 T_1$.

To further evaluate the system performance, we simulate the packet error rate (PER). Let us use F_n to represent the number of OFDM signals in one packet. We assume that a packet error occurs if more than one of the transmitted data bits in one packet are missdetected. Figure 4.7 shows the PER performance for $\Delta f_0 T_1 = 0.625$. The results show that although the BER under such a condition is large even when Eb/No is beyond 28 dB, bit errors will be concentrated in a small number of packets

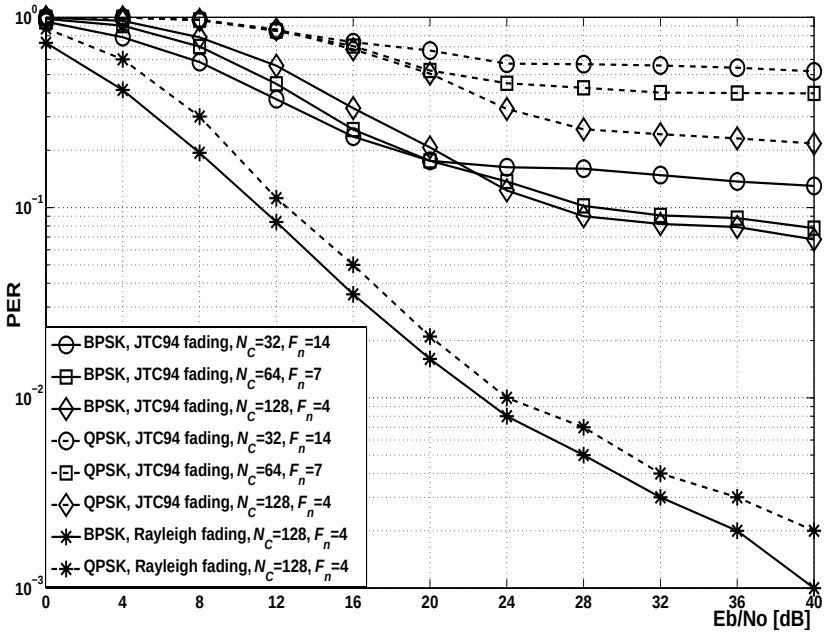

Fig. 4.7 PER of OFDM system with partial signal, $\Delta f_0 T_1$=0.625.

because of worse channel conditions. For example, for BPSK-modulated OFDM with $N_C = 128$ and $F_n = 4$ (each packet can transmit 512 bits), approximately 92% of packets can be correctly demodulated. For $N_C = 128$ and $F_n = 4$ in a QPSK-modulated OFDM system, approximately 81% of packets can be correctly demodulated. Such rates can be improved by increasing N_C.

4.3 Packet Recovery with Partial OFDM Signal

We have described that for OFDM systems, message symbols can be demodulated with the partial OFDM signal. We can utilize this property to recover two collided packets. This method is somewhat similar to the scheme of successive interference cancellation (SIC) [83] which is widely adopted in CDMA systems.

Figure 4.8 illustrates a scenario of the collision of two packets, $y_1(t)$ from user 1 and $y_2(t)$ from user 2. Both packets consist of several OFDM signals, each of which can be expressed by formula (4.1). The duration of each OFDM signal is T_S. We

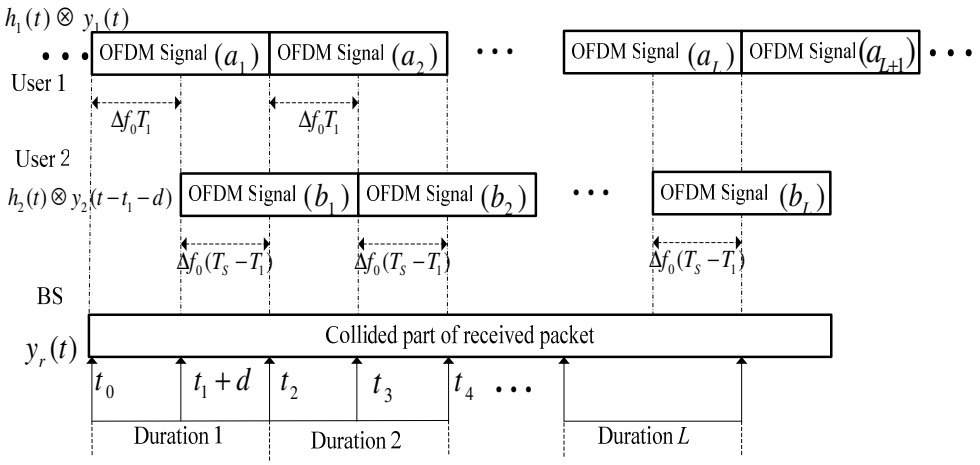

Fig. 4.8 Collisions of two packets.

assume that user 1 is the principal user who is transmitting a long packet and user 2 is a hidden terminal who has just started to build a connection with a short packet at time t_1. Therefore, after the transmission over the respective channels $h_1(t)$ and $h_2(t)$, packet $y_1(t)$ collides with packet $y_2(t)$ at time $t_1 + d$, where d is the transmission delay of user 2. The relative delay of $y_2(t)$ from the first collided OFDM signal a_1 of user 1 is $t_1 + d - t_0 (t_1 \in [t_0, t_2])$. Therefore, the received signal $y_r(t)$ can be represented as

$$y_r(t) = h_1(t) \otimes y_1(t) + h_2(t) \otimes y_2(t - t_1 - d) + n(t). \tag{4.14}$$

$y_r(t)$ can also be represented over $t \in [t_0, t_2]$ as (see also Fig. 4.8)

$$y_r(t) = \begin{cases} h_1(t) \otimes y_1(t) + n(t) & t \in [t_0, t_1 + d] \\ h_1(t) \otimes y_1(t) + h_2(t) \otimes y_2(t - t_1 - d) & \\ \qquad + n(t) & t \in [t_1 + d, t_2]. \end{cases} \tag{4.15}$$

As can be seen from (4.15), there is no collision in $t \in [t_0, t_1 + d]$. Therefore, collided packets $y_1(t)$ and $y_2(t)$ can be recovered iteratively from $y_r(t)$ by the following steps.

(a) By the method described in Sect. 4.2, the receiver (BS) recovers the message symbols carried by OFDM signal a_1, using the partial signal of $y_r(t)$ $(t \in [t_0, t_1 + d])$.

(b) The receiver reconstructs $h_1(t) \otimes y_1(t)(t \in [t_0, t_2])$ with the recovered message symbols and channel information $h_1(t)$, and subtracts it from $y_r(t)$. By this, the receiver can obtain signal $y_r^{'}(t)(t \in [t_1 + d, t_2])$, which is the received signal without OFDM signal a_1.

(c) The receiver recovers the message symbols carried by OFDM signal b_1 using the partial signal of $y_r^{'}(t)$ $(t \in [t_1 + d, t_2])$.

(d) The receiver reconstructs $h_2(t) \otimes y_2(t - t_1 - d)(t \in [t_1 + d, t_3])$ with the recovered message symbols and channel information $h_2(t)$, and subtracts it from $y_r^{'}(t)(t \in [t_1 + d, t_3])$. By this, the receiver can obtain received signal $y_r^{''}(t)(t \in [t_2, t_3])$, which is the received signal without OFDM signal b_1 in $y_r^{'}(t)(t \in [t_1 + d, t_3])$. The new $y_r^{''}(t) = h_1(t) \otimes y_1(t) + n(t)(t \in [t_2, t_3])$ can be treated as $y_r(t)$ in the next duration to recover the message symbols of OFDM signal a_2.

The receiver repeats processes (a) to (d) until all the collided parts of the two packets are recovered (i.e., until OFDM signal a_{L+1} is recovered).

4.4 Some Factors which Influence Performance of Recovery

To achieve better recovery performance, $\Delta f_0 T_1$ and $\Delta f_0(T_S - T_1)$ in Fig. 4.8 should be adopted appropriately. Such a requirement can be realized with the aid of time slots. We assume that all long packets are transmitted at the beginning of time slots, and the short packets are delayed in their transmissions by $t_1 - t_0$ from the beginning of time slots. On the basis of Fig. 4.8 and the above process of collision recovery, we can infer that the performance of recovery depends on the following factors.

4.4.1 Propagation Delay between Transmitters and Receiver

Propagation delay d cannot be a large value. For example, in Fig. 4.8, if t_1+d equals t_2, then $\Delta f_0(T_S - T_1) = 0$. Such a condition will invalidate the recovery method. The maximum delay depends on the allowable maximum transmission distance between BS and transmitters. For wireless LAN or the ad hoc network, the maximum transmission distance is often assumed to be 30 [m] to 60 [m] for an indoor situation and within 300 [m] to 600 [m] for the outdoor case. Thus d is 0.1 [μs] or 0.2 [μs], at most, in the indoor case and 1 [μs] or 2 [μs] in the outdoor case. Compared with the duration of the OFDM signal, for example, 4 [μs] in Table 4.1, the delay changes $\Delta f_0 T_1$ and $\Delta f_0(T_S - T_1)$ only 2.5% to 5% in the indoor situation. Such values will not significantly decrease the performance of the recovery. Furthermore, the system can adopt a large T_0 (or equivalently, N_C) to increase the duration of the OFDM signal. Therefore, if the maximum propagation distance is small, such an influence can be negligible.

4.4.2 Detection of Collision Position

The receiver must detect the position of collision, which means the position of t_1+d in Fig. 4.8. On the basis of the recovery method and Fig. 4.8, BS can utilize partial duration $(t_1 - t_0)/T_0$ of OFDM signal a_1 of user 1 to remove it from $y_r(t)$. After that, BS can detect $t_1 + d$. Therefore, the first step of the detection of the collision position is equivalent to the detection of collision occurrence.

One simple detection method of collision occurrence is that BS checks the received signal power over the GI signal of user 1. Since a long packet utilizes the ZP-GI T_g, which is longer than τ_{L_P}, and the signals of late paths undergo high power attenuations, the received signal $y_r(t)$ will be only the noise component during the late period of the GI if there is no collision from user 2. Therefore, if the received power of $y_r(t)$ increases

rapidly during the GI of user 1, BS can assume that collision has occurred and can carry out the recovery algorithm using partial duration $(t_1 - t_0)/T_0$ of the OFDM signal of user 1. Then BS removes user 1's signal during $t \in [t_0, t_2]$ and checks the propagation delay d of user 2. Such a simple detection can be used even in the situation with a weak near-far effect. We will describe a preamble-based method of obtaining d in the following subsection. Otherwise, if there is no distinct increase of power during the GI of user 1, the receiver can assume that no collision happens. Then the receiver can demodulate the data of the long packet using one-tap equalizer, which is identical to the ZP-OFDM system [65].

4.4.3 Estimation of Channel Information $h_2(t)$ of User 2

Generally speaking, the packet utilizes preamble to obtain channel information; for example, IEEE 802.11a adopts the 16 [μs] preamble, which includes the duration of four OFDM signals, to estimate the channel information. Figure 4.9(a) illustrates the preamble structure specified in IEEE 802.11a [66]. The preamble consists of ten identical short training symbols (D_1), each of which is 0.8 [μs], and two identical long training symbols (S), each of which is 3.2 [μs] plus a 1.6 [μs] prefix (G_1) which precedes the long training symbols. The short training symbols are used for timing, signal detection, automatic gain control (AGC) level setting, coarse timing synchronization and coarse carrier frequency offset correction by auto-correlation and cross-correlation methods [84]. The long training symbols are used for fine carrier frequency offset and channel estimation.

The preamble of IEEE 802.11a cannot be used for user 2 because the short training symbols that are utilized to achieve coarse frequency and timing synchronization are corrupted. Fortunately, there are many preamble designs for OFDM systems [85]-[87], particularly, Minn etal. utilized one OFDM training symbol to estimate the channel in-

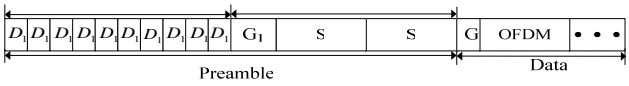

(a) IEEE 802.11a preamble and packet format.

(b) Packet format that includes Minn etal.'s preamble [88],[89].

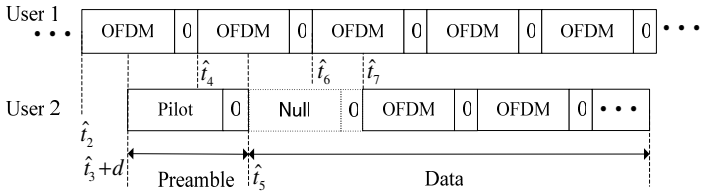

(c) Preamble recovery from the collision.

Fig. 4.9 Packet format and preamble recovery from the collision.

formation and to implement the frequency and timing synchronization [88], [89]. Figure 4.9(b) shows the packet format that is Minn etal.'s preamble and data part. This preamble uses one specifically designed training symbol having a steep rolloff timing metric trajectory. It can implement the frequency, timing synchronization and channel estimation iteratively and can be adopted in many types of time-varying multipath fading channels. The simulated performances of timing, frequency synchronization and channel estimation can be found in [88]. Minn etal.'s also presented a sliding-observation-vector-based maximum-likelihood combined timing and frequency synchronization and channel estimation method using a repetitive training OFDM signal [89].

We can utilize this preamble to estimate $h_2(t)$ and implement the timing and fre-

quency synchronization. Figure 4.9(b) shows the packet format that includes one pilot OFDM signal as the preamble and several OFDM signals to transmit the data. To improve the performance of estimation, the first OFDM signal of the data part only transmits a null OFDM signal. This structure of the preamble also simplifies the detection of collision occurrence.

Suppose that BS knows the impulse response $h_1(t)$ and that user 2 starts the transmission of a short packet at $\hat{t}_3$. After propagation delay d, it collides with the long packet. The pilot training symbol can be obtained by the following process. Using the partial OFDM signals of user 1 during $[\hat{t}_2, \hat{t}_3]$ and $[\hat{t}_5, \hat{t}_6]$ ($\hat{t}_3$ is a known parameter for the BS and transmitters, and $\hat{t}_5 = \hat{t}_3 + d + T_S$ can be determined from the maximum propagation delay), BS can remove two OFDM signals (during $[\hat{t}_2, \hat{t}_6]$) of user 1. Then the preamble of user 2 (during $[\hat{t}_3 + d, \hat{t}_5]$) can be obtained. Utilizing the methods described in [88] and [89], BS can estimate channel information $h_2(t)$, implement the frequency and timing synchronization, and then obtain the timing of collision d.

4.5 Simulated Results of Collision Recovery

In this section, we present the simulated results of the collision recovery described in the above section. It is assumed that each user experiences independent multipath fading, and the fading model is JTC'94 (indoor residential B, delay spread=70ns), which has been described in Table 4.1. The common specifications of simulations are identical to those listed in Table 4.1. The duration of time slots is an integer multiple of T_S, and the long packets include 250 OFDM signals which are transmitted at the beginning of time slots. User 2 delays short packet transmission by $0.5T_S$ from the beginning of time slots. The maximum transmission distance between BS and transmitters is 30 [m]. These conditions cause $\Delta f_0 T_1$, $\Delta f_0 T_2 = \Delta f_0 (T_S - T_1)$ of Fig. 4.8 to be 0.625.

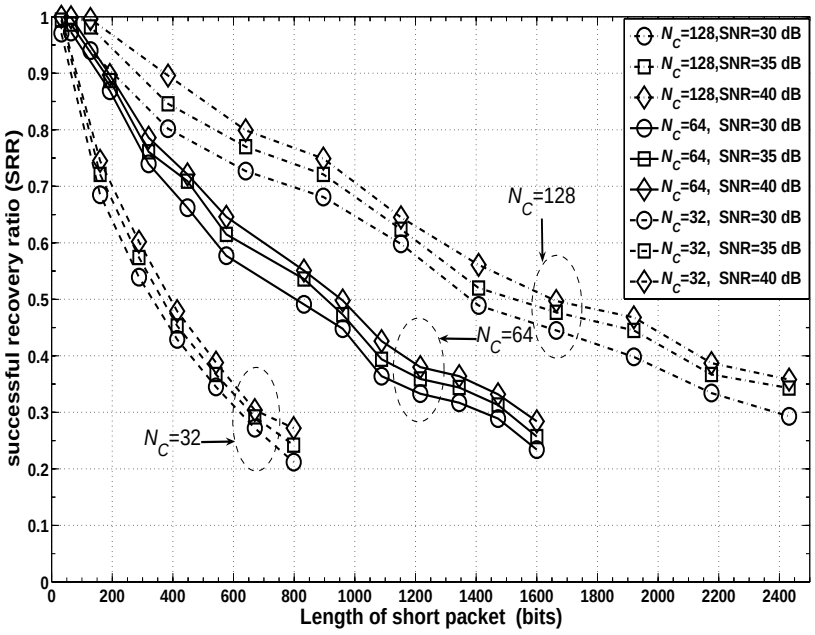

Fig. 4.10 Performance of collision recovery (user 1 and user 2 transmit packets with BPSK-modulated OFDM).

Each user utilizes an identical duration T_S. We assume that BS implements timing and frequency synchronization and obtains $h_1(t)$ and $h_2(t)$ using Minn etal's preamble, the performance of which has been theoretically proved and simulated [88], [89]. Such a preamble can also be utilized to detect the occurrence of collision, as can be seen from Fig. 4.9(c).

4.5.1 Simulated Results of Two Users with Equal SNR and Identical Modulation

We give the simulated results for different N_C and SNR in the case where two users transmit data with BPSK in Fig. 4.10 and QPSK in Fig. 4.11, respectively. The simulated results show that, for different lengths of the short packet (without the length of preamble), the collided part can be recovered with a different successful recovery ratio (SRR) which is defined as the ratio of the times of successful recovery of collided parts

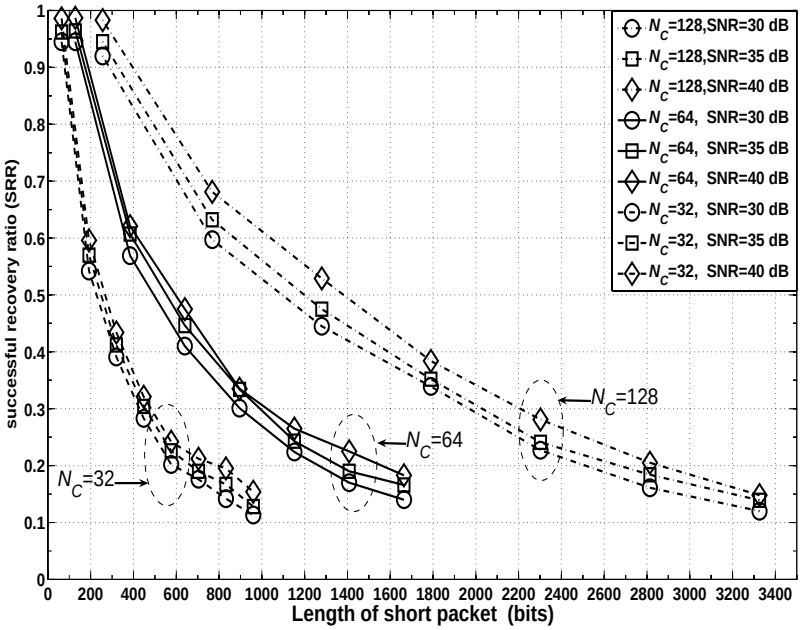

Fig. 4.11 Performance of collision recovery (user 1 and user 2 transmit packets with QPSK-modulated OFDM).

of both packets to the times of all collisions. It is assumed that N_C is 32, 64 or 128. Due to the error floor of the demodulation, SNR has little influence on SRR when SNR varies from 30 [dB] to 40 [dB]. N_C=128 can yield the best performance in Fig. 4.10 and Fig. 4.11 because precise equalization can be achieved as described in Sect. 4.2.

4.5.2 Simulated Results of Two Users with Equal SNR and Different Modulation

It is often assumed that the long packet transmits data with QPSK to achieve a higher transmission rate, and that a short packet, such as ACK, RTS or CTS, utilizes BPSK to send control signals. Figure 4.12 shows the simulated results of collision recovery versus length of short packet (without the length of preamble), it indicates the similar performance of SRR shown in Figs. 4.10 and 4.11.

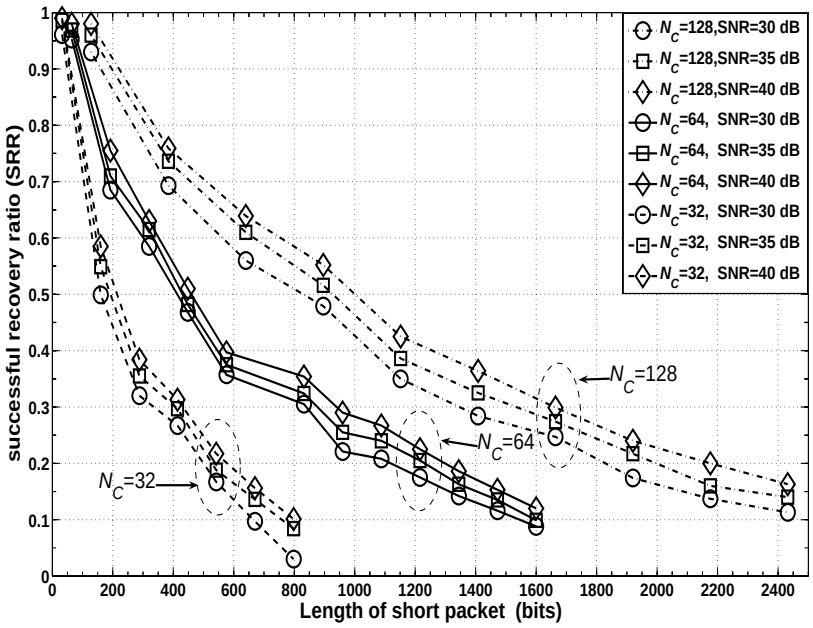

Fig. 4.12 Performance of collision recovery (user 1 transmits packet with QPSK-modulated OFDM, user 2 transmits short packet with BPSK-modulated OFDM).

4.5.3 Simulated Results of Two Users with Weak Near-far Effect

Figures 4.13 and 4.14 show the simulated SRR in the presence of a weak near-far effect. N_C is assumed to be 128 in all simulations. We chose the values of SNR for user 1 to be 30, 35, or 40 [dB] and SINR for user 1 to be -10, -5, 5, or 10 [dB] in Fig. 4.13, which shows the recovery performance versus length of short packet (without the length of preamble). QPSK is assumed for both users. The results indicate that SRR with (SNR, SINR) = (40 [dB], 10 [dB]) for user 1 is approximately identical to that with (SNR, SINR) = (30 [dB], -10 [dB]) for user 2 with increasing length of the short packet. When the packet for user 2 is extremely short, for example, one OFDM signal (without the length of preamble), the different powers of $y_r(t)(t \in [\hat{t}_6, \hat{t}_7]$ in Fig. 4.9(c)) for SINR=10 [dB] and -10 [dB] make SRR different.

Figure 4.14 shows the SRR performance versus length of short packet (without the

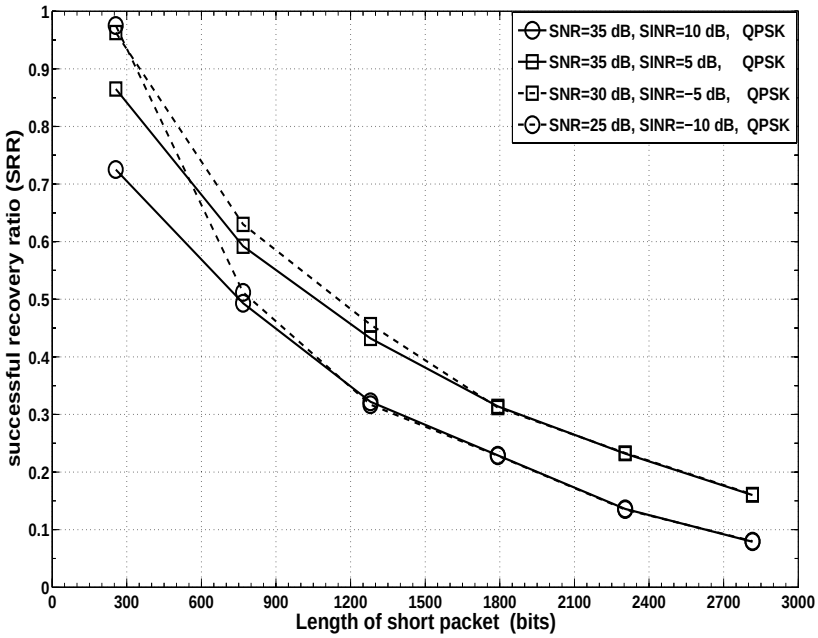

Fig. 4.13 Performance of collision recovery (both packets utilize QPSK-modulated OFDM; the values of SINR and SNR are those for user 1).

length of preamble) of the case that user 1 transmits a long packet by QPSK-modulated OFDM and user 2 transmits a short packet by BPSK-modulated OFDM. Because of the different modulations, SINR=10 [dB] and -10 [dB] for user 1 cannot yield the equal SRR when the length of the short packet increases. However, both Figs. 4.13 and 4.14 show that better SRR can be obtained under a weaker near-far condition.

4.6 Performance of OFDM System with Partial Signal Using 8- and 16-QAM Modulation over the Multipath Channel

In the proposed method, we use the M-algorithm to reduce the complexity of MLSE when only a portion of transmitted signal is received. The M-algorithm can keep demodulation complexity (C_p) as $P^U + (N_C - U)MP$ for each partial OFDM

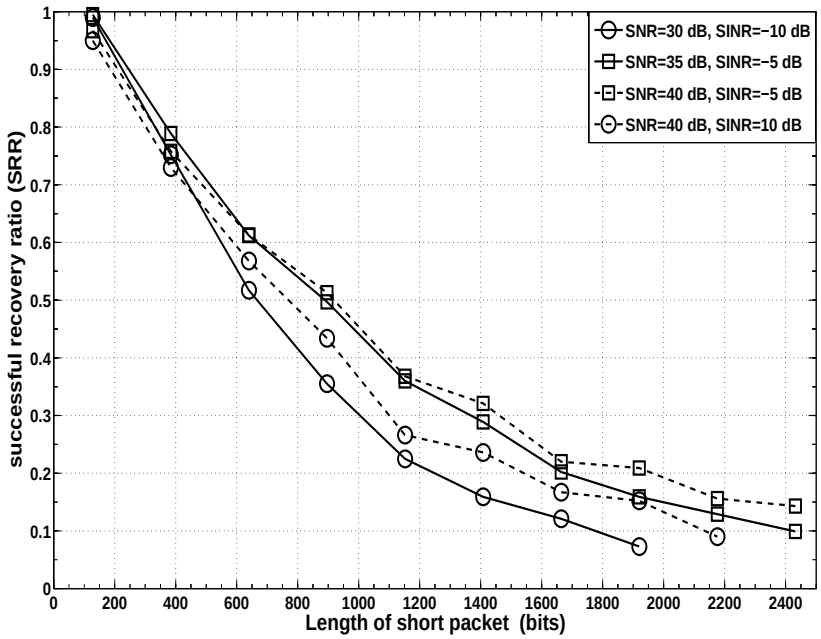

Fig. 4.14 Performance of collision recovery (user 1 transmits packet with QPSK-modulated OFDM but user 2 transmits a short packet with BPSK-modulated OFDM; the values of SINR and SNR are those for user 1).

signal, where P, U and M, are modulation type, depth of initial candidate path and number of survivors for each iteration, respectively.

The BER and PER performance for the system using BPSK and QPSK modulations is acceptable, but there will be large degradation of performance using the 16-QAM or 64-QAM modulation. The reason derives from the main factor: the acceptable demodulation complexity or the number of survivors for each iteration (parameter M) of the M-algorithm. Generally speaking, larger M will achieve better BER or PER performance but increase the demodulation complexity. When the system adopts 8-QAM (P=8) or 16-QAM (P=16) modulation, which increases the value of P, for the identical demodulation complexity to that of using BPSK modulation or QPSK modulation, the BER or PER performance will be dramatically degraded. Even when the M-algorithm moderately increases the value of M, the error propagation will still decrease the BER

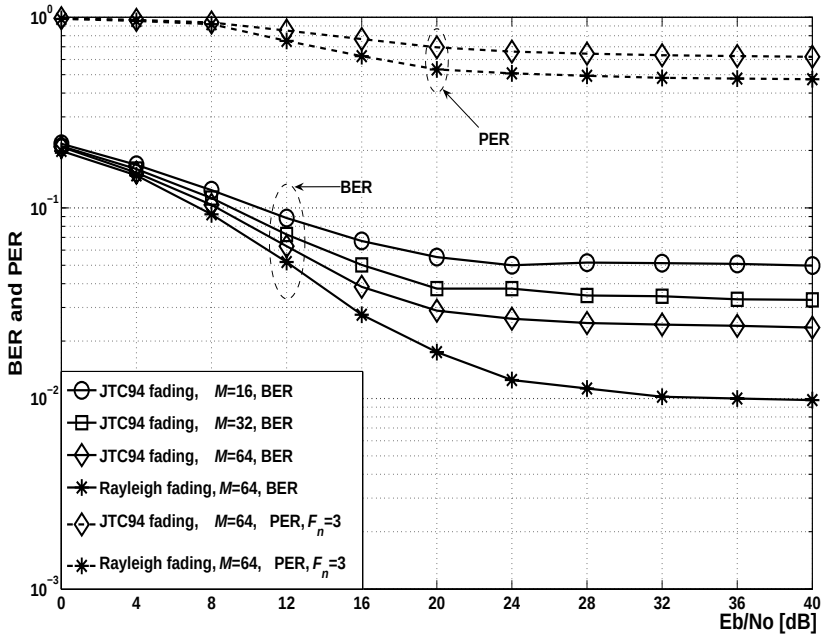

Fig. 4.15 BER and PER performance of 8-QAM-modulated OFDM system with partial signal, $\Delta f_0 T_1$=0.625, $U = 2$, N_C=64.

or PER performance for large N_C.

Figures 4.15 and 4.16 show the BER and PER performance of 8-QAM-modulated OFDM system with partial signal, respectively. The common specifications of simulations are identical to that listed in Table 4.1. The system chooses $\Delta f_0 T_1$=0.625, 0.75 and N_C=64. For each value $\Delta f_0 T_1$, we make M (the number of survivors for each iteration) be 16, 32 and 64, respectively, which enable to increase the BER performance of the system as can be seen from Figs. 4.15 and 4.16. However, compared with that using the BPSKor QPSK, there exists large degradation of performance. Even for the system over a Rayleigh fading channel (N_C=64), which can be regarded as the performance of the system over the multipath fading channel with N_C increasing to infinity, the system with $\Delta f_0 T_1$=0.625 cannot dramatically improve the system performance by increasing N_C to infinity. But for $\Delta f_0 T_1$=0.75, the BER and PER performance can be improved by increasing N_C and M. Therefore, the proposed method can be utilized in

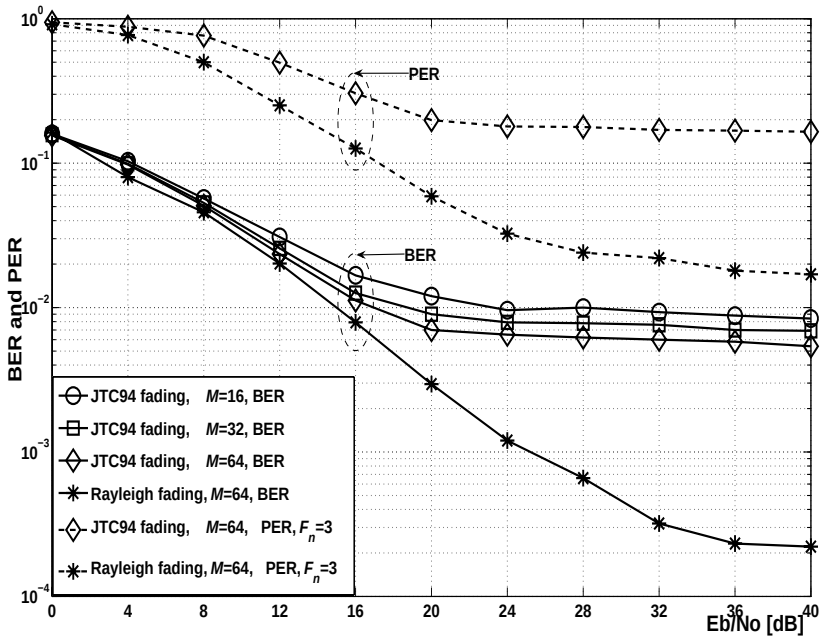

Fig. 4.16 BER and PER performance of 8-QAM-modulated OFDM system with partial signal, $\Delta f_0 T_1$=0.75, $U = 2$, N_C=64.

the syetem where the long packet is modulated by 8-QAM OFDM but the short packet adopts BPSK or QPSK OFDM (in such a case, we must choose $\Delta f_0 T_1 = 0.75$ and $\Delta f_0(T_S - T_1) = 0.5$ in Fig. 4.8.) The simulated results in Fig. 4.17, which 16-QAM-modulated OFDM system chooses $\Delta f_0 T_1$=0.75 and N_C=64, show that there exists large degradation of BER and PER performance. Therefore, it seems that the proposed method cannot be utilized for the QAM-modulated OFDM system using M-algorithm when the number of constellation $P \geq$16. It is also a challenging topic in our future research.

4.7 Conclusions

We have presented an effective method of collision recovery for OFDM-based communications. Because the modulated message data can be demodulated using the partial OFDM signal, the partial signal can be employed to reconstruct the whole OFDM signal

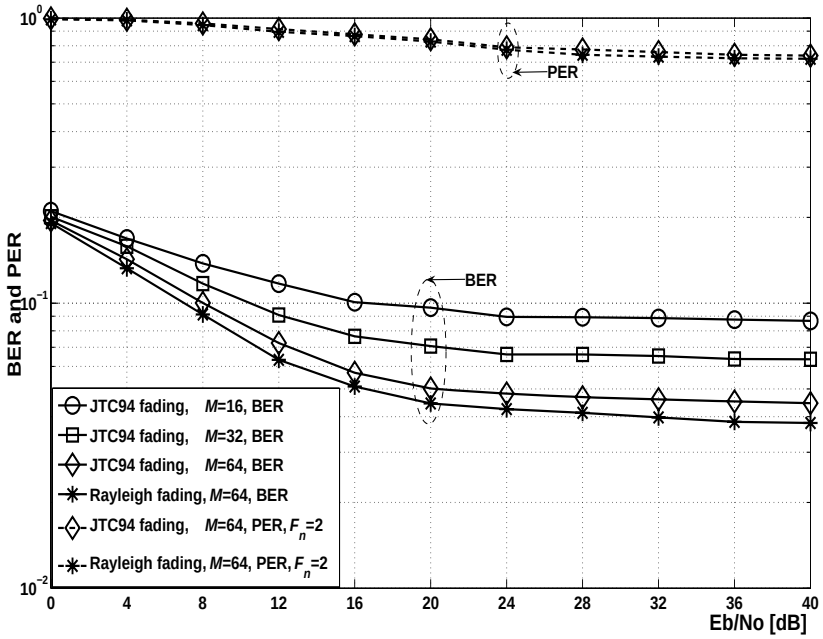

Fig. 4.17 BER and PER of 16-QAM-modulated OFDM system with partial signal, $\Delta f_0 T_1$=0.75, $U = 1$, N_C=64.

using estimated channel information. We utilized this advantageous property to recover the collided parts of two OFDM packets. Since most collisions involve a long packet colliding with short packets, the collided parts are short and can be recovered by our method.

Generally speaking, the performance of recovery depends on many factors such as the conditions of channel fading, number of subcarriers, modulation and more importantly, $\Delta f_0 T_1$. A larger number of subcarriers can lead to better recovery performance, as was revealed in all simulations. Therefore, the performance of our method can be improved by using a WiMAX (802.16a) system that can support a maximum of 2048 subcarriers [90].

It should be pointed out that almost all limitations of this proposed method are a result from demodulation. In this study, we chose the M-algorithm for demodulation because it is simple and has low complexity. However the performance of demodulation

also limits the selections of many factors such as $\Delta f_0 T_1$. For example, if the demodulation can recover all OFDM message data with a smaller T_1, it can recover the collision generated by more than two packets by a similar method.

Chapter 5

PAPR Reduction for Ad-hoc Devices Using Flexible Multicarrier System

5.1 Introduction

5.1.1 Related Work

OFDM signals yield higher values of PAPR than that of single carrier transmission. This necessitates a high linearity for power amplifier in the transmitter even in a low power mobile communication system, which obviously increases power consumption and the cost of the devices. If the peak transmitter power is limited by either regulatory or application constraints, transmission power must be reduced. This results in a reduction of the range of multicarrier transmission. Moreover, to prevent spectral growth of the multicarrier signal in the form of intermodulation among subcarriers and out-of-band radiation, the transmitter power amplifier must be operated in its linear region (i.e., with a large input backoff), where the power conversion is inefficient. This may have a deleterious effect on battery lifetime in mobile ad-hoc applications. In many low-cost applications, the drawback of high PAPR may outweigh all the potential benefits of multicarrier transmission systems.

One effective PAPR reduction is clipping, which deletes the signal components that exceed some fixed amplitude [91]. The amplitude clipping limits the peak envelope of the input signal to a predemetermined value or otherwise passes the input signal through unperturbed device, which only reduces the values of peak samples of signal amplitude but retains the orignal phases of those samples. However, the clipping expands the transmssion signal spectrum, which causes interference to adjacent systems. The combination of clipping and filtering was proposed to remove out-of-band components of the expanded transmission signal spectrum [92], [93]. Althrough filtering can suppress the spectrum expansion, the peak reduction provided by clipping is decreased by the filtering. On the other hand, if the clipping level is set sufficiently low to achieve the smaller PAPR, the bit-error rate (BER) performance will be deteriorated. So in most realistic cases, particularly, when the desired error probability is low, the PAPR values of the OFDM signals have to be set high enough such that clipping is a rare event.

Other different methods of reducing the PAPR of OFDM signals are proposed in many papers, such as coding [94]-[96], partial transmit sequence (PTS) [97]-[99], active constellation extension (ACE) [100], tone reservation (TR) [101], tone injection (TI) [101], interleaving [102] and selected mapping (SLM) [103], [104]. These techniques achieve PAPR reduction at the expense of transmit signal power increase, bit-error rate (BER) increase, data rate loss, computational complexity increase, and so on.

5.1.2 Contributions and Outline of This Chapter

Since OFDM system can choose the partial time-domain OFDM signals to send the data, it can select the signal during some specific durations, which can achieve the promising PAPR, to transmit the equal bits of data. So in this Chapter, we propose a novel PAPR reduction technique named as partial signal transmission (PST) for multicarrier systems. Firstly, for each OFDM signal, the transmitter selects some specific

durations where both larger and smaller amplitudes appear. Then the transmitter replaces the envelopes during those durations with the zero-amplitude signals. For the receiver, after the detections of the positions of zero-amplitude samples from analog-to-digital (A/D) conversion with oversampling, the receiver can demodulate the modulated data using M-algorithm. The PST can dramatically decrease the PAPR of the OFDM signal and achieve an acceptable BER performance.

The remainder of this Chapter is organized as follows. The model of OFDM system with the PST and M-algorithm are introduced in Sect. 5.2. The PAPR and BER performance of the OFDM system with the PST are presented in Sect. 5.3. Conclusions are presented in Sect. 5.4.

5.2 OFDM System with Partial Signal Transmission

5.2.1 Model of OFDM System with Partial Signal Transmission

Figure 5.1 shows the transmitter and receiver for the OFDM system with partial signal transmission. Suppose the data, which can be expressed by a vector whose elements are $x(k)(k = 0, \ldots, N_C - 1)$, is transmitted in each symbol duration. In the transmitter, $(L-1)N_C$ zeros are tacked on $x(k)$ as padding at the input of the inverse discrete Fourier transform (IDFT), then LN_C samples $y(n)(n = 0, \ldots, LN_C - 1)$ are generated at the IDFT output. The operation of padding zeros is for mitigating the aliasing in the frequency domain caused by the IDFT and for interpolation for the samples in the time domain. When the entire samples $y(n)$ are transmitted, the transmitter output $y(t)$ will form the ordinary OFDM waveforms after parallel-to-serial (P/S) and digital-to-analog (D/A) conversions, which exhibits a large value of PAPR. For simplicity, the time-domain OFDM signal $y(t)$ and its discrete samples $y(n)$ are

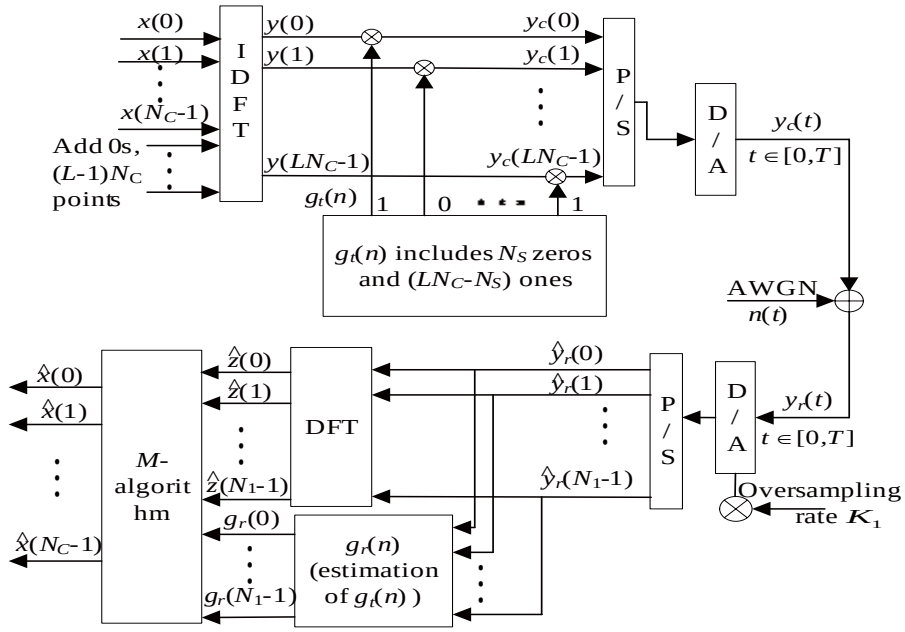

Fig. 5.1 Transmitter and receiver of the OFDM system with partial signal transmission over the AWGN channel.

expressed in complex base-band notation as

$$y(t) = \sum_{k=0}^{N_C-1} x(k) e^{j2\pi k \Delta f_0 t/L} \quad t \in [0, T_0], \tag{5.1}$$

$$y(n) = \sum_{k=0}^{N_C-1} x(k) e^{j2\pi kn/(LN_C)} \quad n \in [0, LN_C - 1], \tag{5.2}$$

where Δf_0 is the subcarrier frequency spacing, T_0 is the symbol duration. The PAPR of the transmitted OFDM signal is defined as

$$PAPR = \frac{max_{0 \le t \le T_0} |y(t)|^2}{P_{in}}, \tag{5.3}$$

where P_{in} is the average power of the transmitted OFDM signals.

For the samples of each OFDM signal $y(n)(n = 0, \ldots, LN_C - 1)$, the transmitter will generate a signal-selected function $g_t(n)(n = 0, \ldots, LN_C - 1)$ corresponding to the LN_C samples of $y(n)$. The $g(n)$ consists of N_S zeros and $(LN_C - N_S)$ ones. The positions of N_S zeros of $g_t(n)$ are decided by the amplitudes of $y(n)$. For $y(n)(n =$

$0, \ldots, LN_C - 1$) of each OFDM signal, the transmitter selects N_{Smax} samples and $N_{Smin}(= N_S - N_{Smax})$ samples, whose amplitudes are larger and smaller than other $(LN_C - N_S)$ samples, respectively. The corresponding positions of N_S samples of $y(n)$ in $g_t(n)$ will be zeros. After multiplied by the signal-selected function $g_t(n)$, LN_C samples $y_r(n)(= y(n)g_t(n), n = 0, \ldots, LN_C - 1)$ are transmitted after P/S and D/A conversions.

The receiver generates N_1 discrete-time samples, $\hat{y}_r(m)(m = 0, \ldots, N_1 - 1)$, from the received signal $y_r(t)$ after A/D conversion with oversampling rate K_1. For simplicity of analysis, we assume $K_1 = L$ in this paper, therefore, $N_1 = LN_C$. Before the operation of the discrete Fourier transform (DFT), the receiver estimates the signal-selected function $g_t(n)(n = 0, \ldots, LN_C - 1)$ from the received samples $y_r(n)$ by the following process. The receiver chooses N_S samples, whose amplitudes are smaller than other $(LN_C - N_S)$ samples, from $y_r(n)$. Suppose the postions of these N_S samples are $p(i)(i = 1, \ldots, N_S)$, therefore, the positions of N_S zeros of the estimated signal-selected function $g_r(n)$ can be simply fixed by $p(i)(i = 1, \ldots, N_S)$. It can be intuitively inferred that the correctness of estimation for $g_r(n)$ will be improved in the situation of larger signal-to-noise ratio (SNR).

Finally, the estimates $\hat{x}(k)(k = 0, \ldots, N_C - 1)$ of $x(k)$ are recovered through the demodulation stage with the samples $\hat{z}(n)$ and $g_r(n)(n = 0, \ldots, LN_C - 1)$. Since the system removes N_S samples from the OFDM samples, the recived signal $y_r(t)$ and its discrete samples $\hat{y}_r(n)$ will generate the intercarrier interference (ICI) among the samples $\hat{z}(n)(n = 0, \ldots, LN_C - 1)$ after DFT operation. Therefore, the usual demodulation algorithm, that is, each subcarrier is demodulated independently, cannot utilized in this systems. But we can use the M-algorithm for the OFDM system with PST in this Chapter.

5.2.2 M-Algorithm for OFDM System with Partial Signal Transmission

We briefly introduce the M-algorithm to demodulate the partial OFDM signal. Readers can find the detailed process and performance in [64].

Step 1: Generate partial message vectors $\mathbf{X}_u^{(1)}$ =$[x(0), \ldots, x(U-1), \ldots, 0](u = 0, \ldots, P^U - 1$; $U \leq N_C$; $P = 2$ for BPSK, $P = 4$ for QPSK) of length N_C. Utilizing $\mathbf{X}_u^{(1)}$, produce P^U kinds of replica vectors $\mathbf{Z}_u^{(1)} = [z(0), \ldots, z(LN_C - 1)]$ by the same operation using the estimated signal-selected function $g_r(n)$ as shown in Fig. 5.1 without AWGN noise. Euclidian distances $d_u^{(1)}(u = 0, 1, \ldots, P^U - 1)$ between $\mathbf{Z}_u^{(1)}$ and $\hat{\mathbf{Z}}$ are first evaluated using their elements partially as

$$d_u^{(1)} = \left(\sum_{l=0}^{U-1} |z(l) - \hat{z}(l)|^2 + \sum_{l=N_C}^{LN_C-1} |z(l) - \hat{z}(l)|^2 \right)^{1/2}. \tag{5.4}$$

Then $M(M < P^U)$ kinds of $\mathbf{Z}_u^{(1)}$, which indicate small Euclidean distances, are chosen as $\mathbf{Z}^{(1)(r)}(r = 0, 1, 2, ..., M-1)$ from among P^U kinds of $\mathbf{Z}_u^{(1)}$, and vectors $\mathbf{X}_u^{(1)}$ which produce $\mathbf{Z}^{(1)(r)}$ are stored as $\mathbf{X}^{(1)(r)}$ $(r = 0, \ldots, M-1)$. The elements of vectors $\mathbf{X}^{(1)(r)}$ become candidates for the partial message symbols $\hat{x}(0), \ldots, \hat{x}(U-1)$.

Step 2: Redefine partial message vectors $\mathbf{X}_w^{(2)}(w = 0, \ldots, MP - 1)$ of length N as $\mathbf{X}_w^{(2)}$=$[\mathbf{X}^{(1)(r)}, x(U), 0, \ldots, 0]$. Therefore, MP kinds of replica vectors $\mathbf{Z}_w^{(2)}$ = $[z(0)...z(LN_C-1)]$ are produced. Euclidian distances $d_w^{(2)}(w = 0, \ldots, MP-1)$ between $\mathbf{Z}_w^{(2)}$ and $\hat{\mathbf{Z}}$ are evaluated by

$$d_w^{(2)} = \left(\sum_{l=0}^{U} |z(l) - \hat{z}(l)|^2 + \sum_{l=N_C}^{LN_C-1} |z(l) - \hat{z}(l)|^2 \right)^{1/2}. \tag{5.5}$$

Then, M kinds of $\mathbf{Z}_w^{(2)}$, which indicate small Euclidian distances, are chosen as $\mathbf{Z}_w^{(2)(r)}(r = 0, \ldots, M-1)$ from among MP kinds of $\mathbf{Z}_w^{(2)}$, and vectors $\mathbf{X}_w^{(2)}$ which produce $\mathbf{Z}_w^{(2)(r)}$ are stored as $\mathbf{X}^{(2)(r)}(r = 0, \ldots, M-1)$. The elements of vectors $\mathbf{X}^{(2)(r)}$

become new candidates for the partial message symbols $\hat{x}(0), \ldots, \hat{x}(U)$. Thus, $\hat{x}(U)$ is added to the candidates obtained in Step 1.

Step 3: MP kinds of $\mathbf{Z}_w^{(N_C-U+1)}$ are obtained by repeating Step 2 $N_C - U$ times. Finally, vector $\mathbf{X}^{(N_C-U+1)}$, which produces the minimum Euclidian distance, contains all the message symbols $\hat{x}(0), \ldots, \hat{x}(N_C - 1)$.

5.3 Simulation Results of OFDM signal with PST

We define two parameters T_{ratio} and Z_{ratio} as $T_{ratio} = (1 - N_S/(LN_C))$ and $Z_{ratio} = N_{Smax}/N_S$. The parameter T_{ratio} can be regarded as the ratio of transmitted samples to all samples. The N_{Smax} zero-amplitude samples are used to decrease the values of high amplitudes among each OFDM samples, N_{Smin} zero-amplitude samples are utilized to improve the correctness of estimation for $g_r(n)$. Therefore, the parameter Z_{ratio} can be regarded as an adjustment between N_{Smax} and N_{Smin}. On the other hand, to evaluate the performance of OFDM system with the PST, we also give the simulated preformance of OFDM system with the technique of amplitude clipping [91]. The amplitude clipping is performed digitally on the samples $y(n)$. If L is larger than four, the discrete samples $y(n)$ can totally approximate the continuous time-domain signal $y(t)$. For the clipping, the amplitude of the time-domain signal samples are limited by a threshold A_{th}. The value of clipping ratio (CR) is often definded as CR$= A_{th}/\sqrt{P_{in}}$. Let $\bar{y}(n)$ be a clipped time sample with the phase unchanged, then

$$|\bar{y}(n)| = \begin{cases} |y(n)| & if \quad |y(n)| \le A_{th} \\ A_{th} & if \quad |y(n)| > A_{th}. \end{cases} \tag{5.6}$$

The distortion caused by amplitude clipping can be viewed as another source of noise. The noise caused by amplitude clipping falls both in-band and out-of-band. Since filtering after clipping can reduce out-of-band radiation but may also cause some peak regrowth so that the signal after clipping and filtering will exceed the clipping level at

some point, we only simulate the performance of OFDM system with the technique of amplitude clipping without filtering to compare with the performance of OFDM system with the PST.

5.3.1 CCDF of PAPR for OFDM Signal with Partial Signal Transmission ($N_C = 64$)

The PAPR of the signal of OFDM signal with partial signal transmission can be defined as

$$PAPR = \frac{\max_{0<t<T_0} |y_c(t)|^2}{P_{AV}}, \tag{5.7}$$

where P_{AV} is the ensemble average of the power of time-domain OFDM signals with the PST $y_c(t)$. We randomly generate millions of time-domain OFDM signals with PST by computer to obtain the approximate value $\hat{P}_{AV}$ of P_{AV}. To capture the peaks of the OFDM signal, we adopt 4 times oversampling ($L = 4$) time-domain samples which can totally approximate the continus time-domain signal [68]. We use the complementary cumulative density function (CCDF) of the PAPR (Prob[PAPR>PAPR_0]) to identify the PAPR characteristics.

Figures 5.2 to 5.4 show the simulated CCDF of PAPR of OFDM system with the PST. T_{ratio} was chosen to be 0.9, 0.8 and 0.6. The number of subcarrier is 64 ($N_C = 64$). For each T_{ratio}, the PST will decrease the PAPR with the different values of Z_{ratio}. For $T_{ratio} = 0.9$, it is shown in Fig. 5.2 that ordinary QPSK-modulated OFDM with 64 subcarriers has a PAPR that exceeds 10.7 [dB] with the probability of 0.1%, but with $Z_{ratio} = 0.1$, OFDM system using the PST is only 8.6 [dB] to achieve the identical probability, therefore, 2.1 [dB] PAPR reduction can be obtained. But 4.6 [dB] reduction will be achieved if system chooses $Z_{ratio} = 1$ which can be found in Fig. 5.2. For $T_{ratio} = 0.8$ in Fig. 5.3, $Z_{ratio} = 0.5$ can almost achieve the identical CCDF of PAPR to that of $Z_{ratio} = 1$. Particularly for $T_{ratio} = 0.6$ in Fig. 5.4, $Z_{ratio} = 1$

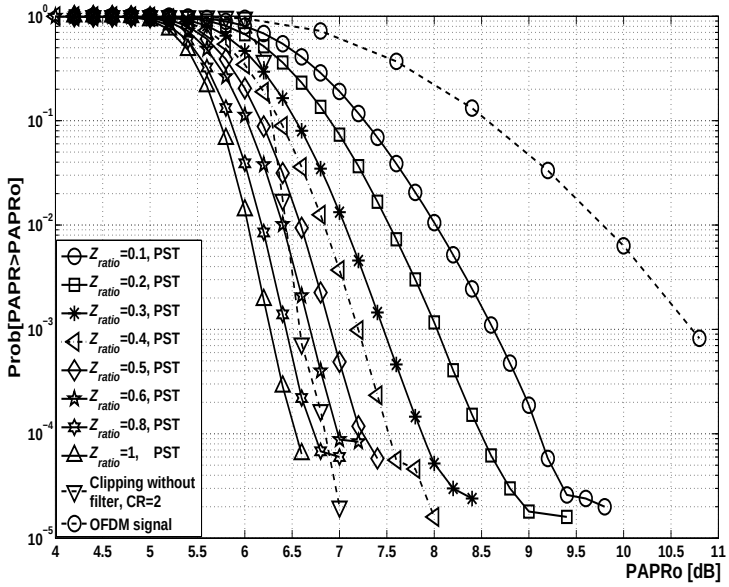

Fig. 5.2 CCDF of PAPR of OFDM system with partial signal transmission ($T_{ratio} = 0.9$, $N_C = 64$, QPSK).

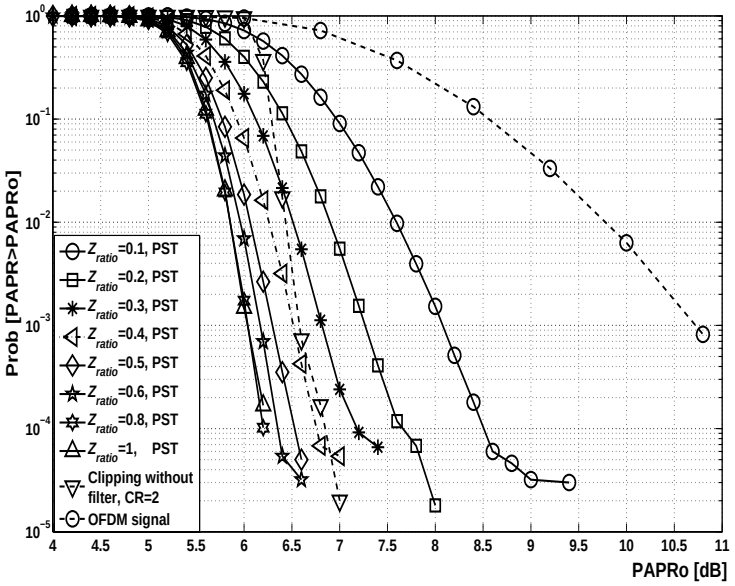

Fig. 5.3 CCDF of PAPR of OFDM system with partial signal transmission ($T_{ratio} = 0.8$, $N_C = 64$, QPSK).

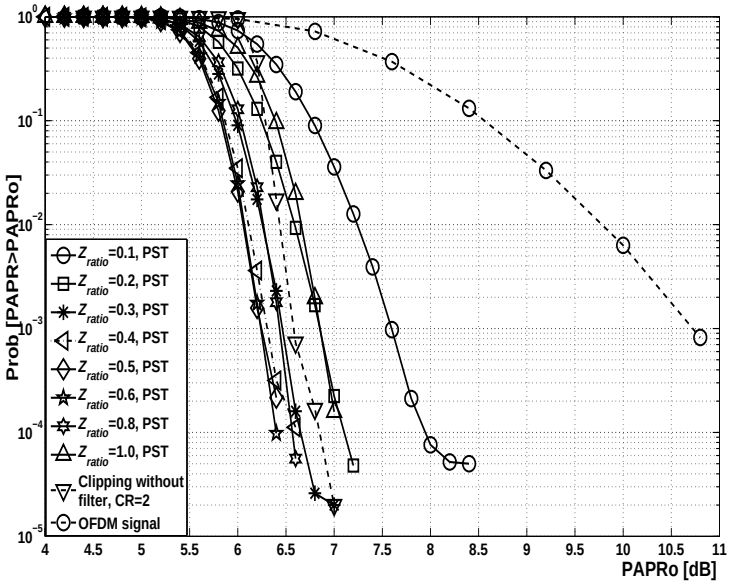

Fig. 5.4 CCDF of PAPR of OFDM system with partial signal transmission ($T_{ratio} = 0.6$, $N_C = 64$, QPSK).

cannot obtain the best CCDF of PAPR because $N_{Smax}(= N_S)$ zero-amplitude samples for the high amplitudes among each OFDM samples will decrease the peak values of OFDM signal but also decrease the average power $\hat{P}_{AV}$. Therefore, $Z_{ratio} = 0.5, 0.8$ can achieve the best CCDF of PAPR than that of other Z_{ratio} for $T_{ratio} = 0.6$. Figures 5.2 to 5.4 confirm that OFDM system with the PST can obtain the promising PAPR characteristics by choosing appropriate Z_{ratio} and T_{ratio}. On the other hand, we also simulate the PAPR characteristic of OFDM signal after amplitude clipping with CR=2 and compare it to OFDM signal after PST with above T_{ratio} and Z_{ratio} in Figs. 5.2 to 5.4, which also show that OFDM system using the PST with $T_{ratio} = 0.9, Z_{ratio} \in [0.6, 1]$, $T_{ratio} = 0.8, Z_{ratio} \in [0.5, 0.8]$ and $T_{ratio} = 0.6, Z_{ratio} \in [0.3, 0.8]$ can achieve better CCDF of PAPR than that of OFDM system using amplitude clipping with CR=2.

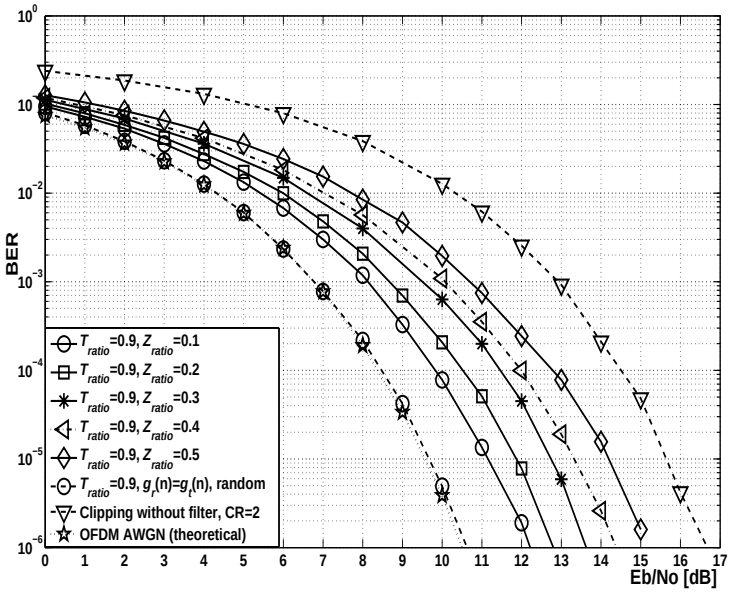

Fig. 5.5 BER performance of the OFDM system with partial signal transmission over AWGN channel ($T_{ratio} = 0.9$, $N_C = 64$, QPSK).

5.3.2 BER performance for OFDM System with Partial Signal Transmission ($N_C = 64$)

Figures 5.5 to 5.7 show the simulated BER performance of the OFDM system with partial signal transmission over AWGN channel. T_{ratio} was to be 0.9, 0.8 and 0.6. The number of subcarrier is 64 ($N_C = 64$). For each T_{ratio}, the system chooses Z_{ratio} from 0.1 to 0.5. From Figs. 5.5 to 5.7, we can find that, for all values of T_{ratio}, the system with small Z_{ratio} will achieve better BER performance than that of large Z_{ratio}. The reason is that smaller Z_{ratio} will improve the correctness of estimation for $g_r(n)$. For the system with $T_{ratio} = 0.9, Z_{ratio} = 0.1$, which can achieve 2.1[dB] PAPR reduction for Prob $[PAPR < PAPR_O]$=0.1% in Fig. 5.2, there will be 1.5 [dB] loss for the requirement of BER=10^{-5}. For the system with $T_{ratio} = 0.9, Z_{ratio} = 0.5$, which can achieve 4.1 [dB] PAPR reduction for Prob $[PAPR < PAPR_O]$=0.1%, such a loss for the requirement of BER=10^{-5} will be increased to 4 [dB]. The similar characteristics of BER

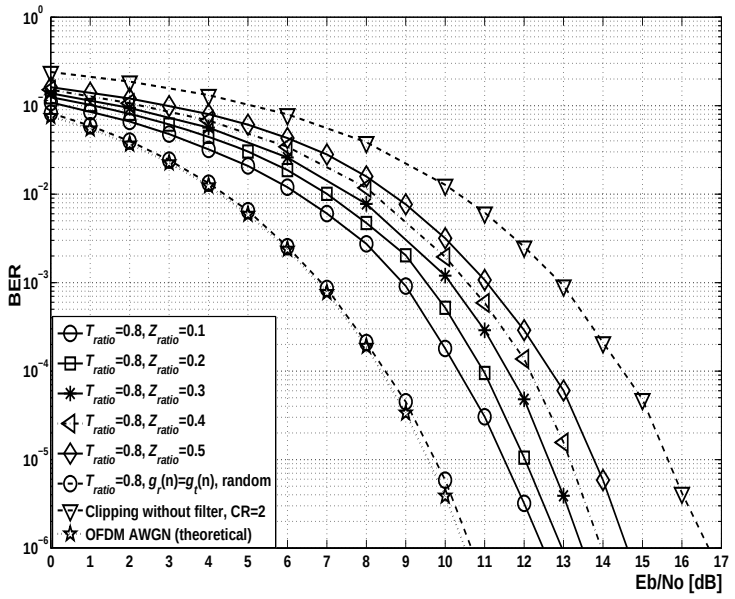

Fig. 5.6 BER performance of the OFDM system with partial signal transmission over AWGN channel ($T_{ratio} = 0.8$, $N_C = 64$, QPSK).

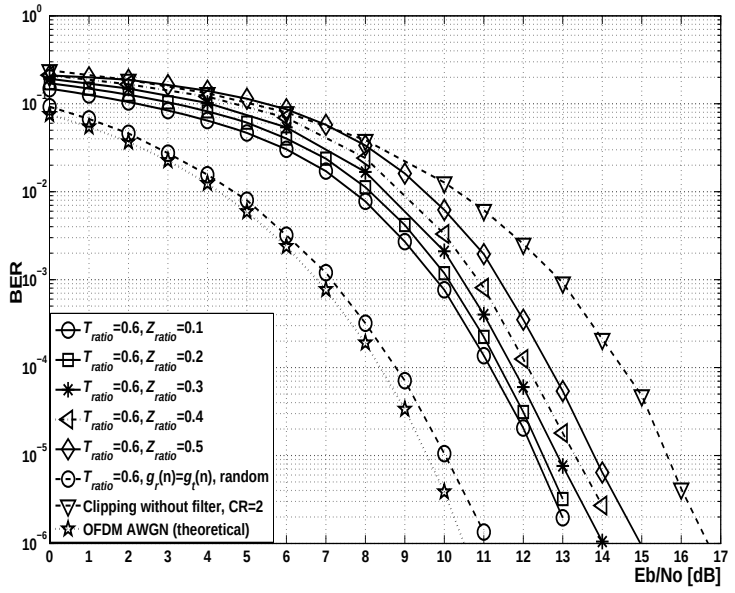

Fig. 5.7 BER performance of the OFDM system with partial signal transmission over AWGN channel ($T_{ratio} = 0.6$, $N_C = 64$, QPSK).

performance can also be found in Figs. 5.6 and 5.7. Therefore, OFDM system with the PST adopts the tradeoff between the BER performance and PAPR reduction. On the other hand, we also give the simulated BER performance of system for each T_{ratio} when the signal-selected function $g_t(n)$ is correctly detected ($g_r(n) = g_t(n)$). It is assumed that N_S samples are selected randomly among LN_C samples of each OFDM signal. The simulated results show that the deterioration of BER performance mainly results from the mis-detection of the signal-selected function $g_t(n)$. The BER performance will be further improved if the estimation of $g_t(n)$ is promoted. At the same time, we also simulate the BER performance of the OFDM system after amplitude clipping with CR=2 and compare it to OFDM signal after the PST with above T_{ratio} and Z_{ratio} in Figs. 5.5 to 5.7 which also show that OFDM system using the PST for all T_{ratio} and Z_{ratio} can achieve better BER performance than that of OFDM system using amplitude clipping with CR=2.

5.3.3 CCDF of PAPR and BER performance of OFDM System with Partial Signal Transmission (N_C=128)

Figures 5.8 and 5.9 show the CCDF of PAPR and BER performance of OFDM system using the PST with N_C=128 and QPSK modulation, respectively. T_{ratio} is choosen as 0.9, 0.8 and 0.6. For each T_{ratio}, the system only adopts Z_{ratio} to be 0.5 and 0.4. From Fig. 5.8, we can find that OFDM system with the PST can obtain the promising PAPR characteristics by choosing appropriate Z_{ratio} and T_{ratio} for $N_C = 128$. for example, OFDM system using the PST with $Z_{ratio} = 0.8, 0.6$ and $T_{ratio} = 0.5, 0.4$ can obtian better PAPR characteristics than that of the OFDM system after amplitude clipping with CR=2. Compared with the ordinary QPSK-modulated OFDM with 128 subcarriers has a PAPR that exceeds 11 [dB] with the probability of 0.1%, OFDM system using the PST with $Z_{ratio} = 0.8, 0.6$ and $T_{ratio} = 0.5, 0.4$ can achieve about 5 [dB] PAPR

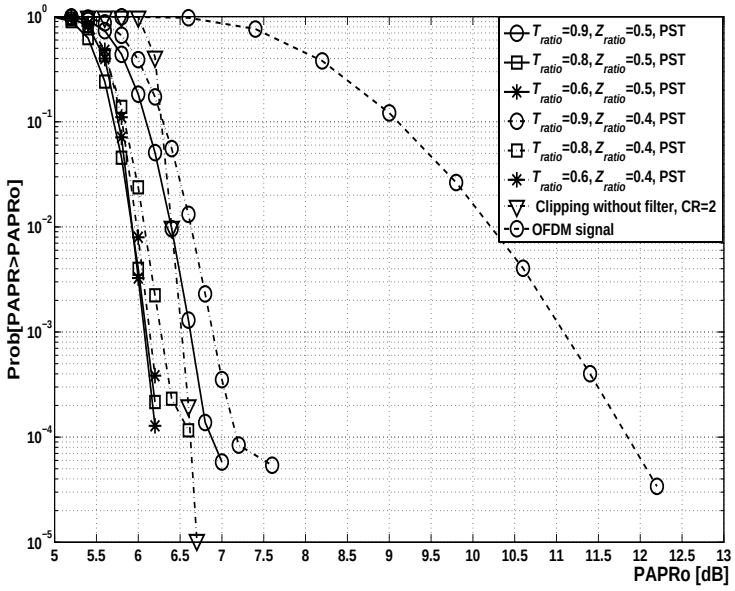

Fig. 5.8 CCDF of PAPR of OFDM system with partial signal transmission ($N_C = 128$, QPSK).

reduction for the identical probability of PAPR. The simulated BER performance in Fig. 5.9 also confirms that OFDM system using the PST with appropriate T_{ratio} and Z_{ratio} can achieve the better BER performance than that of OFDM system using amplitude clipping with CR=2.

5.4 Conclusions

Based on adaptive properties of HC-MCM, OFDM system can choose the partial time-domain OFDM signals to send the data. Therefore, OFDM system can select the signal during some specific duration, which can achieve the promising PAPR, to transmit the equal bits of data. So in this Chapter, we have proposed a novel PAPR reduction technique named as partial signal transmission (PST) for ad-hoc network using OFDM-based WLAN. PST can dramatically decrease the PAPR of the OFDM signal and achieve the promising BER performance. Therefore, those technologies will

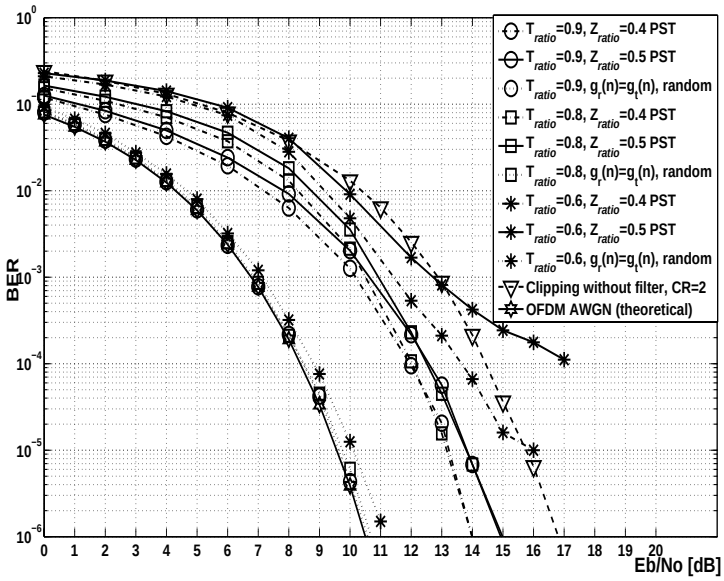

Fig. 5.9 BER performance of the OFDM system with partial signal transmission over AWGN channel ($N_C = 128$, QPSK).

decrease the devices cost of ad-hoc networks.

Chapter 6

Conclusions and Future Directions

6.1 Conclusions of This Dissertation

Bandwidth efficiency is the primary concern in the design of future communication systems. One efficient technique that increases the bandwidth efficiency is to utilize multilevel modulation, such as M-QAM, which increases the spectral efficiency of link, measured in [bits/sec/Hz], by sending multiple bits per symbol, the spectral efficiency can be dramatically improved with high-order M-QAM. However, since wireless channel is subject to severe propagation impairment which results in a serious degradation in the link carrier-to-noise ratio (CNR), even though the efficient techniques of compensation are used, the high order M-QAM cannot achieve the optimal performance. Therefore, the OFDM of high order M-QAM will also be limited to the special applications with the above reason. In addition, the high order M-QAM often chooses $M = 2^k$ and k is an integer. So physical layer adaptation using adaptive M-QAM is not robust to obtain the appropriate M. If the M could be positive real number, there will be more useful for the physical layer adaptation.

One novel flexible multicarrier system (high compaction multi-carrier modulation: HC-MCM) which can attain higher spectral efficiency than that of the original OFDM has been designed. The HC-MCM system has a high affinity with exiting OFDM system,

and it can flexibly control the transmission rate and quality of communication. More importantly, only utilizing BPSK or QPSK modulation, the HC-MCM achieves the transmission rate of high order M-QAM OFDM, even the M could be any positive real number. It can also flexibly adjust the length of frame according to the radio channel condition. In this dissertation, we have extended this flexible multicarrier systems for ad-hoc wireless network. The underlying philosophy in all problems that are considered in this dissertation is a synergy between the physical and the MAC layers of ad-hoc networks.

In Chapter 2, we explained that the flexible transmission including adaptive modulation and variable length of frame can cause different link goodput, range and energy efficiency. In such a case, the nodes of ad-hoc network can realize the tradeoff between goodput, range and energy efficiency by the flexible transmissions. We also gave the results which show that there is much to be gained from adaptive modulation and variable frame length in terms of goodput, range and energy consumption for ad-hoc networks. We obtain three rules of design for the tradeoff for wireless node.

Physical layer adaptation using adaptive M-QAM is not robust to obtain the appropriate M due to wireless channel and high order M-QAM is restricted to be adopted in wired or optical networks. High order M-QAM also cannot be used for WLAN-based ad-hoc networks. So in Chapter 3, based on the parallel combinatory OFDM (PC-OFDM) and HC-MCM, we proposed a novel adaptive modulation, that is, parallel combinatory/high compaction multi-carrier modulation (PC/HC-MCM) for ad-hoc networks. The PC/HC-MCM can achieve any transmission rate of M-QAM that corresponds to not only integer M but also real number M. The PC/HC-MCM can also realize the adaptive length of frame which can be utilized to physical layer adaptation with the adaptive length of packet for ad-hoc networks. Two types of PC/HC-MCM systems, which have been named as the modulated PC/HC-MCM system and

PC/HC-MCM (un-modulated) system, were designed by PC/HC-MCM. The modulated PC/HC-MCM system can achieve better BER performance than that of HC-MCM system with the equal BWE by employing appropriate parallel combinatory coding. The PC/HC-MCM (un-modulated) system can obtain excellent peak-to-average power ratio (PAPR) characteristics by selecting the optimal constellations for its subcarriers. On the other hand, since the PC/HC-MCM can divide the duration of PC-OFDM symbol into multiple time-slots, the advantages of frequency hopping (FH) can be applied in the PC/HC-MCM systems. Therefore, we also combine the PC/HC-MCM and frequency hopping multiple accesses (FHMA) to propose a new multiple access (MA) system. This MA system can synchronously transmit multiple users' data within one symbol duration of the PC-OFDM.

Since most collisions occur when one user starts to build a connection or sends a response with a short packet, such as RTS (request-to-send), CTS (clear-to-send) or ACK (acknowledgement), to one node while a principal user is transmitting a long packet including data to an identical destination. Therefore, the collided part is not as long as the principal long packet. For example, the long packet of IEEE 802.11a (64 subcarriers) can convey 8184 [bits] (payloads) without preamble and control bits, but the length of ACK, RTS or CTS is no longer than 300 [bits] which can be carried by only six BPSK-modulated OFDM signals or three QPSK-modulated OFDM signals. Undoubtedly, for the long packet, if such collided parts can be recovered, the system performance, such as throughput and delay, will be dramatically improved. On the other hand, it will also benefit the protocol design of ad-hoc networks because short packets often contain much important information, such as positions and power levels. So in Chapter 4, we proposed a method of collision recovery for ad-hoc networks based on this flexible multicarrier system. We presented the property that, from the flexible multicarrier system, the modulated message data of OFDM signal can be demodulated

using the partial (ΔfT) time-domain OFDM signal. Therefore, the partial signal can be adopted to reconstruct the whole OFDM signal with estimated channel information. Utilizing this advantageous property, a practical method of collision recovery can be realized. The proposed method can be developed to solve the problems of hidden terminals and exposed terminals in ad-hoc networks.

According to the property of flexible multicarrier system, OFDM system can transmit partial time-domain OFDM signals to send the data. Therefore, OFDM system can select the signal during some specific duration, which can achieve the promising PAPR, to transmit the equal bits of data. So in Chapter 5, we have proposed a novel PAPR reduction technique called partial signal transmission (PST) for devices of ad-hoc network using OFDM-based WLAN. PST can dramatically decrease the PAPR of the OFDM signal and achieve the promising BER performance. Therefore, those technologies will decrease the devices cost of ad-hoc networks.

6.2 Future Directions of This Dissertation

In this section, the extension of this work towards the PC/HC-MCM and collision recovery will be discussed in detail.

6.2.1 For PC/HC-MCM

The main weakness of PC/HC-MCM or HC-MCM is the high demodulation complexity. Since the receiver utilizes MLSE to demodulate the transmitted data, the demodulation complexity (C_p) of MLSE increases exponentially with the number of subcarriers N and modulation type P(BPSK: $P = 2$; QPSK: $P = 4, \ldots$), that is, $C_p = P^N$, which is impractical for the demodulation for large N. M-algorithm will keep demodulation complexity (C_p) as $P^U + (N-U)MP$ for each partial OFDM signal,

where P, U and M, are modulation type, depth of initial candidate path and number of survivors for each iteration, respectively. But the performance will be deteriorated for smaller ΔfT and high order M-QAM modulation. On the other hand, almost all limitations of this proposed method of collision recovery are a result from demodulation. The performance of demodulation using the the M-algorithm also limits the selections of many factors. For example, if the demodulation can recover all OFDM message data with a smaller partial time-domain OFDM signal, it can recover the collision generated by more than two packets by a similar method. So the demodulation algorithm for PC/HC-MCM or HC-MCM is a main topic in the future research. The good algorithm should have the acceptable demodulation complexity and BER performance. On the other hand, the algorithm should be considered for the applicaitons which concerns the high mobile situation and multiple antennas.

6.2.2 For Collision Recovery

The most contribution of this dissertation is that the proposed method of collision recovery can dramatically benefit the protocol design of wireless networks, including ad-hoc and sensor networks. Since most collisions occur when one user starts to build a connection or sends a response with a short packet, such as RTS (request-to-send), CTS (clear-to-send) or ACK (acknowledgement), to one node while a principal user is transmitting a long packet including data to an identical destination. But the short packets such as RTS often contain much important information of wireless nodes, such as their positions and desired transmission duration. If the nodes which have sent the RTS have not obtained the responses, they will retransmit the short packets (RTS) after a random delay and such a process will result in another collision. By utilizing our proposed method, the receiver can separate the short packets from the long packet when they are collided with the long packet. So in the next step, the receiver can send

the responses according to the scheduling strategies to all nodes which have sent the RTS packets. On the other hand, in the near-far situation, our method can achieve better recovery performance in the weak near-far condition which is more realistic in the wireless LAN. Therefore, the proposed method can be utilized to solve the hidden terminal or exposed terminal problems and improve the performance of ad-hoc networks that are based on wireless LAN using OFDM techniques. Based on above analysis, the future directions for the collision recovery will include following areas.

Exploring the new methods to improve the successful recovery ratio

Obviously, the improvment of SRR will furthur benefit the performance of ad-hoc networks. Let us suppose the SRR=p, k nodes take turns to send their RTS packets to one receiver during the period of the transmission of one long packet to the identical receiver and only one short packet is involved in each collision with the long packet. Utilizing our method, the probability of recovery will be p^k for the long packet and p for all short packets. Therefore, the recovery performance for the long packet will be decreased exponentially with the value of p. Thereby the performance of ad-hoc network will markedly improved by the increase of SRR.

Many techniques can be combined with our method to improve the performacne of collision recovery based on OFDM system, such as the error correction coding (ECC) and diversity reception. ECC can improve the ability to detect errors that are made due to noise or other impairments in the course of the transmission then can enable localization of the errors and correct them. Therefore, ECC can improve the PER performance of both packets when the system utilizes the partial signal to demodulate the data. Thereby the SSR will be improved. Diversity reception means that the transmitted signal can be received more than once, thereby enabling the receiver to

have more opportunities to determine what was transmitted. It is used to minimize the effects of fading. The SINR of the received signal can be increased at the receiver when using diversity reception is directly dependent on the independence of the fading characteristics. Therefore, diversity reception can improve the BER or PER then SRR performance of the system using the proposed method. These issues will also be new topics in our future research.

Exploring the new protocols of ad-hoc networks based on the method of collision recovery

In multiple access (MA) wireless networks where a common channel is shared by a population of users. A key issue, referred to as medium access control (MAC), is to coordinate the transmissions of all users so that the common channel is efficiently utilized and the quality-of-service (QoS) requirement of each user is guaranteed. The schemes for coordinating transmissions among all users are called MAC protocols. The conventional assumption on the channel is that any concurrent transmission of two or more packets results in the destruction of all the transmitted packets. Based on this assumption, numerous MAC protocols, such as Aloha, CSMA and a class of adaptive protocols have been proposed. Particularly, carrier sense multiple access with collision avoidance (CSMA/CA) has been accepted as the part of standard IEEE 802.11a, which can be used in ad-hoc networks. It is reasonable that the method of collision recovery can be utilized to combine with the techniques of MAC layer.

For Aloha-type protocol, it is difficult to realize the quality-of-service (QoS) requirement of each user because no cooperation exists between the transmitters. On the other hand, the AP (or receiver) cannot decide and assign the channel to some specific nodes because it has no ways to suppress other nodes to access the channel. Using our

method, the AP can obtain the information of other nodes during the transmission of the principal nodes. So, combined with the proposed method, Aloha-type protocal can achieve the quality-of-service (QoS) requirements of each user. On the other hand, the stability of wireless MAC protocol is also improved by the proposed method.

For ad-hoc networks, the protocol of CSMA/CA often has been utilized to guarantee the continus transmission between nodes. But hidden terminal problem will dramatically decrease the system performance. In addition, exposed terminal problem also limits the transmission between other nodes. So we can combine this techniques in a new design of protocol and the new protocol will further improve the transmission performance and stability of ad-hoc networks with large number of nodes. These issues will also be hot topics in our future research.

Exploring the new methods for sensor networks based on the method of collision recovery

One of the most important constraints on sensor nodes is the low power consumption requirement. Sensor nodes carry limited, generally irreplaceable, power sources. Therefore, while traditional networks aim to achieve high quality of service (QoS) provisions, sensor network protocols must focus primarily on power conservation. They must have inbuilt tradeoff mechanisms that give the end user the option of prolonging network lifetime at the cost of lower throughput or higher transmission delay. So for sensor nodes, the number of subcarrier for IFFT or DFT is designed to be small in order to decrease the cost of the sensor. On the other hand, the M-algorithm needs more computation complexity, therefore, power consumption is high. The mathematical model of HC-MCM can be carried on the Cholesky factorization for the small number of subcarrier and appropriate ΔfT. The Cholesky factorization can remove the ISI among

the subcarriers. Therefore, the demodulation complexity for the HC-MCM system and the OFDM system with partial signal can be reduced by the Cholesky factorization. Thereby the proposed method can be utilized for the sensor networks based on OFDM communications using the small number of subcarriers. On the other hand, sensor nodes can communicate each other using the lower throughput or higher transmission delay. Therefore, collision recovery will further reduce the retransmission process of packet and save the power consumption. These issues will also be given in our future research.

6.2.3 For Partial OFDM Signal

The partial time-domain OFDM signal can be utilized to demodulate the OFDM data or to be utilized to recover the whole time-domain OFDM signal. Such a property can be applied in many applications. We have presented that a flexible multicarrier can be realized using this property and this property also can be developed to solve the problem of hidden terminals or exposed terminals. It also can be utilized to decrease the PAPR of multicarrier signal. So such a property will also be useful in many other fields such as multiple antennas system [105], since, due to correlation of the fading channel, it seems to enable to improve the system performance if some some antennas only transmit the partial signals. The property also can be utilized in the multiuser system in the mode of TD-FDMA, for example, the AP can sent the data of two users in one duration (T_0) of OFDM signal and i-user can hold different $T_i (i = 1, 2)$ ($T_1 + T_2 = T_0$). Such a TD-FDMA system maybe furthur improves the performance and diversity of the multi-user systems. We will give more applications on this property in our future research.

Acknowledgement

First of all, I would like to appreciate Kochi University of Technology, Fudan University and President of KUT, Prof. Hajime OKAMURA, for giving me this chance to study here and offering three years of expense support. Without the special scholarship program (SSP) for international cooperation between KUT and Fudan University, China, I cannot complete my doctoral research successfully. At the same time, I want to appreciate Prof. Shiyong Zhang and Prof. Yiping Zhong, my advisors of Fudan University, for their persistent warmhearted support and help to give me so long period for my Ph. D study in both universities.

Next, I am very thankful of my advisor of KUT, Prof. Masanori Hamamura, for three years of encouragement, guidance and support. Prof. Masanori Hamamura has guided me into the exciting area of wireless communications and signal process. Moreover, his research enthusiasm and insight into wireless communications make me deep impression. Especially, his patience and serious spirit for study and instructing students will affect my career forever. The work presented here would not have been possible without his constant guidance and helpful recommendation. I am especially grateful for his untiring effort to teach me how to think to tackle the problems in my research world. I believe his good thinking way and research skills will be beneficial to my study in the future.

I would like to appreciate the great support of Prof. Kazunori SHIMAMURA, Prof. Makoto IWATA, Prof. Akihiro SHIMIZU and Prof. Masahiro FUKUMOTO for helpful comments on my thesis work. I also would like to thank the other professors of the Department of Information Systems Engineering especially Prof. Keizo SHINOMORI, Prof. Xiangshi REN for their advice on my research.. Moreover, I acknowledge the

secretaries of the Department for their help and the staffs of the International Relations Center, for their kindness and warmness.

Third, I am grateful of the fellow students in Hamamura Lab. It would have been far more difficult to complete this work without their help. Special thanks to Shinji Takahashi, Teruhiko Miyatake, Keiichirou Tsuyuki, Jun Hyuga, Mizuki Kageyama and Jotaro Kikuchi for their helpful discussion and advice. I would have never forgotten their help and warmness which made my academic experience at KUT most enjoyable. Again, I would like to thank the other SSP students of KUT for their help.

References

[1] M. Weiser, The Computer for the Twenty-First Century, Scientific American, 1991.

[2] E. Anceaume, A. K. Datta, M. Gradinariu, G. Simon, "Publish/subscribe scheme for mobile networks," Proc. ACM Workshop on Principles of Mobile Computing 2002, pp. 74-81.

[3] Special issue "Special feature on middleware for mobile and pervasive," ACM Mobile Computing and Commun. vol. 6, no. 4, Oct. 2002.

[4] C. Mascolo, L. Capra, W. Emmerich, " Middleware for mobile computing (a survey)," in Enrico Gregori, Giuseppe Anastasi, Stefano Basagni (Eds.), Advanced Lectures on Networking, LNCS 2497, Springer, Berlin, 2002.

[5] E. Belding-Royer, Routing Approaches in Mobile Ad-hoc Networks, IEEE Press and John Wiley and Sons, New York, 2004.

[6] C. E. Perkins, Ad-hoc Networking, Addison-Wesley, Reading, MA, 2000.

[7] P. Kuosmanen, "Classification of ad-hoc routing protocols," Finnish Defence Forces, Naval Academy, Finland. Available from (http://keskus.hut.fi/opetus/s38030/k02/Papers/12-Petteri.pdf).

[8] E. M. Belding-Royer, C.K. Toh, "A review of current routing protocols for ad-hoc mobile wireless networks," IEEE Personal Commun. Mag., vol.6, no.2, pp.46-55, Apr. 1999.

[9] M. S. Corson, J. P. Maker, J. H. Cernicione, "Internet-based mobile ad-hoc networking," IEEE Internet Computing, vol.3, no.4, pp.63-70, 1999.

[10] M. Conti, "Body, personal, and local wireless ad-hoc networks," in Handbook of Ad-hoc Networks (Chapter 1), CRC Press, New York, 2003.

[11] W. Stallings, Local and Metropolitan Area Networks, Prentice Hall, Englewood

Cliffs, NJ, 1996.

[12] Web site of the IEEE 802.11 WLAN: http://grouper.ieee.org/grups/802/11/main.html.

[13] Web site of the Bluetooth Special Interest Group: http://www.bluetooth.com/.

[14] C. Bisdikian, "An overview of the Bluetooth wireless technology," IEEE Commun. Mag., vol. 39, no. 12, pp. 86-94, Dec. 2001.

[15] Specification of the Bluetooth System, Ver. 1.1, Feb. 2001.

[16] B. A. Miller, C. Bisdikian, Bluetooth Revealed, Prentice Hall, Englewood Cliffs, NJ, 2000.

[17] IEEE standard for Wireless LAN-Medium Access Control and Physical Layer Specification, P802.11, Nov. 1997.

[18] L. M. Feeney, "An energy-consumption model for performance analysis of routing protocols for mobile ad-hoc networks," ACM/Kluwer Mobile Networks and Applications (MONET), vol.6, no.3, pp.239-249, June, 2001.

[19] E. Mingozzi, "QoS support by the HiperLAN/2 MAC protocol: a performance evaluation," Cluster Computing Journal, vol.5, no.2, pp.145-155, Apr. 2002.

[20] G. Zaruba, S. Das, "Off-the-shelf enablers of ad-hoc networks," Ad-hoc Networking (Chapter 2), IEEE Press Wiley, New York, 2003.

[21] G. Anastasi, M. Conti, E. Gregori, "IEEE 802.11 ad-hoc networks: protocols, performance and open issues," in Ad-hoc Networking (Chapter 3), IEEE Press Wiley, New York, 2003.

[22] B. Sklar, "Rayleigh fading channels in mobile digital communication systems part I: characterization", IEEE Commun. Mag., vol. 35, no. 9, pp. 136-146, Sept. 1997.

[23] F. A. Tobagi, L. Kleinrock, "Packet switching in radio channels: Part II the hidden terminal problem in carrier sense multiple access modes and the busy tone solution", IEEE Trans. on Commun., vol.23, no.12, pp.1417-1433, Dec. 1975.

[24] S. Khurana et al., "Effect of hidden terminals on the performance of IEEE 802.11

MAC protocol, Proc. IEEE LCN 98,pp. 12-20, Oct. 1998.

[25] C. L. Fullmer, J. Garcia-Luna-Aceves, "Solutions to hidden terminal problems in wireless networks", Proc. ACM SIGCOMM 97, 1997.

[26] A. J. Goldsmith, S. B. Wicker, "Design challenges for energy-constrained ad-hoc wireless networks," IEEE Wireless Commun. Mag., vol. 9, no.4, pp. 8-27, Aug.2002.

[27] T. Keller and L. Hanzo, "Adaptive multicarrier modulation: a convenient framework for time-frequency processing in wireless communications", Proceedings of the IEEE, vol.88, no.5, pp.611-640, May 2000.

[28] J. S. Chow, J. C. Tu, J. M. Cioffi, "A discrete multitone transceiver system for HDSL applications", IEEE Journal on Selected Areas in Commun., vol.9, no.6, pp.895-908, Aug. 1991.

[29] I. Koutsopoulos, L. Tassiulas, "Carrier assignment algorithms in wireless broadband networks with channel adaptation", Proc. of IEEE ICC 01, vol.5, pp. 1401-1405, 2001.

[30] B. Vucetic, "An adaptive coding scheme for time-varying channels", IEEE Trans. on Commun., vol.39, no.5, pp.653-663, May 1991.

[31] M. B. Pursley, S. D. Sandberg, "Variable-rate coding for meteor-burst communications", IEEE Trans. on Commun., vol.37, no.11, pp.1105-1112, Nov. 1989.

[32] J. G. Proakis, Digital Communications, Mc Graw-Hill, 2000.

[33] N. Morinaga, M. Nakagawa, R. Kohno, "New concepts and technologies for achieving highly reliable and high-capacity multimedia wireless communication systems", IEEE Commun. Mag., vol.37, no.1, pp.34-40, Jan. 1997.

[34] T. Ue, S. Sampei, N. Morinaga, K. Hamagushi, "Symbol rate and modulation level-controlled adaptive modulation/TDMA/TDD system for high-bit rate wireless data transmission", IEEE Trans. on Vehicular Tech., vol.47, no.4, pp.1134-1147, Nov. 1998.

[35] A. J. Goldsmith, S. G. Chua, "Variable-rate variable-power M-QAM for fading channels", IEEE Trans. on Commun., vol.45, no.10, pp.1218-1230, Oct. 1997.

[36] N. Morinaga, M. Yokoyama, S. Sampei, "Intelligent radio communications techniques for advanced wireless communication systems," IEICE Trans. Commun., vol. E79-B, pp. 214-221, Mar. 1996.

[37] J. R. Treichler, M. G. Larimore, J. C. Harp, "Practical blind demodulator for high-order QAM signals", Proceedings of the IEEE, vol. 86, no.3, pp. 1907-1926, Oct. 1998.

[38] R. Howald, "QAM bulks up once again: modulation to the power of ten," Motorola Broadband Communications Sector, SCTE Cable-Tec, June 2002.

[39] P. Lettieri, C. Fragouli, M. Srivastava, "Lower power error control for wireless links," Proc. of ACM Mobicom 97, Budapest, Hungary, Sep. 1997.

[40] P. Bhagwat, P. Bhattacharya, A. Krishna, S. Tripathi, "Enhancing throughput over wireless LANs using channel state dependent packet scheduling," Proc. of IEEE INFOCOM 96, pp. 1133-140, Mar. 1996.

[41] C. Fragouli, V. Sivaraman, M. Srivastava, "Controlled multimedia wireless link sharing via enhanced class-based queuing with channel state dependent packet scheduling," Proc. IEEE INFOCOM 98, pp. 572-577, Apr. 1998.

[42] C. Chien, S. Nazareth, P. Lettieri, et al., "Design experience with an integrated testbed for wireless multimedia computing," in Mobile Multimedia Communications, Plenum Press, 1997.

[43] P. Lettieri, M. B. Strivastana, "Adaptive frame length control for improving wireless link throughput, range, and energy efficiency", Proc. of IEEE INFOCOM 98, pp. 564-571, San Francisco, USA, 1998.

[44] Z. Lin, G. Malmgren, J. Torsner, "System performance analysis of link adaptation in HiperLAN Type2," Proc. of IEEE VTC 00, pp. 1719-1725, Sep. 2000.

[45] A. Doufexi, et al., "A comparison of the HiperLAN/2 and 802.11a wireless LAN standards," IEEE Commun Mag, vol.40, no.5, pp.172-180, May, 2002.

[46] B. Sklar, Digital Communications: Fundamentals and Applications, Prentice Hall, Jan. 2001.

[47] S. Lin, J. Daniel, Jr. Costello, Error Contorl coding: Fundamentals and Applications, Prentice Hall, 2005.

[48] M. Krunz, A. Muqattash, S. J. Lee, "Trasmission power control in wireless ad hoc networks: chanllenges, solutions, and open issues," IEEE Network Mag., Vol. 18, No. 5, pp. 8-14, Sep. 2004.

[49] Y. Hou, M. Hamamura, S. Zhang, "Performance tradeoff with adaptive frame length and modulation in wireless network," Proc. of IEEE CIT 05, pp. 490-494, Sep. 2005.

[50] Y. Hou, M. Hamamura, "A novel way of saving power in CSMA/CD," Proc. of IEEE CCNC 05, pp. 582-584, Jan. 2005.

[51] Y. Hou, M. Hamamura, "Probability of successful transmission between ad-hoc nodes with random radius and variable length of packets," Proc. of NEINE 05, Shanghai, China, Sept. 2005.

[52] Y. Hou, M. Hamamura, S. Zhang "Performance control of CSMA/CD with variable length of packets," Proc. of NEINE 04, Kochi, Japan, Sept. 2004.

[53] R. D. Katznelson, "Delivering on the 256-QAM promise," Broadband Innovations Inc., SCTE Cable-Tec, June 2002.

[54] T. Schenk, P. M. Smulders, E. Fledderus,"Multiple carriers in wireless communications – curse or blessing?", Tijdschrift van het NERG, vol. 70, no. 4, pp. 112-123, Dec. 2005

[55] G. Kutyniok, T. Strohmer, "Wilson bases for general time-frequency lattices," SIAM J. Math Anal., vol.37, no.3, pp.685-711, 2005.

[56] T. Strohmer, S. Beaver, "Optimal OFDM design for time-frequency dispersive channels," IEEE Trans. on Commun., vol. 51, no.7, pp.1111-1122, July 2003.

[57] Y. Hou, M. Hamamura, "A Novel Modulation with Parallel Combinatory and High Compaction Multi-Carrier Modulation ," Conditionally accepted by IEICE Trans. on Fundamentals.

[58] J. Zhu, S. Sasaki, G. Marubayashi, "Proposal of parallel combinatory spread spectrum communication system (in Japanese)," IEICE Trans. on Commu., vol. J74-B, no. 5, pp.207-214. May 1991.

[59] S. Sasaki, H. Kikuchi, J. Zhu, G. Marubayashi, "Multiple access performance of parallel combinatory spread spectrum commmunication systems in nonfading and Rayleigh fading channels," IEICE Trans. Commun., vol. E78-B, no. 8, pp.1152-1161. Aug. 1991.

[60] P. K. Frenger, N. Arne, B. Svensson, "Parallel combinatory OFDM signaling," IEEE Trans. Commun., vol. 47, no. 4, pp.558-565, Apr. 1999.

[61] M. Hamamura, S. Tachikawa, "Bandwidth efficiency improvement for multi-carrier systems," Proc. of IEEE PIMRC 04, Barcelona, Spain, Sept. 2004.

[62] M. Hamamura, S. Tachikawa, "On high compaction FDM comunication systems(in Japanese)," IEICE Technical Report, Jul. 2003.

[63] Y. Hou, M. Hamamura, "Bandwidth efficiency of PC-OFDM systems with high compaction multi-carrier modulation," Proc. of IEEE WCNM 05, Wuhan, China, Sept. 2005.

[64] S. Takahashi, M. Hamamura, S. Tachikawa, "A demodulation complexity reduction method using M-algorithm for high compaction multi-carrier modulation systems," Proc. of IEEE ISWCS 04, Mauritius, Sept. 2004.

[65] B. Muquet, Z.Wang, G. B. Giannakis, M. de Courville, P. Duhamel, "Cyclic prefixing or zero padding for wireless multicarrier transmissions?," IEEE Trans. Com-

mun., vol. 50, no. 12, pp. 2136-2148, Dec. 2002.

[66] K. Halford, M. Webster, "Multipath measurement in wireless Lan," Intersil Application Note AN9895, Oct. 2001.

[67] B. Tarokh, H.R. Sadjadpour, "Construction of M-QAM signals utilizing QPSK Golay sequences with low PMEPR suitable for OFDM systems," IEEE Trans. on Commun., vol.51, no.1, pp.25-28, Jan. 2003.

[68] C. Tellambura, "Computation of the continuous-time PAR of an OFDM signal with BPSK subcarriers," IEEE Commun. Lett., vol. 5, no. 5, pp. 185-187, May 2001.

[69] W. C. Y. Lee, "CS-OFDMA: A new wireless CDD physical layer scheme," IEEE. Commun. Mag, vol. 43, no.2, pp.74-79, Feb. 2005.

[70] A. Jamalipour, T. Wada, T. Yamazato, "A tutorial on multiple access technologies for beyond 3G mobile networks," IEEE Commun. Mag, vol. 43, no.2, pp.110-117, Feb. 2005.

[71] R. Ramanathan, J. Redi, "A brief overview of ad hoc networks: challenges and directions," IEEE Commun. Mag. vol. 30, no. 5, May 2002.

[72] Y. Hou, M. Hamamura, "Collision recovery for OFDM system over wireless channel," Accepted by IEICE Trans. on Fundamentals.

[73] A. Woo, K. Whitehouse, F. Jiang, J. Polastre, D. Culler, "Exploiting the capture effect for collision detection and recovery", Proc. of IEEE EmNetS-II, Sydney, Australia, May 2005.

[74] S. Ghez, S. Verdu, S. Schwartz, "Optimal decentralized control in the multipacket channel," IEEE Trans. Automatic Control, vol.34, no. 11, pp. 1153-1163, Nov. 1989.

[75] W. Luo, A. Ephremides, " Power levels and packet lengths in random multiple access with multi-packet reception capability," IEEE Trans. on Info. Theory, vol. 52, pp. 46-58, Feb. 2006.

[76] S. Verdu, "Multi-user Detection", Cambridge University Press. 1998.

[77] S. Lin, D. J. Costello, Jr., Error Control Coding: Fundamentals and Applications, second edition, Prentice Hall: Englewood Cliffs, NJ, 2005.

[78] Y. Li, J. C. Chuang, N. R. Sollenberger, "Transmitter diversity for OFDM systems and its impact on high-rate data wireless networks," IEEE J. Select. Areas Comm., vol.17, no.7, pp. 1233-1243, Jul. 1999.

[79] G. Bianchi, "Performance analysis of the IEEE. 802.11 distributed coordination function," IEEE Journal of Selected Areas in Commun., vol. 18, no. 3, Mar. 2000.

[80] L. Tong, Q. Zhao, G. Mergen, "Multipacket reception in random access wireless networks: From signal processing to optimal medium access control," IEEE Commun. Mag., vol. 39, no. 11, pp. 108 -112, Nov. 2001.

[81] Q. Zhao, L. Tong, "A multi-queue service room MAC protocol for wireless networks with multipacket reception," IEEE/ACM Trans. on Networking, vol. 11, no. 1, pp. 125-137, Feb. 2003.

[82] V. Naware, G. Mergen, L. Tong, "Stability and delay of finite user slotted ALOHA with multipacket reception," IEEE Trans. on Info. Theory, vol. 51, no. 7, pp. 2636-2656, July 2005.

[83] J. G Andrews, "Interference cancellation for cellular systems: a contemporary overview," IEEE Wireless Commun., vol. 12, no. 2, pp. 19-29, Apr. 2005.

[84] L. Hanzo, M. Munster, B. J. Choi, T. Keller, OFDM and MC-CDMA for Broadband Multi-user Communications, WLANs and Broadcasting, John Wiley, IEEE Press, Sept. 2003

[85] T. M. Schmidl, D. C. Cox, "Robust frequency and timing synchronization for OFDM," IEEE Trans. on Commun., Vol. 45, pp. 1613-1621, Dec. 1997.

[86] H. Stefan, M. Weinfurtner, "Comparison of preamble structures for burst frequency synchronization," Proc. IEEE Globecom2000, San Francisco, CA. Nov. 2000.

[87] H. Stefan, M. Weinfurtner, "Burst frame and frequency synchronization with a

Sandwich preamble," Proc. IEEE Globecom2001, San Antonio, Texas, Nov. 2001.

[88] H. Minn, V. K. Bhargava, K. B. Letaief, "A robust timing and frequency synchronization for OFDM systems," IEEE Trans. on Wireless Communications, vol. 2, no. 4, pp. 822-839, July 2003.

[89] H. Minn, V. K. Bhargava, K. B. Letaief, "A combined timing and frequency synchronization and channel estimation for OFDM," IEEE Trans. on Commun., vol. 54, no. 3, pp. 416-422, Mar. 2006.

[90] A. Ghosh, J. G. Andrews, R. Chen, D. R.Wolter, "Broadband wireless access with WiMax/802.16: Current performance benchmarks and future potential," IEEE Communications Magazine, vol. 42, no.2, pp. 129-136, Feb. 2005.

[91] R. O'Neill, L. B. Lopes, "Envelope variations and spectral splatter in clipped multicarrier signals," Proc. of IEEE PIMRC 95, pp. 71-75, Toronto, Canada, Sept. 1995.

[92] X. Li, L. J. Cimini, Jr., "Effect of clipping and filtering on the performance of OFDM," IEEE Commun. Lett., vol. 2, no. 5, pp. 131-133, May 1998.

[93] J. Armstrong, "Peak-to-average power reduction for OFDM by repeated clipping and frequency domain filtering," Elect. Lett., vol. 38, no. 8, pp. 246-247, Feb. 2002.

[94] V. Tarokh, H. Jafarkhani, "On the computation and reduction of the peak-to-average power ratio in multicarrier communications," IEEE Trans. Commun., vol. 48, no. 1, pp. 37-44, Jan. 2000.

[95] J. A. Davis, J. Jedwab, "Peak-to-mean power control in OFDM, Golay complementary sequences, and ReedCMuller codes," IEEE Trans. Info. Theory, vol. 45, no. 7, pp. 2397-2417, Nov. 1999.

[96] C. V. Chong, V. Tarokh, A simple encodable/decodable OFDM QPSK code with low peak-to-mean envelope power ration," IEEE Trans. Info. Theory, vol. 47, no. 7, pp. 3025-3029, Nov. 2001.

[97] S. H. Han, J. H. Lee, "PAPR reduction of OFDM signals using a reduced complexity PTS technique," IEEE Sig.Proc. Lett., vol. 11, no. 11, pp. 887-890, Nov. 2004

[98] S. H. Muller, J. B. Huber, A comparison of peak power reduction schemes for OFDM," in Proc. IEEE GLOBECOM' 97, Phoenix, AZ, pp. 1-5, Nov. 1997.

[99] A. D. S. Jayalath, C. Tellambura, Adaptive PTS approach for reduction of peak-to-average power ratio of OFDM signal," Elect. Lett., vol. 36, no. 14, pp. 1226-1228, July 2000.

[100] B. S. Krongold, D. L. Jones, "PAR reduction in OFDM via active constellation extension," IEEE Trans. Broadcast., vol. 49, no. 3, pp. 258-268, Sept. 2003.

[101] J. Tellado, Peak to Average Power Reduction for Multicarrier Modulation, Ph.D. dissertation, Stanford Univ., 2000.

[102] A. D. S. Jayalath, C. Tellambura, "Reducing the peak-to-average power ratio of orthogonal frequency division multiplexing signal through bit or symbol interleaving," Elect. Lett., vol. 36, no. 13, pp. 1161-1163, June 2000.

[103] R. W. Bauml, R. F. H. Fisher, J. B. Huber, "Reducing the peak-to-average power ratio of multicarrier modulation by selected mapping," Elect. Lett., vol., 32, no. 22, pp. 2056-2057, Oct. 1996.

[104] H. Breiling, S. Weinfurtner, J. B. Huber,"SLM peak-power reduction without explicit side information," IEEE Commun. Lett., vol. 5, no. 6, pp. 239-241, June 2001.

[105] Y. Hou, M. Hamamura, "PC/HC-MCM System with Space-Time Block Codes," Proc. of NEINE 06, Kochi, Japan, Sept. 2006.